Università degli Studi della Tuscia di Viterbo

Dipartimento per la Innovazione nei Sistemi Biologici, Agroalimentari e Forestali

Corso di Dottorato di Ricerca in Scienze, Tecnologie e Biotecnologie per la sostenibilità – curriculum Ecologia Forestale e Tecnologie Ambientali - XXXIII ciclo

MAPPING AND MODELLING PLANT SPECIES DISTRIBUTION (NATIVES AND ALIENS) ON COASTAL ECOSYSTEMS USING REMOTE SENSING DATA

Settore scientifico-disciplinare

(**s.s.d. BIO/07**)

Tesi di dottorato di:

Dott. Flavio Marzialetti

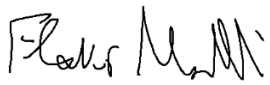

Coordinatore del corso

Prof. Andrea Vannini

Tutore

Prof.ssa Maria Laura Carranza

Co-tutore

Prof.ssa Alicia Teresa Rosario Acosta

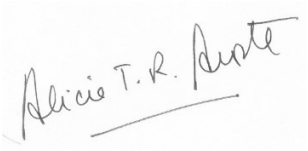

A.A. 2019/20 (A.Y. 2019/20)

A Verdiana per la sua immensa pazienza data in ogni momento,
per essere stata il mio sostegno in tutti i miei momenti di smarrimento
e di ansia nel non raggiungere i risultati sperati.

Index

Short abstract

The preservation and sustainable management of Nature is one of the major challenges of the humanity in the next future. Remote Sensing (hereafter RS) being effective on reporting earth surface status and changes at different scales has a great potential for supporting innovative monitoring tools and methodologies.

This research thesis explored the potential of free RS data (e.g. Sentinel-2, PlanetScope LiDAR) for monitoring coastal dune landscapes in the Mediterranean. The thesis, organized in 4 main chapters, addressed several issues related with RS applications on ecological monitoring. The first chapter stressed the usefulness of free RS, specifically LiDAR data, for modelling and mapping the invasion of a woody alien plant (*Acacia saligna* (Labill.) H. L. Wendl.) on coastal landscapes. Invasive Species Distribution Models (iSDM) are crucial for dealing with biological invasions, and the performed research gave new evidences of RS data usefulness for improving SDMs procedures and results. The second and third chapters tested the potential of RS for mapping coastal dune vegetation through semi-automatic and automatic classification procedures stressing the RS vegetation phenology (second chapter) and the RS yearly variability of three basic elements of coastal dunes landscapes (vegetation, water and bare soil; third chapter). The good temporal, spatial and spectral resolution of Sentinel-2 RS data, allowed to effectively map a dynamic and heterogeneous mosaics like those of coastal dunes .

The fourth chapter explored the relationship between field measured and remote sensed biodiversity and tested such relation on coastal dunes. This chapter, gave new evidences concerning the potential of the "Spectral Variability Hypothesis" (SVH) for depicting floristic biodiversity on well preserved and disturbed (e.g. *Carpobrotus acinaciformis* (L.) L. Bolus, *Carpobrotus edulis.* (L.) N. E. Br. invaded) coastal dune landscapes.

The results presented in this thesis have highlighted several strengths and limits of using RS data for modelling and mapping coastal dune ecosystems.

Keywords

Invasive species distribution model, *Acacia saligna* and *Carpobrotus* spp. invasions, Coastal dune vegetation monitoring, Multispectral satellite images, Multitemporal analysis,

Extended abstract

The preservation and sustainable management of Nature is one of the major challenges of the humanity in the next future. At present natural biodiversity and ecosystem functioning are highly endangered by several processes as climate and land use change, invasive alien species and pollution. To address these challenges, innovative environmental monitoring tools and methodologies are urgently needed and among them Remote Sensing (hereafter RS) which is considered effective on reporting environmental changes at different scales is very promising. Furthermore, the constant improvement of satellite images spatial, spectral and temporal resolutions, along with the increasing availability of computing resources and updated algorithms have enlarged the monitoring application of RS to complex and dynamic ecosystems as river beds or coastal dunes.

In these we adopted as training ground for exploring the RS potential for environmental monitoring, costal dune ecosystems. Coastal landscapes are transition zones between terrestrial and marine environments characterized by highly specialized flora and fauna, which provide several benefits to human wellbeing (e.g. erosion and storm protection, wind shelter, carbon stock, recreation). At the same time, these landscapes are among the most threatened ones worldwide, and in the Mediterranean this human pressure is particularly severe.

The main scope of this thesis is to develop and test innovative monitoring tools supported by free satellite RS data and to explore the potential of the new available images with improved spatial and temporal resolution for coastal ecological monitoring. To best describe the research carried out during this period I've organized the PhD final report into 4 chapters.

The first chapter explored the potential of RS for modelling and mapping plant invasions on Mediterranean coasts. Alien invasions are one of the major drivers of biodiversity loss which also could negatively affect public health and local economy. Effective prevention/management of alien invasions requires to know the major pathways of introduction and secondary spread, the areas more prone to invasion, and the early warning signs. In this context invasive alien species distribution models (iSDM) and derived habitat suitability maps could offer reliable information necessary to inform decision makers. Relatively recent research gave evidence of a wide range of variables that RS data can provide (e.g. biomass, water bodies, vegetation/cover types) to improve SDMs. Indeed, several variables, derived in the past from thematic maps, can be now depicted using RS updated data. RS data have revolutionized methods and updating tools for thematic mapping. In this chapter, as a presentation for demonstration an iSDM for the invasive plant of European concern (*Acacia saligna*) was developed using mixed variables (derived from thematic maps and remote sensed data) was developed. In this chapter, we provided an exploratory analysis of the environmental

characteristics that promote the rapid growth and development of *A. saligna* in Italian dune ecosystems, contributing to filling the gap between theory and practice in conservation decision-making. The use of remotely sensed data allowed to model the invader-landscape relationship on a large geographic extent and to highlight the coastal sectors that are most likely to be invaded in the future.

The second chapter focused on semi-automatic ecosystem monitoring exploring the potential of RS phenological vegetation properties for coastal dune ecosystem classification. Vegetation mapping was among the first products derived from RS data. However, vegetation mapping was often based on the integration of visual interpretation and floristic data which make the procedure time-consuming and sometimes subjective. Concerning coastal dune vegetation mapping, it was traditionally based on photointerpration of ortophotos as the utilization of satellite images was less common. The main limitation of mapping coastal dunes using RS data was related with spatial resolution which, in the old satellite missions (e.g. Landsat), was too coarse to detect the fine scale dune mosaics. Still the availability of open access, remotely sensed data with increasing spatial and spectral resolution (e.g. Sentinel-2) offer new information to perform automatic and semi-automatic vegetation mapping on complex mosaic as coastal dunes. In this chapter, we tested the strength of a RS phenology-based vegetation mapping approach using of open source products (Sentinel-2 and Snap toolboxes) across all the processing chain. The obtained vegetation maps as those derived from RS automatic and semi-automatic methodologies allowed to reduce the subjectivity of the interpreter and increased the repeatability of the method in others environments. Notice that the high temporal resolution of some RS data offers extra information for classification procedures that besides the widely used multispectral bands and spectral indices can include temporal variability (e.g. vegetation phenology) which is extremely important for discriminating different elements on complex and dynamic mosaics as those in coastal landscapes.

The third chapter investigated the potential of RS data for depicting vegetation temporal variability and its contribution on automatic vegetation mapping and monitoring. We analyzed coastal dunes which conforms a typical vegetation zonation encompassing the sea-to-inland gradient. Each coastal dune vegetation type is characterized by a specific phenology and seasonality. In this chapter we developed and tested a landscape classification approach accounting for the within-year temporal variability of the main components of the coastal mosaic: vegetation, bare soil and water surfaces. Specifically, we stressed the potential of Rao's Q diversity for summarizing spectral variability over time. The use of diversity metrics depicting RS temporal variability (e.g. seasonal cycles) allowed to integrate several landscape features the within a single tool. Multitemporal RS analysis proved to be

an effective support for mapping a highly seasonal and heterogeneous landscape such as coastal dunes.

The fourth chapter explored the relationship between the field measured and RS biodiversity and specifically tested such relation on coastal dunes. The improvement of biodiversity monitoring tools is currently a pressing need and combining field collected and remotely sensed (RS) data represents one of the most promising approaches for an extensive and up-to-date ecosystem assessment. This chapter investigated the potential of the so called "Spectral Variability Hypothesis" (SVH) in linking field collected and remote sensed data in a complex and dynamic landscape. This chapter provided a pioneering assessment of the relation between floristic and spectral RS diversity in Mediterranean coastal dune habitats providing strong evidence about the potential of RS for estimating and monitoring diversity in coastal landscapes.

The results obtained in this research have evidenced several strengths of using free RS data analyzed with automatic and semi-automatic approaches for depicting and monitoring coastal dune ecosystems. Processing RS data by automatic and semi-automatic approaches assured objective and repeatable products. Furthermore the proposed data analysis and methodologies could be extended to other environmental conditions.

Plant species nomenclature conforms the updated checklist of the vascular flora of Bartolucci et al. 2018 and Galasso et al. 2018.

Chapter 1: Modelling plant invasions on coastal landscapes though an integrative approach using remote sensing. The case of *Acacia saligna* on LTER sites in the Adriatic coast

1.1. Introduction

Biological invasions are one of the major global drivers of biodiversity loss, often resulting in economic damage and public health care problems (Hulme *et al.* 2009, Simberloff *et al.* 2013).
The establishment, growth and expansion of invasive alien species depend on a combination of mechanisms related to both ecology of the species and the assembly of environmental factors (Lockwood *et al.* 2005, Richardson and Pyšek, 2006, Malavasi *et al.* 2018). Indeed, biological invasions are promoted by a wide range of drivers that can be schematically grouped into three main components, the so called PAB factors: Propagule pressure (P), Abiotic characteristics of the invaded ecosystem (A) and Biotic interaction between invasive species and recipient community (B, Catford *et al.* 2009). It is well known that invasions cannot occur without adequate propagule pressure (P), defined as the frequency of plant propagule introductions (Eppstein and Molofsky, 2007). Although several authors agree that P represents the key driver in the invasion process (Lockwood *et al.* 2005, Colautti *et al.* 2006, Simberloff *et al.* 2013), abiotic drivers also play an essential role as the invasion will fail if the invading species cannot survive the environmental conditions of a site (Weiher and Keddy, 1995, Gallien *et al.* 2014). Finally, an alien species entering into a new area can either gain or lose biotic interactions capable of facilitating or constraining the invasion (Mitchell *et al.* 2006).
In order to deal with biological invasions and for preventing their negative effects on ecosystem biodiversity and functioning (Hulme *et al.* 2009), the European Union adopted a new regulation (EU-No 1143/2014, hereinafter EU Alien regulation) which sets guidelines for the management of Invasive Alien Species (IAS). This regulation underlines the importance of invasion prevention, early warning and rapid response followed by eradication and control measures (Genovesi *et al.* 2015). As stated by the EU Alien regulation, preventing biological invasions should be the most cost-effective way to minimise the impact of IAS on biodiversity. Still, new methodologies aimed at identifying early signs of invasion are needed (Sitzia *et al.* 2016). In this context, the use of invasive Species Distribution Models (iSDMs), aimed at investigating the relationship between alien occurrence and PAB factors, should offer an effective tool to better understand biological invasions (Guisan and Thuiller 2005, Tulloch *et al.* 2016). Specifically, iSDMs analyze the statistical relationship between the presence of alien species (dependent variable) and environmental predictors (independent variables, Elith and Leathwick, 2009); they also allow both identification of the strength of the relationship between species presence and environmental variables and project the probability of occurrence of the species in wide areas in which the species is not present. Over the last twenty years,

iSDMs have been widely implemented for conservation and management purposes (Elith and Leathwick 2009, Franklin 2010). Part of the research efforts has been devoted to unravelling the influence of different invasion drivers on the occurrence of some invasive species (Bazzichetto *et al.* 2018a, Bellard *et al.* 2016, Thuiller *et al.* 2005) and predicting the probability of invasion of one taxon (e.g. Gutierres *et al.* 2011) or a group of taxa (e.g. Malavasi *et al.* 2018).

Despite all these efforts, further research is still necessary, orientated towards implementing invasive species distribution models for supporting IAS management. A taxon for which important research efforts have been undertaken, but still requiring multivariate analysis of the different invasion drivers, is the Australian genus *Acacia*. *Acacia* sp. is a highly aggressive genus and one of the major invaders in the world (Castro-Díez *et al.* 2011, Richardson *et al.* 2011, Richardson and Rejmánek, 2011). Amongst them, *A. saligna* (Labill.) H. L. Wendl. is one of the most invasive taxa of the genus (Richardson and Rejmánek, 2011) and its spread is particularly worrisome in Italy and the rest of Europe (Wilson *et al.* 2011). Although the high potential of invasion of *A. saligna* is acknowledged and the role of several environmental factors in driving its invasion has been separately investigated (Hadjikyriakou and Hadjisterkotis, 2002, Nsikani *et al.* 2017, Yelenik *et al.* 2004), studies exploring the simultaneous influence of these factors are needed.

In light of this, the present chapter sets out to model the occurrence of *A. saligna* in coastal landscapes of central Italy (Adriatic coast) while accounting for the simultaneous effect of propagule pressure, abiotic and biotic factors. By implementing an iSDM, based on field and cartographic geo-referenced data, we explored the relationship between the presence of *A. saligna* and PAB factors. We assumed that the invasion by *A. saligna* across the dune mosaic is not homogeneous, but varies through space, according to the distribution of the main PAB factors.

By identifying the factors related to higher occurrence values of the alien taxa and by mapping the areas with different probabilities of occurrence, we can identify new tools able to contribute to the prioritization of conservation actions in coastal ecosystems, as required by the EU Alien regulation.

It is also worth mentioning that such iSDM implementation benefitted from the presence within the study area of two Long-Term Ecological Research sites (LTER, http://www.lter-europe.net/), which actively contributed to the description of the considered ecosystem status and its possible future trends. Indeed, the LTER network in which ecosystem experts monitor a wide range of environmental variables may offer a rich overview of alien species distribution and invasion drivers across different ecosystems and geographical areas.

1.2. Materials and methods

1.2.1. Target species

A. saligna is one of the most invasive taxa of the genus *Acacia* (Richardson and Rejmánek, 2011). The species was introduced into the coastal areas of South Africa and of the Mediterranean basin for reforestation, dune stabilization and ornamental purposes (Bar Kutiel *et al.* 2004, Gutierres *et al.* 2011,Wilson *et al.* 2011). It expanded in an uncontrolled manner in coastal areas of Algeria, Cyprus, Israel, Italy, Kenya, Morocco, Portugal, South Africa and Spain (Wilson *et al.* 2011, Yelenik *et al.* 2004). It successfully colonized arid environments of the Mediterranean region with poor and periodically burnt soils (Bell *et al*. 1993). In Italy, *A. saligna* was introduced in the 1950s for the stabilization of inner dunes (Izzi *et al.* 2007, Tulloch *et al.* 2016). Nowadays, the species is present in many coastal areas of Italy (Celesti-Grapow *et al.* 2010, Del Vecchio *et al.* 2013) and it tends to colonize a narrow coastal strip between the Mediterranean scrubs and the *Pinus* sp. woodlands of the fixed dunes (Del Vecchio *et al.* 2013, Figure A1).

A. saligna has several ecological features that favor its expansion in non-native environments. The clonal and sexual reproduction, high rate of growth, short juvenile period and high tolerance to environmental stress (Del Vecchio *et al.* 2013, Milton and Hall, 1981, Witkowski 1994) are all traits that allow its expansion in a wide variety of ecosystems. Furthermore, the production of a huge number of long-lived seeds and the secretion of allelopatic substances ensure the persistence of the species in the soil seed bank and its chance to sprout over long periods (Mehta 2000, Abd El-Gawad and El-Amier, 2015, Strydom *et al.* 2012). *A. saligna* forms dense monospecific stands in which several native species are excluded (Yelenik *et al.* 2004), leading to a simplification of the structure and diversity of native plant communities (Calabrese *et al.* 2017, Cohen and Bar Kutiel, 2017, Del Vecchio *et al.* 2013, Hadjikyriakou and Hadjisterkotis, 2002). It also alters the soil properties as its invasion promotes changes in microclimatic conditions (Mehta 2000, Richardson *et al.* 2011, Calabrese *et al.* 2017) and to hydrological and nutrient cycles (Witkowski 1991, Yelenik *et al.* 2004), in particular the N-cycle (Yelenik *et al.* 2004; Le Maitre *et al.* 2011).

1.2.2. Study area

The study was carried out on a representative tract of the Adriatic coast of central Italy (Molise region). The coast is mainly composed of recent sandy dunes (Holocene), which occupy a narrow strip along the seashore. The dune system has a simple structure, being usually characterized by a single dune ridge with low elevation (less than 10 meters, Acosta *et al.* 2009, Carranza *et al.* 2008). Here, the psammophilous vegetation distributes following a well-defined coastal zonation due to the presence of a sea-inland environmental gradient (Acosta *et al.* 2003, Prisco *et al.* 2012).

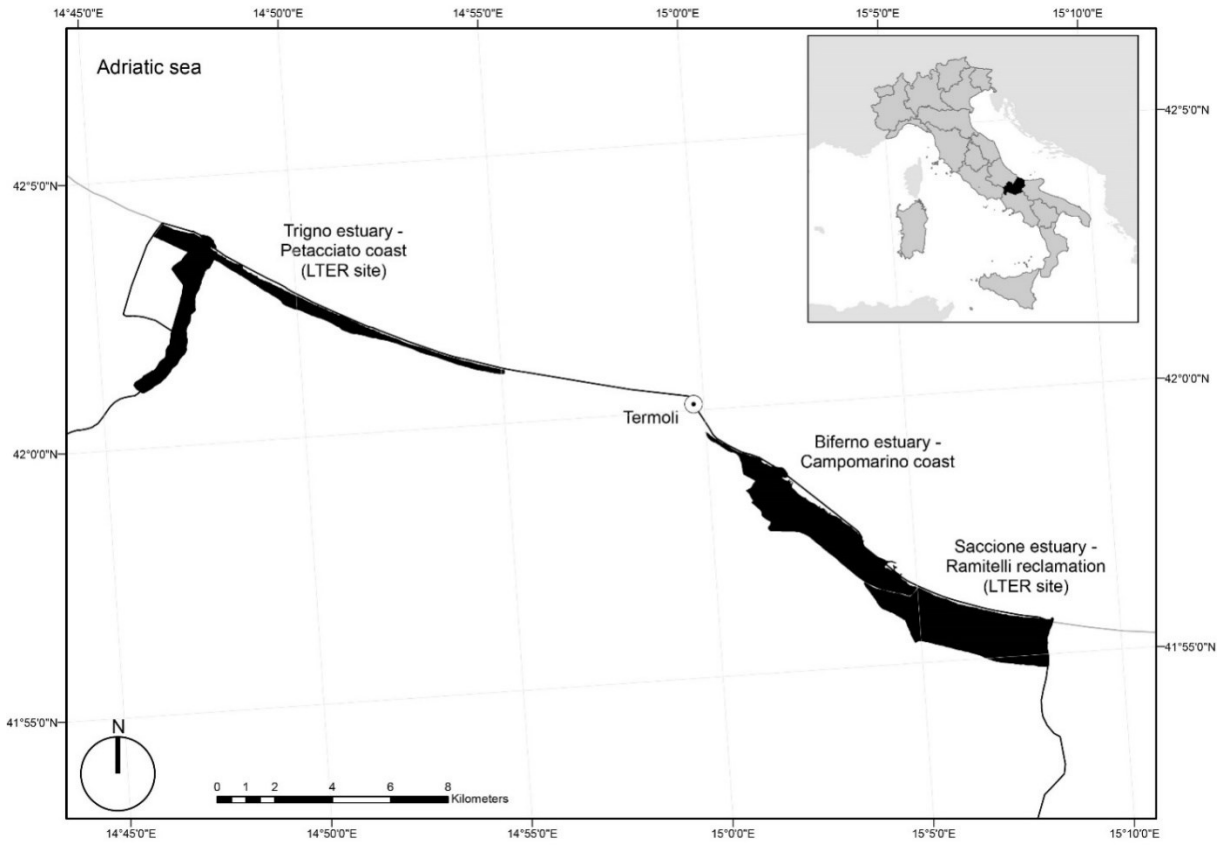

Figure. 1. Study area. Sites of European Conservation concern and LTER sites are shown in black. Coordinates are given in Datum: WGS 84.

The intense and rapid land use change (Malavasi *et al.* 2013, Malavasi *et al.* 2016) and the introduction of exotic species are amongst the main threats affecting native communities of Adriatic coastal ecosystems (Romano and Zullo, 2014, Calabrese *et al.* 2017, Malavasi *et al.* 2018). Nonetheless, the coastal dunes of Molise still host many ecosystems of conservation concern in Europe (the so-called EU habitat types according to the European Directive 92/43/EEC; Stanisci et al. 2014). Most of the analysed coastal sectors are included in Sites of European Conservation Concern (Foce Trigno – Marina di Petacciato: IT7228221; Foce Biferno – Litorale di Campomarino: IT7222216; Foce Saccione – Bonifica Ramitelli: IT7222217) and belong to the European LTER network (Bertoni 2012, Drius *et al.* 2013, Figure 1).

1.2.3. *Acacia saligna* occurrence records

To implement the analysis, we used presence data of *A. saligna* mostly collected inside LTER sites during the years 2013-15 (Calabrese *et al.* 2017, Del Vecchio *et al.* 2013). We used 30 presence points and 95 random-absences collected at a minimum distance of 100 m between each other and distributed along the whole coastal dunes in the area (Hijmans 2012). The number of absences was chosen in order to guarantee model adequacy and provide an accurate prediction (Franklin 2010).

1.2.4. Environmental data

In an ArcGIS environment (ArcGIS 10.2.2), a set of environmental variables was computed related to propagule pressure (P), abiotic (A) and biotic factors (B) and which were expected to influence the expansion of *A. saligna*. We selected road distance as a proxy of propagule pressure *(Bazzichetto et al.* 2018a), while sea distance and river distance were used as surrogates of abiotic conditions (Gutierres *et al.* 2011, Bazzichetto *et al.* 2018a). Finally, *Pinus* sp. wooded dune land cover and herbaceous dune vegetation land cover were used as a proxy of biotic conditions (Del Vecchio *et al.* 2013, Table 1). Concerning propagule pressure, the distance from roads was considered because of its acknowledged role in favouring alien species dispersal (Jørgensen and Kollmann, 2009, Le Maitre *et al.* 2004). Road distance was computed as the Euclidean distance between each point of occurrence of the invasive species and the closest road, including paved roads and secondary pathways (road data retrieved from https://planet.openstreetmap.org/; OpenStreetMap contributors 2017) that cross the dune systems. For abiotic factors, sea distance was considered because, in coastal dunes, it properly depicts the ecological conditions along the sea-inland stress gradient (Acosta *et al*. 2003, Drius *et al.* 2013, Bazzichetto *et al.* 2016). This sea distance was measured as the Euclidean distance of each point of occurrence from the shore line (obtained through photo-interpretation by Malavasi *et al.* 2013). Considering that *A. saligna* tends to prefer mesic conditions on arid landscapes, we used river/stream distance as a proxy of water supply (Le Maitre 2004, Gutierres *et al.* 2011). The distance from rivers was derived using the hydrography map and measured as the Euclidean distance of each point from principal rivers and streams of the Molise region (river data retrieved from https://planet.openstreetmap.org/; OpenStreetMap contributors 2017). Finally, as biotic factors, we considered the relationship between *A. saligna* occurrence with two natural dune vegetation types widely spread along the coast and characterised by different spatial structures and plant strategies: closed formations of *Pinus* woods and the herbaceous dune vegetation growing on fore dunes. We derived the percentage (%) of *Pinus* sp. woodlands and of herbaceous dune vegetation by applying a moving window procedure (buffer 30 m radius) FRAGSTATS (McGarigal *et al.* 2012) across a fine scale (1:5000) land-cover map (Malavasi *et al.* 2013). The land-cover map conforms to the CORINE land-cover mapping procedure extended to a fourth level of detail for the forested and semi-natural categories (see Acosta *et al.* 2005 for details). The considered cover categories in the study area are linked with habitats of European conservation concern: Wooded dunes with *Pinus pinea* and/or *Pinus pinaster* (EC-2270) and herbaceous dune vegetation, that includes the embryonic shifting dunes (EC-2110), shifting dunes along the shoreline with *Calamagrostis arenaria* supsp. *arundinacea* (EC – 2120) and *Malcolmietalia* dune grasslands (EC – 2230). All the variables were reported into raster layers with 5 m resolution, which is an adequate spatial resolution for analysing the coastal dune

environments in the Mediterranean basin (Bazzichetto *et al.* 2018a, Malavasi *et al.* 2018).

1.2.5. Species Distribution Models

The iSDM was based on a binomial Generalised Linear Model (GLM) aimed at analysing the relationship between the occurrence of *A. saligna* and the PAB variables (Hosmer and Lemeshow, 2000). First, we performed collinearity analysis between these variables (see Appendix A.1 for details) in order to exclude multi-collinearity (Brauner and Shacham, 1998). Collinearity was assessed by means of Spearman's rank correlation (P_S) and by computing the Variance Inflation factor (VIF, Brauner and Shacham, 1998, Guisan and Thuiller, 2005). A predictor was excluded by the model in case of high correlation, i.e. whenever the Spearman's correlation coefficient (P_S) was higher than 0.7 or lower than -0.7 and when VIF was higher than 3 (see Appendix 1 for collinearity analysis and variables selection).

Table 1 Predictors analysed. Propagule pressure (P), abiotic (A) and biotic (B) factors along with the corresponding proxy variables (predictors) used for implementing the iSDM.

Factor	Proxy variables (predictors)	Description
P	Road distance (m)	- Euclidean nearest distance (m) from paved roads and secondary pathways.
A	Sea distance (m)	- Euclidean distance (m) from shoreline.
	River distance (m)	- Euclidean distance (m) from nearest river (main streams, river courses)
B	% *Pinus* sp. wooded dunes	- percentage of *Pinus* sp. wooded dunes within a 30 m radius window. Includes EU Habitat: 2270 – Wooded dunes with *Pinus pinea* and/or *Pinus pinaster*.
	% Herbaceous dune vegetation	- percentage of herbaceous vegetation within a 30 m radius window. Includes embryonic shifting dunes (EC-2110), shifting dunes along the shoreline with *Calamagrostis arenaria* subsp. *arundinacea* (EC – 2120) and *Malcolmietalia* dune grasslands (EC –2230).

Model performance was evaluated using two measures: the McFadden's R squared (McFadden 1973) and the area under the receiver operator curve (AUC, Pearce and Ferrier, 2000). The McFadden's R squared index, as the classical R squared, can assume continuous values from 0 to 1, with 0 indicating minimum and 1 maximum variability "explained" by the model (McFadden 1973). AUC has been widely used as a standard measure for assessing the predictive accuracy of SDMs (Jiménez-Valverde 2012, Lobo *et al.* 2008, Pearce and Ferrier, 2000). In particular, the AUC was used to estimate the capacity of the model in predicting the presence of the species in location where the species was actually present and its absence where it was not recorded. AUC values between 0.5 and 0.7 indicate a poor discrimination capacity of the model, values between 0.7 and 0.9 represent a reasonable discrimination and an AUC greater than 0.9 indicates a very good discrimination capacity of the model (Pearce and Ferrier, 2000). A robust estimation of the AUC can be gathered by cross-validating

the model and averaging the single AUC values obtained from each cross-validation run. With this aim, the dataset was randomly partitioned into five subsets, using a 75% for model training and the remaining 25% to test prediction accuracy. Then, a final AUC value was computed by averaging between a single AUC obtained in each cross-validation run (Le Dell *et al.* 2015, Millar *et al.* 2011).

1.3. Results

According to the GLM model, the different PAB factors showed specific and significant relationships with the occurrence of *A. saligna*. (Table 2).

Table 2. GLM model outcome. Response variable: *Acacia saligna* presence/absence; predictors: Propagule pressure, abiotic and biotic factors. For a detailed description of the predictors and the land cover types see Table 1. ('***' $p < 0.001$; '**' $p < 0.01$; '*' $p < 0.05$).

Predictors	Estimate	Std. Error	Z value	p-value
Intercept	2.08	1.24	1.68	p>0.05
P (Propagule pressure)				
Road distance	-0.004	0.002	-2.059	*
A (Abiotic)				
Sea distance	-0.025	0.010	-2.639	**
River distance	-0.001	0.000	-2.289	*
B (Biotic)				
Pinus sp. dune wood	0.073	0.019	3.884	***
Herbaceous dune vegetation	0.003	0.016	0.202	p>0.05

The variables, considered for modelling species occurrence, were independent with no significant Spearman's rank correlation coefficient and VIF values (see Appendix A, Table A for details).

The occurrences of *A. saligna* were associated with propagule pressure (P, Table 2), with higher probabilities of finding the species in proximity to roads (Figure 2). Concerning the abiotic variables (A), sea distance showed a significant and negative relationship with the presence of *A. saligna*, indicating that the species occurred in a specific sector of the dune system (50 – 100 meters to sea) (Table 2; Figure 2). Similarly, *A. saligna* showed a significant negative relationship with river distance, indicating a link to humid conditions (Table 2; Figure 2). Amongst the biotic factors (B), *A. saligna* was significantly associated with *Pinus* sp. dune woods. In particular, the probability of occurrence of *A. saligna* increased with higher percentages of *Pinus* dune woods (Figure 2).

A zoomed area of the suitability map for Molise for *A. saligna* is reported in Figure 3.

The fitted GLM explained 0.70 of the variability (McFadden's R squared= 0.70) and good predictive power (AUC mean = 0.96).

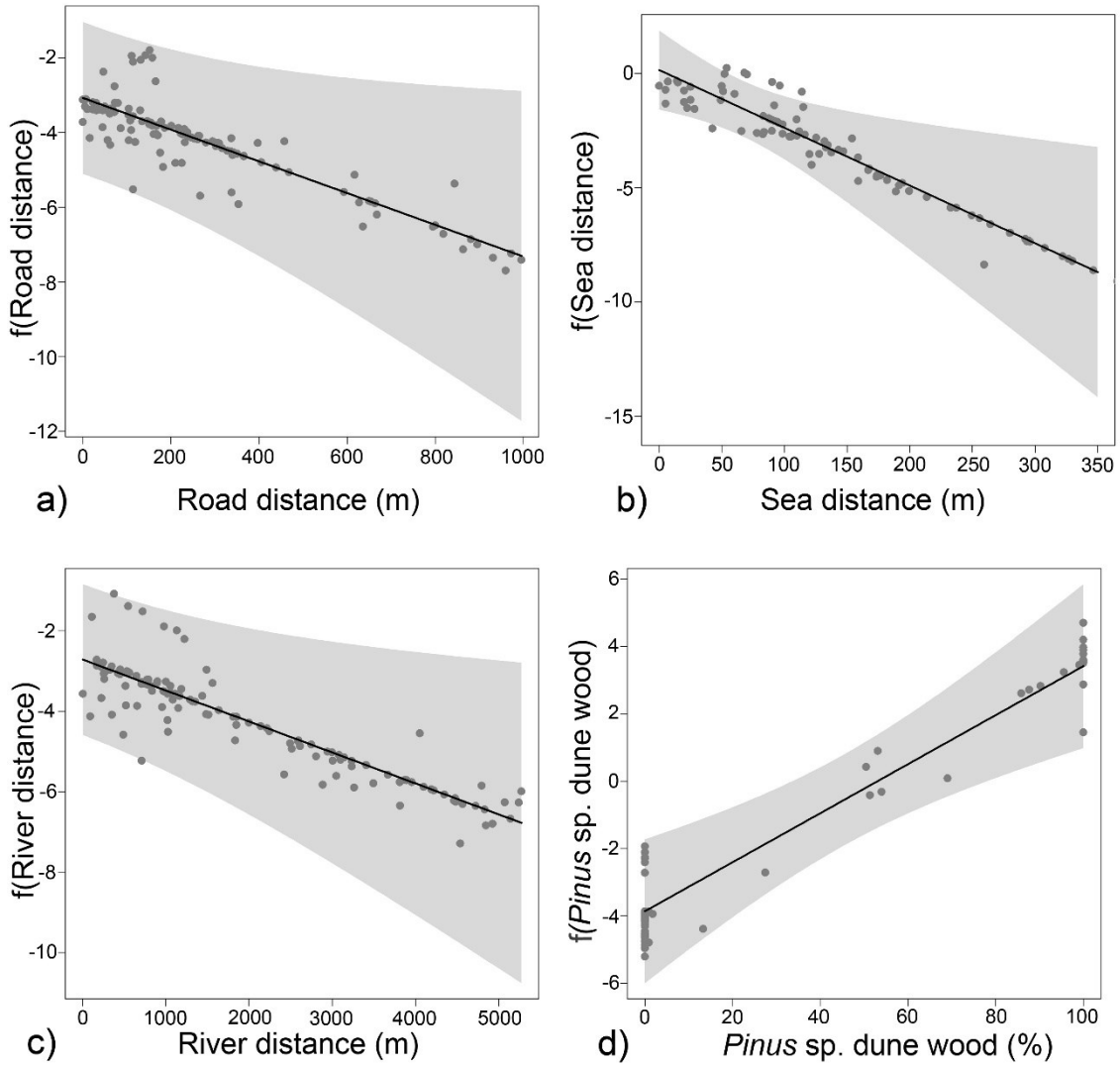

Figure 2. Regression curves. Relationship between *A. saligna* occurrence and the PAB predictors (a – Road distance, b - Sea distance, c – River distance, d – % of *Pinus* sp. dune wood). On the x-axis: predictors with the corresponding unit of measurement. On the y-axis: the residual values for each predictor.

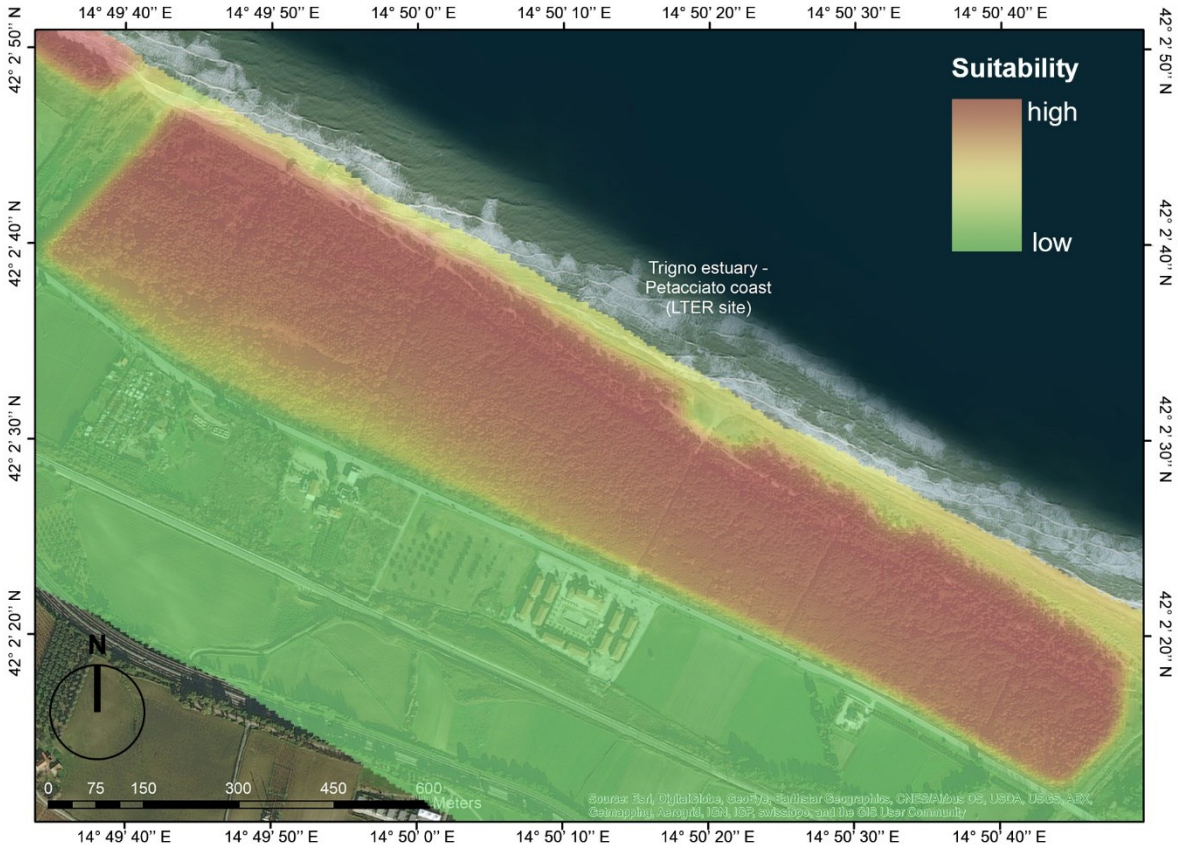

Figure 3. Zoomed area reporting the suitability map for *Acacia saligna* obtained by the spacialization the iSDM in the Molise coast (Marina di Pettaciato).

1.4. Discussion

In this study, we modelled the occurrence of *A. saligna* along the Adriatic coast in central Italy and identified the specific role of propagule pressure, abiotic and biotic factors in determining the presence of the species. The model showed a good power of prediction, as highlighted by the explained variability of the McFadden's R squared and predictive accuracy of the mean AUC, obtained through cross-validation.

Our results highlighted that the invasion by *A. saligna* was not spatially homogeneous, but varied across the coastal landscape, following the spatial distribution of the different PAB factors. *A. saligna* preferentially occurred close to the coastal pine forest, at an intermediate distance from the coastline, preferably 50-100 meters from sea and its presence was also related to distance from roads and rivers. Specifically, *A. saligna* occurrence is promoted by propagule pressure, which along the Mediterranean coasts can be related to distance from roads (Arévalo *et al.* 2005, Bazzichetto *et al.* 2018b). In addition to the acknowledged role of roads in supporting alien species dispersal (Jørgensen and Kollmann, 2009, Le Maitre *et al*. 2004), roads can also fragment forested areas, thus altering the undergrowth light conditions (Gutierres *et al.* 2011) and creating gaps of favourable habitat for *A. saligna* (Flory and Clay, 2006, Gutierres *et al.* 2011, Parendes and Jones, 2000). Indeed, forest edges

are characterised by microclimatic conditions of temperature and soil moisture (Brothers and Spingarn 1992, Gehlhausen *et al.* 2000) that promote the growth of edge species (Carranza *et al.* 2012), most of them being weeds and aliens (Spellerberg 1998).

Moreover, the model also highlighted that abiotic factors regulated *A. saligna* invasion. Coastal dune ecosystems are characterised by a mosaic of habitats in which the gradual change in abiotic conditions shapes the growth of the species, thus determining the typical sea-inland ecological gradient (Acosta *et al.* 2003, Drius *et al.* 2013). Sea distance is a good proxy of such gradient (Bazzichetto *et al.* 2016) and the observed correlation of *A. saligna* occurrence with sea distance underlined the influence of this complex environmental gradient on the invasion process. Indeed, *A. saligna* tends to invade specific sectors of the dune system (Cohen *et al.* 2008, Midgley and Turnbull, 2003) and, according to our results, this species preferentially occurred on sparsely vegetated fixed dunes. Probably this trend is also related with soil characteristics that, in the inner dune sectors, are more compact and with lower salt concentration (Santoro *et al.* 2011).

Similar behaviour was observed in other ecosystems characterised by dry sandy soils, (e.g. South-African fynbos, coastal sand dunes of Israel) in which *A. saligna* invades areas with open or patchy vegetation (Mehta 2000, Bar Kutiel *et al.* 2004) and it was attributed to its good competitive strategy for using water resources (Witkowski 1991, Yelenik *et al.* 2004).

In confirmation of this, river distance (a proxy of soil moisture) seems to favour *A. saligna* growth in this Adriatic sector. The observed correlation highlighted the tendency of the species to grow and develop in the most humid areas of arid coasts of the Mediterranean climatic region (Bar Kutiel *et al.* 2004; Gutierres *et al.* 2011). Due to its preference for mesic conditions on arid landscapes, *A. saligna* is commonly associated with areas close to the river courses on both inland sectors and dunes (Gutierres *et al.* 2011). Furthermore, the proximity of rivers, besides indicating the availability of moisture, should imply the presence of disturbance that removes competing plants, making such landscapes particularly sensitive to invasion (Mehta 2000, Gutierres *et al.* 2011).

Biotic conditions also affected the distribution of *A. saligna*, which preferentially invaded areas close to pine forests. The preference of the invader for pine forests on Mediterranean coasts is particularly worrisome because this formation, with high historical and social value for the territory (Del Vecchio *et al.* 2013), is a priority habitat of European conservation concern (Habitat 2270* Wooded dunes with *Pinus pinea* and/or *P. pinaster,* Bonari *et al.* 2017, Bonari *et al.* 2018). Thus, our results pinpointed the need for defining adequate management actions to counteract the invasion risk. Most of the areas covered by Wooded dunes with *Pinus pinea* and/or *P. pinaster* in the Italian peninsula derive from old afforestations (Falcucci *et al.* 2007) carried out to protect the inner coastal plains and for land reclamation purposes (Malavasi *et al.* 2013). The structure and floristic composition of these

old pine formations has evolved over time and now is characterised by the presence of a good cohort of Mediterranean scrub species that forms the understorey corresponding to canopy gaps. The presence of canopy gaps that allow the settlement of fast-growing and light-demanding species would make old pine forests particularly vulnerable to alien invasions (Burnham and Lee, 2010, Del Vecchio *et al.* 2013, Gray 2005, Selmants and Knight, 2003) and be threatened specifically by *A. saligna*. The results obtained using LTER data, should offer the basis for prioritising monitoring efforts on areas more susceptible to invasion, thus optimising the resources and time devoted to managing alien species expansion.

Similarly to that observed by Malavasi *et al.* (2018) using the LifeWatch biological database, the utilization of LTER networks constitutes a sound tool for modelling biological invasions, promoting the sharing of unprecedented amounts of data amongst ecologists. Furthermore, the multi-temporal nature of LTER data offers a unique opportunity to monitor variations in environmental conditions over time and also to identify, through multi-temporal iSDMs (e.g. Carone *et al.* 2011), the factors and phenomena that underlie the changes occurring in invasive alien species distribution over time.

1.5. Conclusion

This integrative analysis of the occurrence of the non-native species *A. saligna* in coastal landscapes, including a single model using the simultaneous effect of propagule pressure, abiotic and biotic factors, allowed us to effectively depict those critical drivers for determining the presence of this highly invasive plant in the Mediterranean dunes and to define areas with different probabilities of invasion. Invasion by *A. saligna* was not homogeneous but varied across the coastal landscape, following the spatial distribution of different factors. Indeed, invasion preferentially occurred on coastal fixed dunes close to pine forests. The implemented iSDM provided valuable insights into the invasion process and it supplied an efficient prediction of the invasion processes in this stretch of the Adriatic coast, providing the necessary instruments for the assessment of invasion risks claimed by the EU Alien regulation (EEC 2014).

Finally, as the presence of a valuable amount of data collected across a network of LTER sites supported the implementation of a more effective iSDM, it is also true that the LTER network benefitted from such research, confirming its relevance in providing useful information for modelling and monitoring invasion processes. Furthermore, by monitoring variations in environmental conditions, it is possible to identify, through multi-temporal iSDMs, the factors and phenomena that allow alien species expansion over time. With this in mind, we hope that other LTER network-based case studies could be further carried out to provide integrated information across a wide range of monitored ecosystems and for increasingly larger areas.

1.6. Appendix A

Figure A1. An example of the invasion process by *A. saligna* along coastal dune system of central Italy (author of the photo: Francesco Maria Tozzi).

The variables considered for modelling species occurrence are lower than threshold values both Spearman's rank correlation coefficient and VIF values (Table). Sea distance and herbaceous dune vegetation are the variables with greater correlation score (- 0.6), instead the lowest correlation was found between herbaceous dune vegetation and roads distance (0.00). *Pinus* dune wood in the multicollinearity test has the higher VIF (2.56), while roads distance has the lowest one (1.12).

Table A. Correlation analysis. Spearman's rank correlation coefficient and Variance Inflation factor (VIF) for all predictors.

Predictors	**Spearman's rank correlation**					**VIF**
	Pinus sp. dune wood	Roads distance	Herbaceous dune vegetation	Sea distance	Rivers distance	
Pinus dune wood						2.56
Roads distance	0.15					1.12
Herbaceous dune vegetation	0.01	0.00				1.22
Sea distance	-0.35	-0.05	-0.6			1.43
Rivers distance	-0.07	0.17	-0.04	0.06		1.19

Chapter 2: Mapping coastal dune vegetation by a RS phenology-based mapping approach: exploring the potential of Sentinel-2

2.1. Introduction

Environmental monitoring is essential to identify and understand the structure, integrity and conservation status of different habitats forming landscape mosaics (Díaz-Delgado *et al.* 2017). Next to traditional field-based techniques (Adam *et al.* 2010), Remote Sensing (RS) methods are useful tools for ecosystems monitoring, as they are able to capture a wide range of properties of vegetation in a standard and replicable way (Lawley *et al.* 2016).

During the last few decades, satellite images have supported vegetation mapping and monitoring of wide landscapes (Xie *et al.* 2008), with a continuous improvement in spatial resolution and use of multi/hyperspectral sensors consistently boosting the performance of remotely sensed data for mapping highly fragmented areas (Adamo *et al.* 2016, Wu *et al.* 2017, Betbeder *et al.* 2015). In particular, for the interpretation of particularly complex or very fine-grained vegetation mosaics such as those commonly encountered on sand dunes, high-resolution data are an essential requirement (Rapinel *et al.* 2014, Zhang and Bass, 2012). Indeed, complex landscapes have long represented a challenge for vegetation mapping and multi-temporal monitoring applications, which still need further development (Malavasi *et al.* 13, Valentini *et al.* 2015). In this context, several space agencies (e.g., ESA, NASA/USGS, CBERS, ISRO) deliver free remotely sensed products with several resolutions that represent a reliable support for different applications of ecosystem monitoring and management. Among these, the free access Sentinel-2 mission of ESA (European Space Agency), with a 10 m spatial resolution for bands in the spectral range of the blue (B2-490 nm), green (B3-560 nm), red (B4-665 nm) and infra-red (B8-842 nm) and a revisit rate of approximately five days, represents an important support for environmental mapping in the Mediterranean area (Drusch *et al.* 2012, Chatziantoniou *et al.* 2017). The relatively recent release of Sentinel-2 mission (Sentinel-2A launched on 23 June 2016 and Sentinel-2B launched on 7 March 2017) still has several potentialities to be explored (Recanatesi *et al.* 2018).

In order to achieve their full potential for accurate mapping of complex vegetation mosaics, RS techniques must be coupled with proper approaches able to capture spatial and temporal vegetation patterns (Díaz-Delgado *et al.* 2017). For instance, the analysis of vegetation phenological properties, describing recurring biological events (e.g., seasonality, Lloyd 1990), is very effective for mapping intense seasonal biomass variations (Dudley *et al.* 105) as those characterizing Mediterranean landscapes. Among the remotely sensed data, vegetation indices, depicting ecosystem spectral properties, are very efficient tools to map vegetation and its temporal pattern (Huete 2012, Vrieling

et al. 2018). Among these, Normalized Difference Vegetation Index (NDVI, Rouse *et al.* 1973, Tucker 1979) is a good proxy of canopy biomass (Campbell and Wynne, 2011), and its application for environmental monitoring is highly appreciated (Stoms and Hargrove, 2000, Honeck *et al.* 2018). Furthermore, the monthly variation of NDVI values across an entire year proved to be a sound surrogate of ecosystem phenology (Vrieling *et al.* 2018, Pettorelli *et al.* 2005, Tomaselli *et al.* 2017), which allows for discriminating contiguous vegetation cover types featuring different seasonality (Helman *et al.* 2015, Sun *et al.* 2018, Bajocco *et al.* 2019).

Coastal dune landscapes are complex mosaics that develop in the transition zones between terrestrial and marine environments, occupying strips parallel to the seashore (van der Maarel 2003). Along the sea-inland gradient, coastal dunes are ruled by a large variety of constraining environmental conditions, such as soil salinity, substrate instability, wind and marine aerosol (Jones *et al.* 2008, Santoro *et al.* 2011, Bazzichetto *et al.* 2016). By shaping the biomass levels, this gradient determines the occurrence of a mosaic of highly specialized and diverse plant communities coexisting in a relatively narrow area which represents a hotspot of exclusive biodiversity (Bazzichetto *et al.* 2016). In spite of their high biodiversity value and complex ecosystem functioning, coastal dunes are among the most threatened ecosystems worldwide (Acosta *et al.* 2009, Schlacher *et al.* 2007). In the Mediterranean areas, the loss and degradation of coastal dune ecosystems have been particularly severe in the last few decades (Schlacher *et al.* 2007, Cori 1999, Speraniddi *et al.* 2019), with the main threats being urban expansion (Malavasi *et al.* 2013, Couch *et al.* 2007, Carranza *et al.* 2008), coastal erosion (Jolicoeur and O'Carroll, 2007) and invasion by alien species (Malavasi *et al.* 2018, Sun *et al.* 2017, Marzialetti *et al.* 2019, Janssen *et al.* 2016). In order to prevent these and other endangered habitats from further degradation, all European Member States adopted the Council Directive 92/43/EEC (hereafter Habitats Directive, HD). By signing the HD, the States committed themselves to maintain, restore and monitor habitats and species of European conservation concern (listed in dedicated annexes) and to report their conservation status every six years. Each habitat type (mainly identified by plant communities) is characterized by specific biotic and abiotic factors (Evans 2006). In this light, innovative and scientifically sound instruments are needed for setting conservation priorities and providing management indications for the coastal dune habitat types (Acosta *et al.* 2003, Carboni *et al.* 2009, Doody 2013, Dius *et al.* 2019). Until now, coastal dunes mapping procedures have mostly been based on the integration of visual interpretation (e.g., photointerpretation of aerial imagery) and floristic data (Acosta *et al.* 2005, Malavasi *et al.* 2013). However, the use of these mapping procedures presents some shortcomings in linear and fragmented ecosystems characterized by low biomass such as coastal dunes. For instance, photo-interpretation is a time-consuming procedure and its results vary depending on the subjectivity of the interpreter, his

experience and personal knowledge of mapped landscapes (Drake 1996, Green *et al.* 2000). Moreover, as small patches (below the minimum mapping area) are neglected, the photo-interpreted maps can be limited for characterizing the coastal fine scale mosaics and related landscape processes (Drius *et al.* 2013, Sperandii *et al.* 2018).

In consideration of the above, the present work sets out to explore the potential of Sentinel-2 in capturing coastal dune natural vegetation types using a phenology-based mapping approach. In particular, by a multi-temporal analysis of NDVI images of coastal dunes in central Italy, we focused on two main questions: (i) does NDVI phenological profiles allow for identifying and correctly mapping different vegetation types distributed along a coastal zonation? (ii) does the product of a phenology-based classification agree with existing coastal dunes classification systems (i.e., photo interpreted land cover maps and 92/43/EEC habitat distribution)?

2.2. Materials and Methods

2.2.1. Study Area

The study was carried out on a representative tract of the Mediterranean coast, placed in the Tyrrhenian seashore of Central Italy (Lazio Region). The study area includes ca. 250 km of sandy coast, mainly formed by recent (Holocenic) dunes (Figure 4, Acosta *et al.* 2003). These dunes are relatively simple in structure, with a single low dune ridge (lower than 10 m height) occupying a narrow strip (usually no more than 500 m with) along the seashore (Bazzichetto *et al.* 2016). In this area, coastal plant communities mostly range from pioneer vegetation near the shoreline to Mediterranean shrubs on landward fixed dunes (Acosta *et al.* 2003, Acosta *et al.* 2009). Previous studies discriminate eight different habitats occurring along this coastal zonation, of which two have been listed as priority (Table 3, Carranza *et al.* 2008, Sperandii *et al.* 2018). In the analyzed littoral zone, human activities have intensified in the course of the 20th century (Malavasi *et al.* 2013, Carranza *et al.* 2018). Specifically, during the last 60 years, the Tyrrhenian coast faced consistent processes of fragmentation (Malavasi *et al.* 2014), simplification (Acosta et al. 2003) and biodiversity loss (Malavasi *et al.* 2018). Nevertheless, the Tyrrhenian coast still hosts a good number of plant communities of conservation concern in Europe (92/43/EEC Habitats Directive; EEC, 1992) for which monitoring and conservation strategies must be improved.

Table 3. EC Habitat types (Habitat Directive 92/43/EEC) along with a brief description in terms of vegetation types. Asterisk (*) indicates habitats with high priority for conservation.

EC Habitat	Name	Vegetation Types
EC-1210	Annual vegetation of drift line (upper beach).	Pioneer annual vegetation characterizing the strandline zone of the beach.
EC-2110	Embryonic shifting dunes (embryo dune).	Pioneer, perennial community of the low embryo-dunes dominated by *Thinopyrum junceum.*
EC-2120	Shifting dunes along the shoreline with *Ammophila arenaria* (mobile dune).	Seaward and semi-permanent cordons of dune systems dominated by *Calamagrostis arenaria* subsp. *arundinacea*.
EC-2210	*Crucianellion maritimae* fixed beach dunes.	Chamaephytic community of the inland side of fixed dunes dominated by *Crucianella maritima.*
EC-2230	*Malcolmietalia* dune grasslands	Annual, species-rich community colonized by small terophytes in dry, interdunal depressions of the coast.
2250		
EC-2250*	Coastal dunes with *Juniperus* spp. (juniper scrub)	Shrub formations dominated by juniper on the fixed dunes.
EC-2260	*Cisto- Lavanduletalia* dune sclerophyllous scrubs	Shrub formations dominated by sclerophyllous species
EC-2270*	Wooded dunes with *Pinus pinea* and/or *Pinus pinaster*	Coastal dunes colonized by Mediterranean and Atlantic termophilous pines.

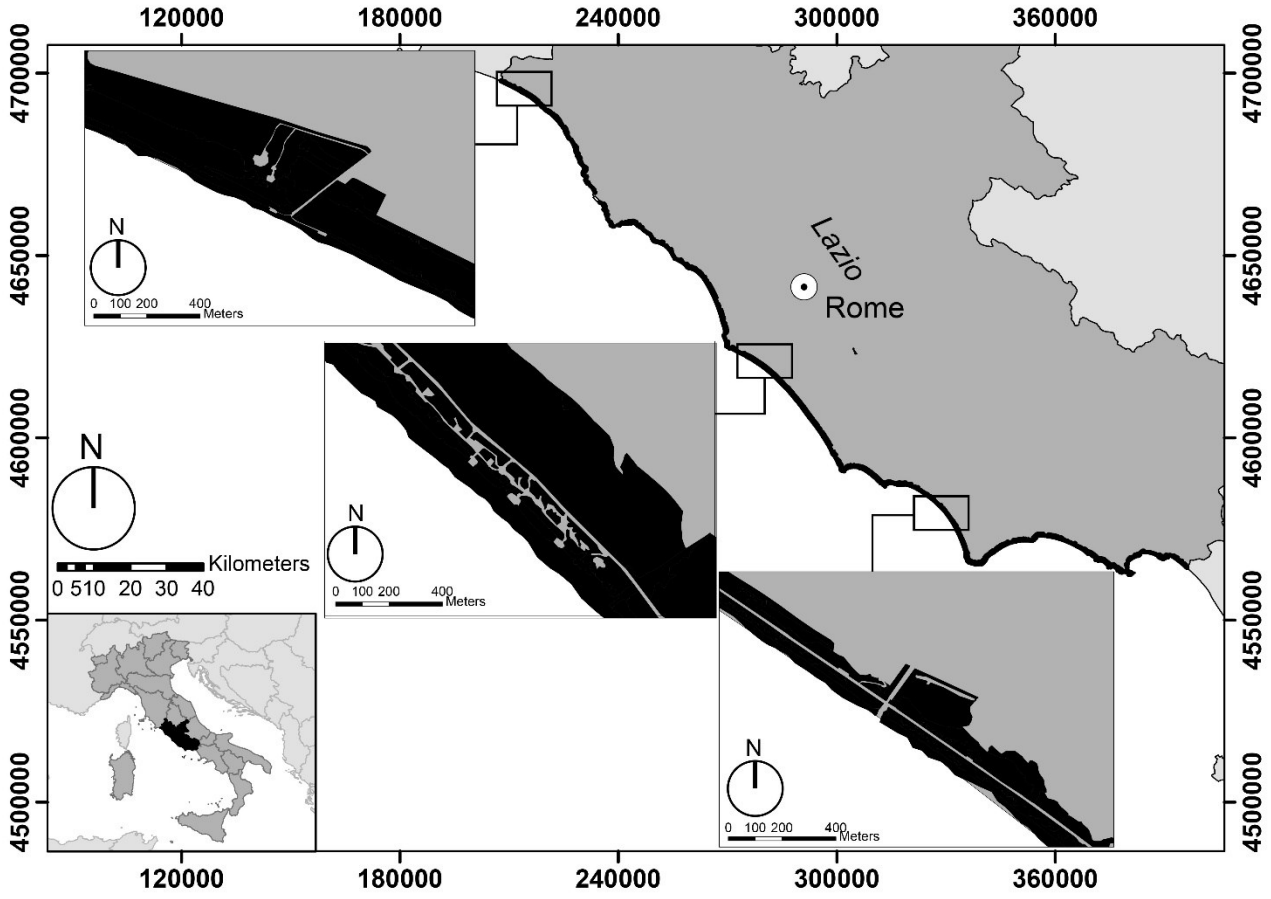

Figure 4. Study area. The coastline of the Lazio Region (Italy). Three zoomed examples at north, center and south are reported in black. Coordinates system: WGS84 UTM 33N (epsg: 32633).

2.2.2. Methodology

We performed a phenology-based classification of coastal dune ecosystem following a sequence of steps (Figure 5): (1) multitemporal dataset collection and image preprocessing, (2) NDVI calculation and data processing, (3) data classification, (4) accuracy assessment, and (5) comparison of phenology-based classes vs. previous studies.

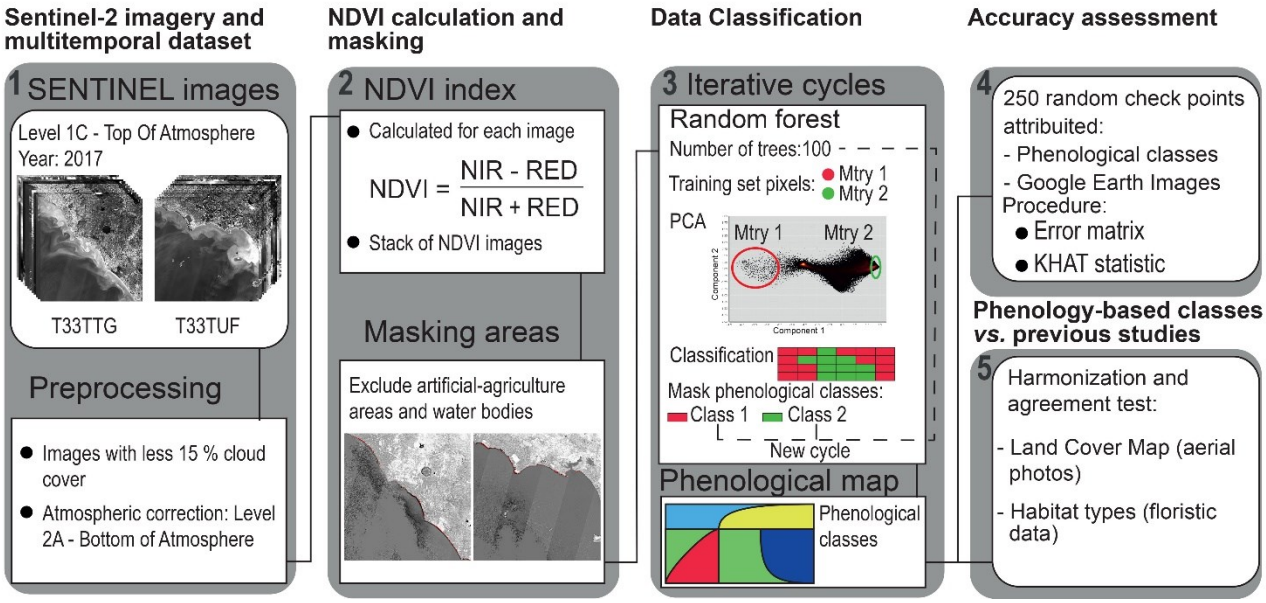

Figure 5. Workflow synthesizing the full mapping procedure of natural dune vegetation with Sentilnel-2 NDVI (Normalized Difference Vegetation Index) time series and Random Forest classification approach.

2.2.2.1. Sentinel-2 Imagery and Multitemporal Dataset

Sentinel-2 is a European wide-swath, multi-spectral imaging mission, constituted by a two-satellite platform: Sentinel-2A and Sentinel-2B (Bertini *et al.* 2012). The Multi Spectral Instrument (MSI) on-board Sentinel-2 can provide images with a temporal resolution of five days at the equator, and a 12-bit radiometric resolution from 492 nm to 1377 nm, which includes the Visible (VIS), Near Infra-Red (NIR), and Short Wave Infra-Red (SWIR) spectra (13 bands). Sentinel-2 images are freely downloadable from the Copernicus Open Access Hub (https://scihub.copernicus.eu/). In this study, we used the red band (R, around 665 nm in the VIS spectrum) and the NIR band (around 833 nm), at 10 meters of resolution (Drusch *et al.* 2012). The study area is included in two Sentinel-2 dataset tiles (T33TTG, T33TUF).

We extracted monthly NDVI images recorded in the year 2017 for the two Sentinel-2 tiles describing the analyzed coast and we built a multi-temporal dataset (stack, see Table B1 - Appendix B). For the analysis, we selected only those images with low cloud coverage (< 15%), excluding March, due to the excess in cloud coverage. The clean stack for the phenology-based classification was composed of 22 images (one per tile and month, excluding March). Only part of the downloaded data was already corrected from atmospheric noise, while the other part was rough. We corrected these others

using Sen2Cor version 2.5.5 (http://step.esa.int/main/third-party-plugins-2/sen2cor/, Luis et al. 2016).

2.2.2.2. NDVI Calculation and Masking

For the entire stack, we calculated NDVI (Equation 1) as follows:

$$\mathrm{NDVI} = \frac{\mathrm{NIR}-\mathrm{R}}{\mathrm{NIR}+\mathrm{R}}. \quad (1)$$

NDVI ranges from – 1 to 1, with increasing values related with growing photosynthetic biomass (Pettorelli *et al.* 2004). The NDVI stack was masked using a fine scale land cover map (1:5000; SITR—Sistema Informativo Territoriale Regionale Lazio) in order to exclude from the classification, at least partially, urban areas, agriculture fields and water bodies.

2.2.2.3. Data Classification

We classified the resulting NDVI stack by implementing a Random Forest algorithm (RF) with a hierarchical logic, using ESA's Sentinel-2 toolbox—ESA Sentinel Application Platform 6.0 (SNAP). RF is a machine learning classification method that operates by constructing a multitude of decision trees (Breiman 2001, Gislason *et al.* 2006). RF algorithm is widely used for classification because of its speed, stability and ability to discriminate differences (Rodriguez-Galiano *et al.* 2012, Pal 2005, Hakkenberg *et al.* 2018).

We cyclically performed different RF analyses, defining for each cycle two parameters: the training set of pixels (Mtry, see the next paragraph) and the number of trees (Ntree, in our case 100 runs per cycle). In order to maximize the efficacy of RF, in the training set, we used a number of pixels that was higher than the square root of the total of the pixels (Breiman 2001, Gislason *et al.* 2006).

In each cycle, the identification of the training set was supported by a Principal Component Analysis (PCA) of the monthly NDVI values (pixels x monthly NDVI values matrix). We projected all the pixels in the PCA1 and PCA2 ordination space (Lasaponara 2006). As objects that are close in the ordination space (similar component values) describe similar cover types (Lasaponara 2006), we therefore selected as the training set for classification the two furthest away clouds of pixels with maximum variance between them (Brown *et al.* 2014). For each tree (run), the training set was split through a bootstrapping procedure in two groups: seed pixels (*inbag*), to build the classification tree, and validation pixels (*out-of-bag*), to estimate the classification performance. Then, all pixels were compared with the *inbag* set using the *Gini* inequality index (Breiman *et al.* 1984) and assigned to a class based on the Lorenz Curve. The latter ranges from 0 (perfectly equality) to 1 (perfectly inequality, Cutler *et al.* 2007). At the end of each run, RF conferred to each pixel an ordinal vote (the minimum value of Lorenz Curve). After the entire cycle of 100 runs, each pixel was definitively

assigned to the more frequently attributed class (Breiman 2001). In each cycle, the performance of classification was assessed by repeating the classification procedure on the basis of the *out-of-bag* data and comparing both classifications (Breiman 2001, Cutler *et al.* 2007).
In each RF cycle, we classified the stack in two vegetation classes, and we carried on all the cycles where the *out-of-bag* error was <50%.

2.2.2.4. Accuracy Assessment

The accuracy of the phenology classification map was assessed through an error matrix (Table B2 – Appendix B) calculating overall accuracy (Equation B1 – Appendix B), producer's accuracy (Equation B2 – Appendix B) and user's accuracy (Equation B3 – Appendix B) and Kappa statistic ($0 \leq Kappa \leq 100$; Equation B4 – Appendix B, Congalton and Green, 2009). We based this assessment on 250 random checkpoints visually inspected on Google Earth images (Tilahun and Teferie, 2015, Mohammed and Landry, 2016, Quin *et al.* 2016). The positional errors of objects in Google Earth images are much lower compared to of the minimum spatial resolution of Sentinel-2 images (Mohammed and Landry, 2016) and their spatial resolution (~1m) is high enough to allow clear visual interpretation of the land cover (Dorai and Cardille, 2011). In our case, the random checkpoints were inspected in Google Earth images for a 5 m radius buffer area (comparable scale of the 10 m pixel of Sentinel-2 images) to limit the scale mismatch errors. We built the error matrix, reporting the assigned phenology-based class in rows, and the Google Earth visual attribution in columns.

2.2.2.5. Phenology-Based Map vs. Previous Vegetation Studies

The error matrix was further used to compare the phenology-based map with two previous studies conducted in the same area. The first study reports an actual vegetation map produced at 1:5000 scale by visual interpretation of aerial orthophotos (Malavasi *et al.* 2016) and the second one refers to the natural dune vegetation types classified according to the Habitats directive (92/43/EEC; Table 3) and identified by floristic field data (Figure B1, Figure B2 – Appendix B). To compare the phenology-based classes with the photointerpreted map, we used 250 random checkpoints, while the congruence with habitat types was tested using 135 floristic plots extracted from "RanVegDunes", a database of randomly distributed floristic surveys (Sperandii *et al.* 2017). For testing the congruence of the phenology-based classification with the existing documents, we aggregated and homogenized the classes of the vegetation map (Table B4 – Appendix B) and the habitat types (Table B5 – Appendix B) on the basis of similarities in physiognomies and ecological conditions (Kosmidou *et al.* 2014). Then, we tested the correspondence among maps and defined their respective levels of agreement through the Kappa statistic (Table B3 – Appendix B).

2.3. Results

2.3.1. Sentinel-2 NDVI Classification

The phenology-based classification allowed for identifying five vegetation classes organized in three hierarchical levels, each one characterized by a specific phenological pattern (Figure 6) referable to different mosaics of plant communities. The first level of classification distinguishes a class of Open Sand from the Vegetated class, the second level divides the Vegetation class in Herbaceous and Woody Vegetation, and the third level divides Herbaceous and Woody Vegetation classes into two further classes (the first in Sparse Herbaceous Vegetation (SHV) and Dense Herbaceous Vegetation and Ruderals (DHVR); the second in Sparse Woody Vegetation (SWV), and Dense Woody Vegetation (DWV)).

The Open Sand class (Figure 6(a)) is characterized by very low biomass. Monthly values are close to 0, except in summer, when NDVI is negative. The Open Sand class is extensively present along the whole coast as thin stripes even on quite urbanized coastal tracts.

The Sparse Herbaceous Vegetation class is characterized by low monthly NDVI values (Figure 6(b1)) that decrease towards 0 in summer. Sparse Herbaceous Vegetation is in contact with Open Sand and covers a narrow discontinuous strip of land between Open Sand and the inner vegetation classes. Sparse Herbaceous Vegetation preferentially occurs on well-preserved coastal tracts characterized by all phenology-based vegetation classes.

The Dense Herbaceous Vegetation and Ruderals class (Figure 6(b2)) is characterized by NDVI values slightly over 0.5 from November to April that decrease during summer. Dense Herbaceous Vegetation and Ruderals include a highly seasonal herbaceous vegetation. This class occurs close to the seashore in sectors exposed to environmental stress and on inner dune sectors characterized by high anthropic pressure.

The Sparse Woody class is composed by sparse evergreen vegetation (Figure 6(c1)) with high monthly NDVI values (>0.5) that slightly decrease in summer. This class tends to occur at intermediate distances from the seashore and in the inner sectors of the dune in contact with densely wooded dunes.

Lastly, the Dense Woody Vegetation class presents high monthly NDVI values (> 0.7; Figure 6(c2)) throughout the year. It occurs in the back-dune zones corresponding to dense shrublands and forests.

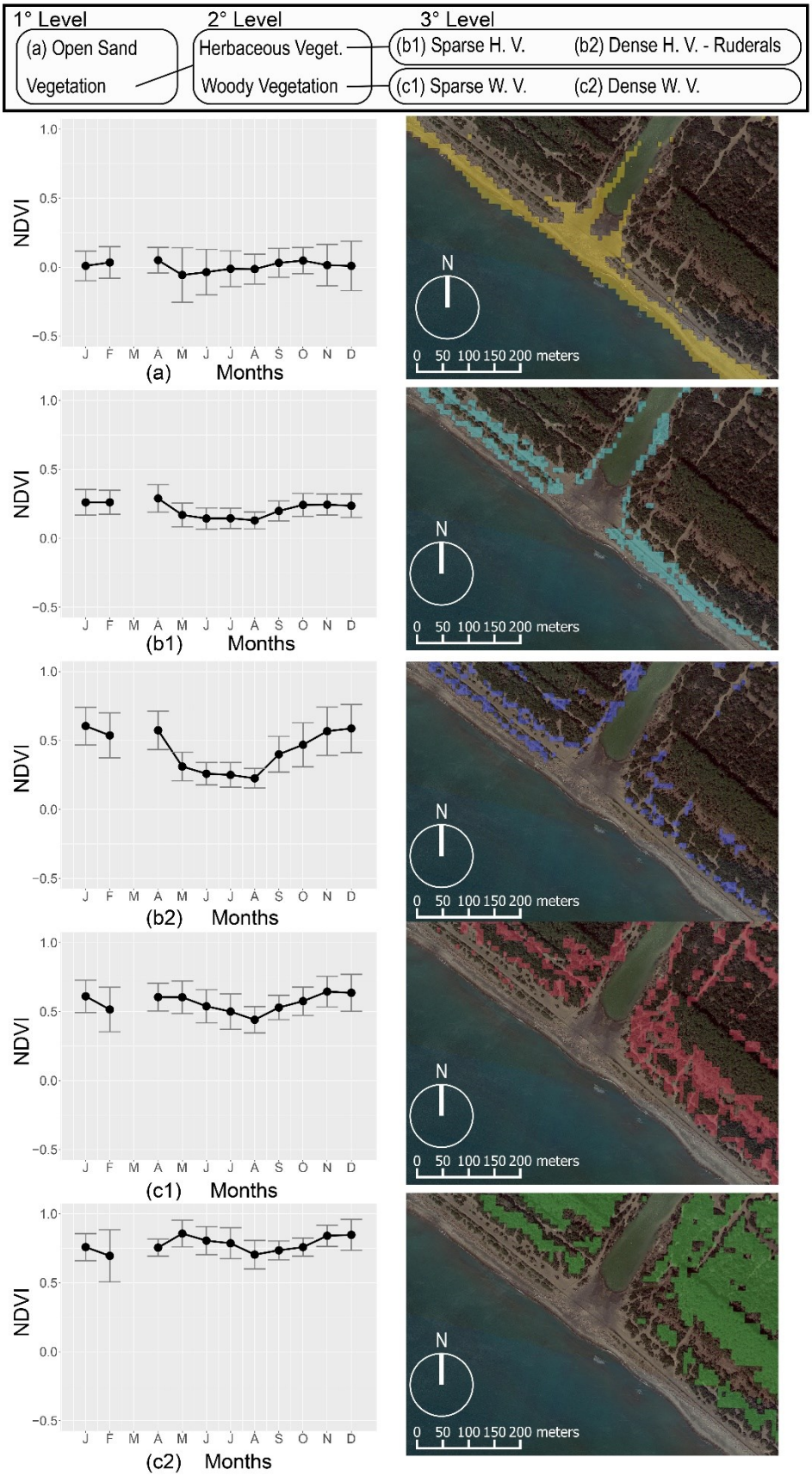

Figure 6. Cartesian diagrams (on the left) of NDVI values with average ± standard deviation (*y*-axis) for each month of the year except March (*x*-axis) of the five phenology-based classes identified by multitemporal classification of Sentinel-2 images, along with mapping examples (on the right) projected on Google Earth View.

2.3.2. Classification Accuracy Assessment

The classification of multi-temporal NDVI data (phenology-based classification) showed a good level of accuracy when compared with the visual interpretation of Google Earth images. The first level of classification (two classes: Vegetation and Open Sand) exhibited very high values of overall accuracy (96%) with both producer's and user's accuracy over 88% and Kappa statistic of 86% (Figure 7(a)). Similarly, the overall accuracy of the second hierarchical level (Herbaceous and Woody Vegetation) was high (88%) with a moderate agreement among classes and reference data given by a Kappa statistic of 79% (Figure 7(b)).

All land cover classes identified at the third level of detail evidenced values of accuracy with producer's accuracy ranging between 69% (Herbaceous Vegetation) and 99% (Woody Vegetation). Similarly, the user's accuracy ranged between 86% (Woody Vegetation) and 90% (Open Sand and Herbaceous Vegetation) (Figure 7(c)).

The correspondence between the third hierarchical level of classification and the set of Google images resulted as moderate as underlined by both overall accuracy (79%) and Kappa statistic (71%, Figure 7(c)). The producer's accuracy was adequate for all classes. In particular, Open Sand and Dense Woody Vegetation had the highest values of producer's accuracy (88% and 96%, respectively). This result defined an elevated precision of the map in these two classes. Moreover, both herbaceous classes showed moderate agreement (75% Sparse Herbaceous Vegetation, 65% Dense Herbaceous Vegetation). Finally, Sparse Woody Vegetation class featured the lowest value of producer's accuracy detected, even though the value showed moderate agreement (56%). The user's accuracy showed the higher values in Open Sand and Dense Herbaceous Vegetation classes (90% and 98%, respectively). Sparse Herbaceous Vegetation and Sparse Woody Vegetation had the lowest values (respectively 63% and 64%). Finally, Dense Woody Vegetation presented user's accuracy (75%).

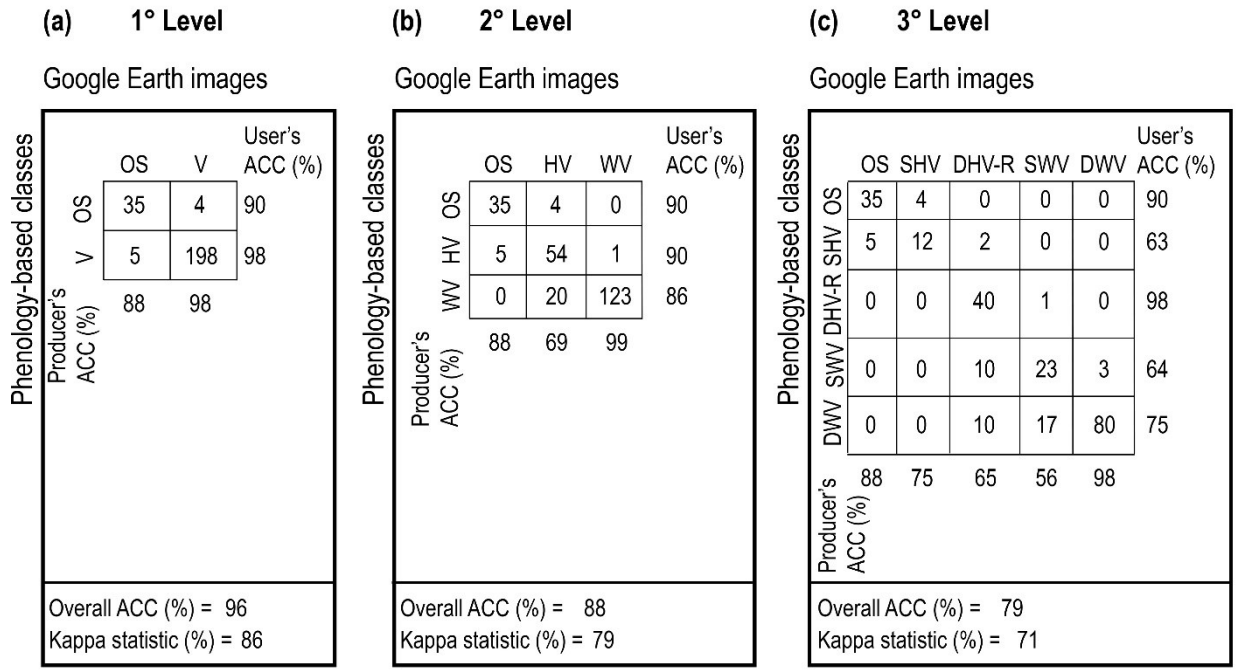

Figure 7. Error matrix, Accuracy (ACC) values, in particular Overall ACC, Producer's ACC, User's ACC, and Kappa statistic of all hierarchical levels of classification–phenology-based classes: Open Sand (OS), Vegetation (V), Herbaceous Vegetation (HV), Woody Vegetation (WV), Sparse Herbaceous Vegetation (SHV), Dense Herbaceous Vegetation (DHV-R), Sparse Woody Vegetation (SWV), and Dense Woody Vegetation (DWV).

2.3.3. Harmonization and Agreement Test with Existing Documents

The NDVI classification showed significant values of agreement with the photointerpreted map (Malavasi *et al.* 2016), and floristic field data with the habitat types (Sperandii *et al.* 2018) at both the first and the second hierarchical levels (Figure 8).

The first hierarchical level showed strong agreement values with the photointerpreted classification map, with 95% of overall accuracy and 83% of Kappa statistic (Table B6 – Appendix B), and also the producer's and user's accuracy showed high agreement values (~100%). The agreement of the second classification level resulted in being quite significant for all of the classes, with high overall accuracy (80%) and Kappa statistic (66 %) depicting a moderate congruence between them. The user's accuracy for the three classes was over 77%. The producer's accuracy ranges between 58 % and 95% (Table B7 – Appendix B).

Finally, at the third level of classification, the agreement test resulted in being moderate, with overall accuracy and Kappa statistic values being approximately 66% and 55%, respectively. However, values of user's accuracy were high only for Open Sand (94%) and Dense Woody Vegetation (85%), while the other classes showed values under 50%. The producer's accuracy ranged between 26% and 81% (Table B8 – Appendix B).

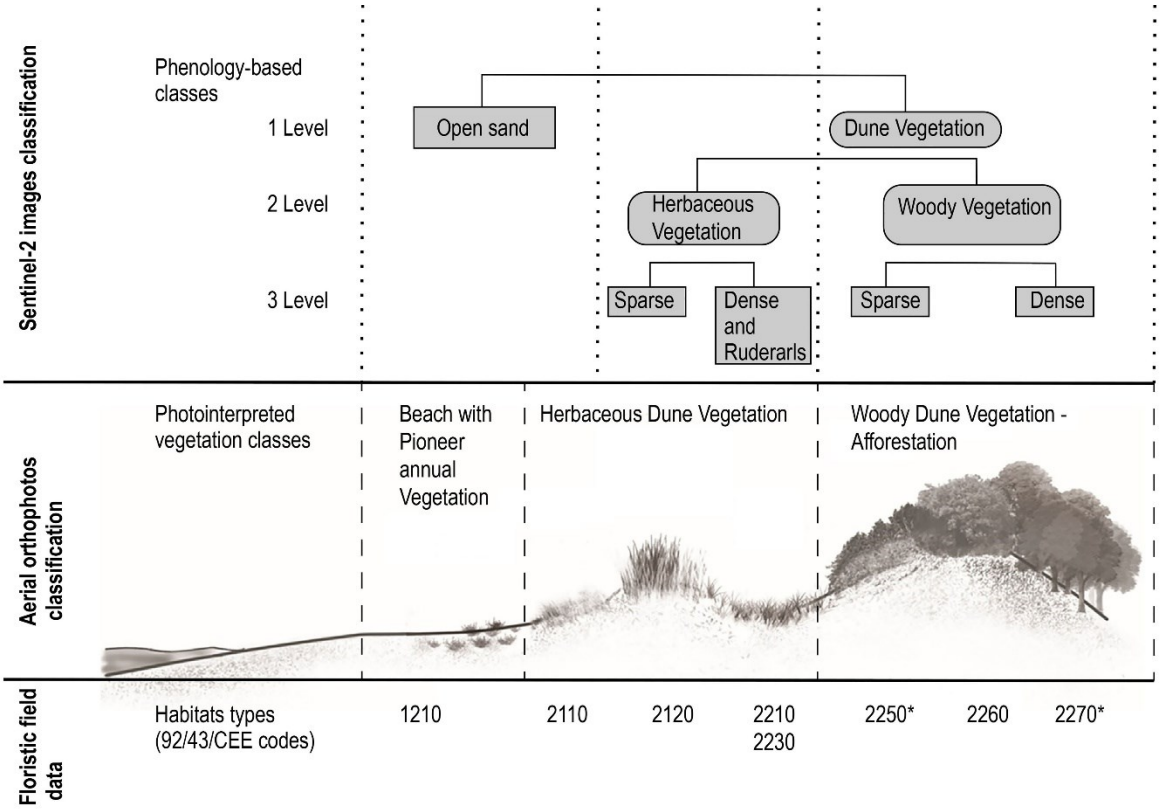

Figure 8. Cross sectional diagram indicating a typical coastal dune zonation along with their corresponding phenology-based classes, habitat types (92/43/EEC; for full habitat names see Table 3) and vegetation classes mapped in a previous study (Malavasi *et al.* 2016).

On the other hand, the agreement values of NDVI phenology-based classification and habitat types assigned by floristic data (Habitats directive 92/43/EEC) showed great differences among the hierarchical levels. At the first two levels, agreement values indicated moderate congruence between the classification systems. At the first hierarchical level, the overall accuracy was ~79% and the Kappa statistic denoted moderate agreement value. User's accuracy was relatively high for both classes, Open Sand (81%) and Vegetation (78%). Producer's accuracy ranged between 53% to 93% (Table B9 – Appendix B).

The agreement test of the second hierarchical level indicated similar consistency, with overall accuracy ~71% and moderate value for the Kappa statistic (58%). The user's accuracy was relatively high for Open Sand and Woody Vegetation (81% and 90% respectively), and the Herbaceous Vegetation manifested moderate values (62%). Similarly, producer's accuracy ranged between 53% and 84% (Table B10 – Appendix B). Finally, the third level of classification exhibited the lowest agreement values. The overall accuracy and Kappa statistic were approximately 53% and 43%, respectively. Moreover, user's accuracy was relatively high only for Open Sand (81%), and moderate agreement for Dense Herbaceous Vegetation and Ruderals (61%) and Dense Woody Vegetation (67%), with the other classes featuring values under 50%. Producer's accuracy ranged between 11% and 73% (Table B11 – Appendix B).

2.4. Discussion

Our results suggest the analysis of remote sensed data (Sentinel-2 images) by a phenology-based classification as an effective approach for monitoring natural landscapes. Sentinel-2 images confirmed their high potential for vegetation mapping (Drusch *et al.* 2012), while the multitemporal analysis of NDVI provided complementary and useful information, proving its convenience even in complex vegetation mosaics, that is to say, beyond their traditional field of application (Vrieling *et al.* 2018, Helman *et al.* 2015, Bajocco *et al.* 2019).

The phenology-based classification using a Random Forest algorithm on a Mediterranean wide coastal area allowed for identifying and mapping five vegetation classes organized in three hierarchical levels. Such classes, each one characterized by specific phenological and ecological features, exhibited high levels of accuracy and clearly depicted the coastal ecosystem zonation ranging from Open Sand, occurring near the seashore line, to Dense Woody Vegetation on the inner dunal sectors (Acosta *et al.* 2003, Forey *et al.* 2009, Belgiu and Csillik, 2018). Sparse Herbaceous Vegetation and Sparse Woody Vegetation occurred discontinuously, while Open Sand and Dense Herbaceous Vegetation and Ruderals formed a continuous strip close to the seashore running along all the analyzed coast. Finally, Dense Woody Vegetation formed regular shaped patches, and, as previously observed (Carranza *et al.* 2008, Bazzichetto *et al.* 2016), occurred in the back-dune zone.

The classification of multi temporal NDVI images, which was successfully used for land cover mapping (Helman *et al.* 2015, Belgiu and Csillik, 2018), is extended here for vegetation mapping on Mediterranean coasts. The phenological analysis that allows for depicting vegetation seasonality (Helman *et al.* 2015, Mannel and Price, 2012, Immitzer *et al.* 2016) enabled to discriminate woody evergreen from herbaceous annual vegetation (Helman *et al.* 2015). Furthermore, by exploring phenological spatial variations occurring in correspondence with biomass transitions, it was possible to distinguish between densely and sparsely vegetation formations and to identify edges (Jones *et al.* 2017, Nagendra *et al.* 2013) between vegetation classes occurring in the analyzed complex mosaic.

Our results respond to the scope of Sentinel mission (Drusch *et al.* 2012, Bertini *et al.* 2012) and give new evidence of its potential for monitoring and mapping coastal dunes with reduced costs and time efforts. The high temporal resolution that assures a continuous release of new clean and fine resolution images (~each 10 days) postulates Sentinel-2 as one of the most effective supports for phenology-based coastal dunes monitoring (Vrieling *et al.* 2018).

The good agreement between phenology-based classification and the photo-interpreted vegetation map (Malavasi *et al.* 2016) suggests the adequacy of Sentinel 2 multi-temporal NDVI classification for producing new vegetation maps of the coastal dune landscapes. Indeed, the phenology based map

is quite consistent with the photo-interpreted vegetation map (scale 1:5000) produced using panchromatic digital aerial ortho-photographs with about one meter of resolution of the year 2008. Furthermore, the hierarchical nature of RF classification offers a good basis for comparing the new remotely sensed classification with existing documents produced with different methodological procedures, data sources and spatial resolution. Linking the new remotely sensed classes with previous maps and mapping supports (as aerial photos) is essential for building a long-term ecological series and for monitoring coastal dune landscapes across time (Kosmidou *et al.* 2014, Herlod *et al.* 2006).

The agreement test of NDVI classes and floristic data referable to EC habitats (92/43/EEC) was significant at the first and second hierarchical level for all classes. At the third level, only Open Sand, Dense Herbaceous Vegetation and Ruderals, and Dense Woody Vegetation showed a relative high congruence with vegetation plots, consequently showing the possibility to discriminate the habitats included in these classes. The lower agreement of NDVI classification and vegetation plots classified in habitat types is probably related with differences in the spatial resolution between the remotely sensed instrument (10x10 m) and the field floristic plots (2x2 m). Furthermore, the Mediterranean coastal dunes, naturally conformed by fine scale ecosystem mosaics (Acosta *et al.* 2003, Acosta *et al.* 2009), are often disturbed by fragmentation processes that alter their biodiversity (Malavasi *et al.* 2018). This probably reduces the possibility of a match between conventional small floristic plots and the 10 m resolution of Sentinel-2 images. This scale mismatch is the principal restriction in this study, and the impossibility to discriminate the single habitat type through this phenology-based approach using 10 m resolution images limits its use to coarse vegetation classes (general physiognomies) (Ghimire *et al.* 2010, Xu *et al.* 2009). In coastal dunes, both subtle variations of environmental factors and human pressure promote the formation of fine scale mosaics of habitats, some of them featuring similar physiognomies but differing in their floristic composition (Thompson and Gergerl, 2008, Santoro *et al.* 202, Feagin *et al.* 2005, Battisti *et al.* 2016, Adam *et al.* 2014, Wu 2004). Implementing the proposed classification do not assure the possibility of computing the extension of habitat types with similar phenologies separately as required by the Annex I of EC habitat directive (92/43/EEC). To deal with such shortcomings, the integration of sentinel data with finer resolution data and tools are advisable. For instance, the use of multispectral satellite images with higher spatial resolution, or the implementation of other classification methodologies as spectral unmixing algorithms able to quantify the percentage of different cover classes inside the single pixels (Machín *et al.* 2018, Lucas *et al.* 2002) should improve the performance of the proposed classification procedure. In any case, the classification performance of each cycle, elaborated by out-of-bag pixels, estimated the uncertainty of the Random Forest result giving an idea of the presence of mixed pixels.

Overall, the potential of Sentinel-2 data in a phenology-based mapping was accomplished with a relative high degree of accuracy assessment and significant congruence with existing previous classifications. It is very promising in the discrimination of annual, deciduous and evergreen vegetation. Moreover, the integration of remotely sensed maps with field data could contribute to continuous update of coastal dune habitats maps, reducing costs and risks of delaying the periodical reporting requested by the Habitat Directive (92/43/EEC).

2.5. Conclusions

The performed phenology-based classification emphasizes the potential of Sentinel-2 images for mapping natural vegetation and extends its field of application to low biomass and highly fragmented systems as coastal dunes. The combined use of NDVI multi-temporal data, machine learning (Random Forest) algorithms, and a pixel-oriented approach allowed for adequately describing with high values of accuracy the complex mosaic of coastal dune vegetation.

The phenology-based classification approach with Sentinel-2 data proposed here is a time saving and more objective approach, complemented with open source earth observation data and implemented through free ESA software, effective and inexpensive instruments for coastal monitoring. Furthermore, the good levels of agreement of phenology-based with previous vegetation maps should allow for building long-term ecological series necessary for exploring and monitoring coastal ecosystems dynamics over time.

Nevertheless, there are several possibilities to improve this phenology-based classification and enhance its potential. For instance, the integration of phenological classification with LiDAR and other remotely sensed data or the implementation of spectral unmixing algorithms could improve the agreement with floristic filed data and should represent new research frontiers to explore.

From an applied perspective, the phenology-based vegetation classification provides relevant knowledge for coastal monitoring and management; therefore, we hope new studies exploring increasingly larger areas will be analyzed to further test the proposed classification and, at the same time, to provide homogeneous information for coasts in the Mediterranean.

2.6. Appendix B

Table B1: The total Sentinel-2 imagery dataset. It shows for each Sentinel-2 image the month, day, platform (Sentinel-2A or Sentinel-2B), the hour of acquisition, the cloud percentage, the processing level (top of the atmosphere – 1C or bottom of the atmosphere – 2A), and the tiles (T33TTG for Lazio north, T33TUF for Lazio south).

Month	Day	Platform	Hour	Cloud (%)	Processing Level	Tiles
January	01	S2A	10.04	0.032	1C	T33TTG
January	01	S2A	10.04	0.778	1C	T33TUF
February	10	S2A	10.01	2.730	1C	T33TTG
February	10	S2A	10.01	5.734	1C	T33TUF
March	12	S2A	10.01	93.575	1C	T33TTG
March	12	S2A	10.00	44.321	1C	T33TUF
April	11	S2A	10.00	9.905	1C	T33TTG
April	11	S2A	10.00	12.132	1C	T33TUF
May	31	S2A	10.00	0.330	2A	T33TTG
May	31	S2A	10.00	1.107	2A	T33TUF
June	21	S2A	10.00	0.661	2A	T33TTG
June	21	S2A	10.00	0.254	2A	T33TUF
July	20	S2A	10.00	0.330	2A	T33TTG
July	20	S2A	10.00	1.107	2A	T33TUF
August	09	S2A	10.00	1.276	2A	T33TTG
August	09	S2A	10.00	3.267	2A	T33TUF
September	23	S2B	10.00	11.252	1C	T33TTG
September	23	S2B	10.00	13.598	1C	T33TUF
October	13	S2B	10.00	0.107	1C	T33TTG
October	13	S2B	10.00	0.488	1C	T33TUF
November	11	S2A	10.03	0.000	1C	T33TTG
November	11	S2A	10.03	2.636	1C	T33TUF
Dicember	22	S2B	10.04	0.459	2A	T33TTG
Dicember	22	S2B	10.04	0.565	2A	T33TUF

Table B2: Example of error matrix. It is a contingency table (k x k array, where k is the number of classes in the classification).

		Google maps attribution = j			Row total
		1	2	k	n_{i+}
Mapped Classes = i	1	n_{11}	n_{12}	n_{1k}	n_{1+}
	2	n_{21}	n_{22}	n_{2k}	n_{2+}
	k	n_{k1}	n_{k2}	n_{kk}	n_{k+}
Column total	n_{+j}	n_{+1}	n_{+2}	n_{+k}	n

Equation B1. Overall accuracy, defined as the total of the correctly classified checkpoints on the total number of the checkpoints where n_{ii} indicates the number of checkpoints classified in the same category both in the satellite mapped classes and the google earth reference data, in other words the elements of the major diagonal.

$$\text{Overall accuracy} = \frac{\sum_{i=1}^{k} n_{ii}}{n}$$

Equation B2. Producer's accuracy: fraction of correctly classified checkpoints in all checkpoints of the produced classification.

$$\text{Producer's accuracy} = \frac{n_{jj}}{n_{+j}}$$

Equation B3. User's accuracy: fraction of correctly classified checkpoints in all checkpoints of the reference data.

$$\text{User's accuracy} = \frac{n_{ii}}{n_{i+}}$$

Equation B4. Kappa statistic ($\widehat{K}$) computed as follows where n_{ij} is the number of observation in row i and column j, n_{i+} and n_{+j} are respectively the total number of observation of row, and the second total number of observation of column.

$$\widehat{\mathrm{K}} = \frac{\mathrm{n}\ \sum_{\mathrm{i}=1}^{\mathrm{k}} \mathrm{n}_{\mathrm{ij}} - \sum_{\mathrm{i}=1}^{\mathrm{k}} \mathrm{n}_{\mathrm{i}+}\mathrm{n}_{+\mathrm{j}}}{n^2 - \sum_{\mathrm{i}=1}^{\mathrm{k}} \mathrm{n}_{\mathrm{i}+}\mathrm{n}_{+\mathrm{j}}} \qquad \text{(D)}$$

Table B3: Classes of Kappa statistic interpretation. The Kappa statistic is a measure of the difference between the actual agreement of real objects observable on google maps with resulted classes, and an agreement due to chance (where real objects are compared with a random classification). Kappa varies between 0 to 100, where values close to 0 represent a poor agreement, and values close to 100 are indicate as excellent level of agreement.

Kappa statistic ($\widehat{K}$) %	Agreement
< 40	Poor agreement
41 – 80	Moderate agreement
81 – 100	Strong agreement

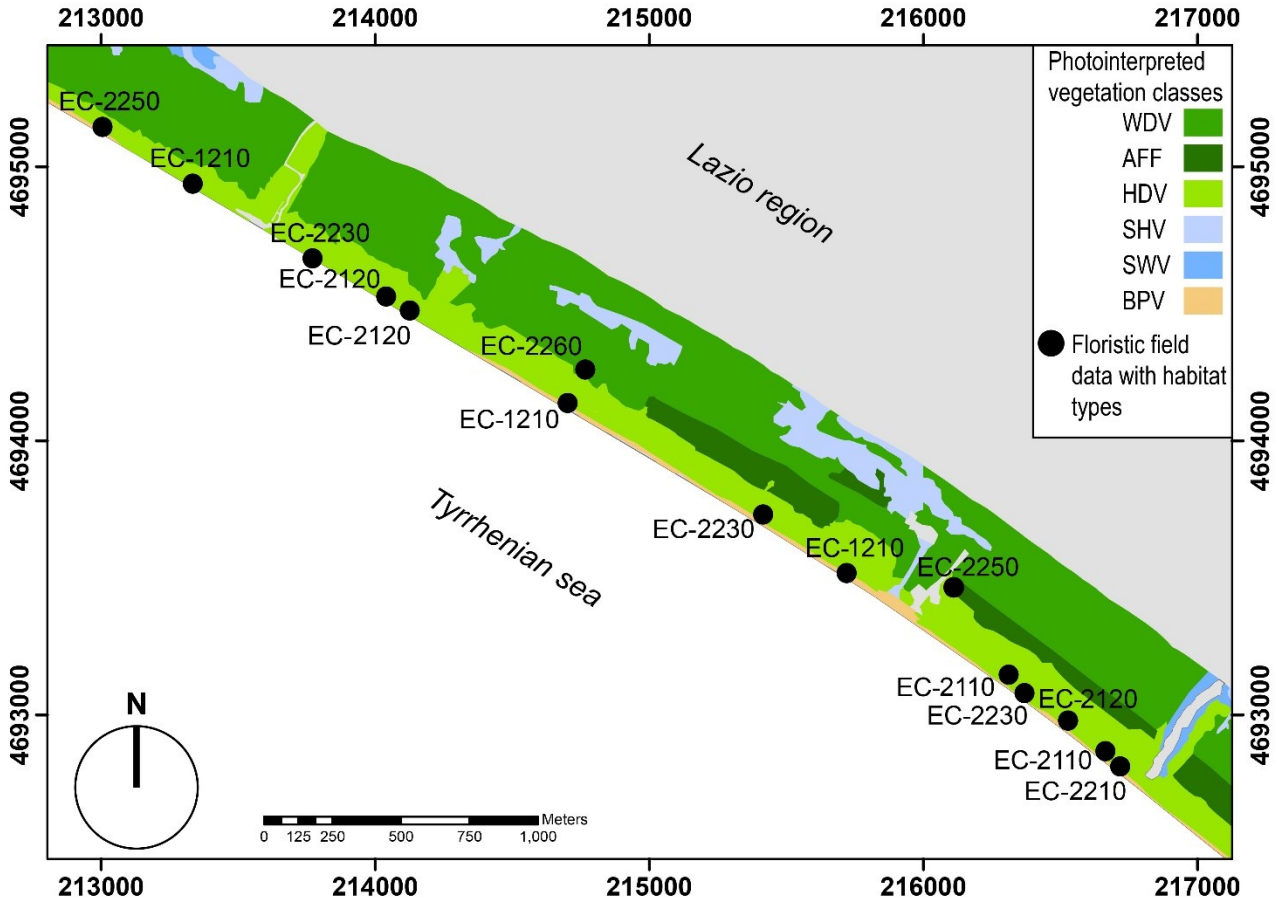

Figure B1: A subset of the photo-interpreted vegetation map produced at 1:5000 scale by visual interpretation of aerial orto-photos, and a subset of the floristic field data classified according with the Habitats directive (92/43/EEC).

Figure B2: Example of floristic field data (2x2 m plots). a) herbaceous vegetation referable to EC-2230, b), shrub vegetation refetable to the EC-2250.

Table B4: Nomenclature homogenization between the produced phenology-based map and the vegetation map.

Vegetation classes (Malavasi, et al. 2016)	**Abbreviation**	**Detailed description**
Beach with pioneer annual vegetation	BPV	Annual, nitrophilous and ephemeral community, exposed to wind disturbance and flooding - Habitat type: EC-1210.
Herbaceous dune vegetation	HDV	Pioneer perennial and halophilous community, dominated by dune-forming plants with low vegetation cover and poor sandy substrate - Habitat type: 2110. Perennial herb community growing on mobile dunes, dominated by the rhizomatous tussock grass (*Calamagrostis arenaria* subsp. *arundinacea*) – Habitat type: 2120. Perennial herbs community, partially sheltered from winds and dominated by chamaephytic species – Habitat types: EC-2210, EC-2230.
Semi-natural herbaceous ruderal vegetation	SHV	Semi-natural herbaceous vegetation, communities with different degrees of degradation or recolonization.
Semi-natural woody vegetation	SWV	Semi-natural woody vegetation: bushy vegetation with scattered trees.
Woody dune vegetation	WDV	Woody dune vegetation growing on fixed dunes. Scrubs with sparse junipers on coastal sand dunes, and evergreen *macchia* dominated by shrub species with high cover values and less exposed to the harsh coastal conditions – Habitat types: EC-2250, EC-2260.
Mediterranean Forest	BMF	Forests dominated by oaks and other broadleaf evergreens – Habitat types: EC-9340.
Afforestation	AFF	Wooded dunes with *Pinus pinea* and/or *Pinus pinaster* – Habitat type: EC-2270.

Level	**Vegetation classes (Malavasi, et al. 2016)**	
1°	BPV.	HDV, SHV, SWV, WDV, BMF, AFF.

2°	BPV.	HDV, SHV.		SWV, WDV, BMF, AFF.	
3°	BPV.	HDV.	SHV.	WDV.	SWV, BMF, AFF.

Table B5. Nomenclature homogenization of the EC habitats (92/43/EEC) types: 1210 (Annual vegetation of drift lines), 2110 (Embryonic shifting dunes), 2120 (Shifting dunes along the shoreline with *Calamagrostis arenaria* subsp. *arundinacea*), 2210 (*Crucianellion maritimae* fixed beach dunes), 2230 (*Malcolmietalia* dune grasslands), 2250 (Coastal dunes with *Juniperus* spp.), 2260 (*Cisto-Lavanduletalia* dune sclerophyllous scrubs), 2270 (Wooded dunes with *Pinus pinea* and/or *P. pinaster*).

Level	**Natura 2000 habitat types**				
1°	EC-1210, EC-2110.	EC-2120, EC-2210, EC-2230, EC-2250, EC-2260, EC-2270.			
2°	EC-1210, EC-2110.	EC-2120, EC-2210, EC-2230.	EC-2250, EC-2260, EC-2270.		
3°	EC-1210, EC-2110.	EC-2120, EC-2210.	EC-2230.	EC-2250.	EC-2260, 2270.

Table B6. Results of the harmonization test (error matrix and Kappa statistic) between phenology-based classes in the first hierarchical level of classification and the photo–interpretation by Malavasi et al. 2016.

		Vegetation classes (Malavasi *et al.* 2016)		
		BPV	HDV-SHV- SWV-WDV-BMR-AFF	User's accuracy (%)
Phenology-based classes	Open Sand	35	6	85
	Vegetation	5	199	98
	Producer's accuracy (%)	88	98	

Overall accuracy (%) = 95; $\breve{K}$ (%) = 83

Table B7. Results of the harmonization test (error matrix and Kappa statistic) between phenology-based classes and the photo–interpretation by Malavasi et al. 2016 in the second hierarchical level of classification.

		Vegetation classes (Malavasi *et al.* 2016)			
		BPV	HDV-SHV	SWV-WDV-BMR-AFF	User's accuracy (%)
Phenology-based classes	Open Sand	33	6	0	85
	Herbaceous vegetation	5	52	6	83
	Woody vegetation	0	32	109	77
	Producer's accuracy (%)	87	58	95	

Overall accuracy (%) = 80; $\breve{K}$ (%) = 67

Table B8. Results of the harmonization test (error matrix and Kappa statistic) between phenology-based classes in the third hierarchical level of classification and the photo–interpretation by Malavasi et al. 2016.

		Vegetation classes (Malavasi *et al.* 2016)					
		BPV	HDV	SHV	WDV	SWV- BMR-AFF	User's accuracy (%)
Phenology-based classes	OS	34	6	1	0	1	94
	SHV	2	7	7	1	0	44
	DHVR	0	1	30	6	3	42
	SWV	0	2	21	11	8	33
	DWV	0	0	13	15	70	85
	Producer's accuracy (%)	81	41	75	26	71	

Overall accuracy (%) = 66; $\breve{K}$ (%) = 55

Table B9. Results of the harmonization test (error matrix and Kappa statistic) between phenology-based classes in the first hierarchical level of classification and habitats of conservation concern (Habitats Directive; 92/43/EEC; table 1) assigned on 2m floristic plots collected in the field.

		Complex of dune habitats		
		EC-1210, EC-2110	EC-2120, EC-2210, EC-2230, EC-2250, EC-2260, EC-2270	User's accuracy (%)
Phenology-based classes	Open Sand	26	6	81
	Vegetation	23	80	78
	Producer's accuracy (%)	53	93	

Overall accuracy (%) = 79; $\breve{K}$ (%) = 50

Table B10. Results of the harmonization test (error matrix and Kappa statistic) of between phenology-based classes in the second hierarchical level of classification and habitats of conservation concern (Habitats Directive; 92/43/EEC; table 1) assigned on 2m floristic plots collected in the field.

		Complex of dune habitats			
		EC-1210, EC-2110	EC-2120, EC-2210, EC-2230	EC-2250, EC-2260, EC-2270	User's accuracy (%)
Phenology-based classes	Open sand	26	6	0	81
	Herbaceous vegetation	23	45	3	62
	Woody vegetation	0	5	27	90
	Producer's accuracy (%)	53	83	84	

Overall accuracy (%) =73; $\tilde{K}$ (%) = 58

Table B11. Results of the harmonization test (error matrix and Kappa statistic) between phenology-based classes in the second hierarchical level of classification and habitats of conservation concern (Habitats Directive; 92/43/EEC; table 1) assigned on 2m floristic plots collected in the field.

		Complex of dune habitats					
		EC-1210, EC-2110	EC-2120, EC-2210	EC-2230	EC-2250	EC-2260, EC-2270	User's accuracy (%)
Phenology-based classes	OS	26	2	4	0	0	81
	SHV	21	16	11	1	1	32
	DHV-R	2	4	14	1	2	61
	SWV	0	0	2	1	6	11
	DWV	0	0	1	6	14	67
	Producer's accuracy (%)	53	73	44	11	61	

Overall accuracy (%) =53; $\tilde{K}$ (%) = 43

Chapter 3: Vegetation mapping based on within-year Remote Sensed spectral diversity. An application using the spectral Rao's Q temporal diversity on coastal dune landscapes.

3.1. Introduction

The increasing impact of human activities and the derived environmental transformations (i.e. climate and land-cover change, invasive species and habitat loss) are promoting changes in global biodiversity at unprecedented rate in human history (Allan *et al.* 2015, Mantyka-Pringle *et al.* 2015, Oliver *et al.* 2015). The effects of such changes are particularly severe on coastal dune landscapes (Brown and McLachlan, 2002, Defeo *et al.* 2009), despite the fact that they host a highly specialized biodiversity (Martínez and Psuty 2008) and provide essential benefits to society (Martínez *et al.* 2007, Drius *et al.* 2019).

Coastal dunes are found at the boundary between continents and seas representing unique transitional mosaics hosting highly dynamic habitats undergoing frequent and substantial changes in physical extent and environmental conditions. Along with this typical transitional condition, seasonality also plays a pivotal role in such ever-changing nature, affecting both abiotic (e.g. magnitude and intensity of weather and sea conditions) and biotic (e.g. phenology) factors, whose interaction finally gives rise to an extremely dynamic and complex mosaic of psammophilous plant communities, bare surfaces and water surfaces (Hesp 1991, Acosta *et al.* 2003). Moreover, being highly endangered, coastal dunes are of conservation concern worldwide and as such, they need updated monitoring and mapping protocols (Henle *et al.* 2013, Janssen *et al.* 2016). Such protocols, traditionally based on field biodiversity data and habitat photointerpretation of aerial imagery (Acosta *et al.* 2005, Malavasi *et al.* 2013), have improved in the last decades with the support of remote sensed images and biomass spectral information (e.g. Brownett and Mills, 2017). Nonetheless, in order to better discriminate between different types of standing biomass, remote sensing approaches for habitat mapping and monitoring in coastal areas are conventionally performed through classification of images captured at the peak of the plant growing season [but see Marzialetti *et al.* 2019). That said, developing an efficient mapping protocol that accounts for the dynamic nature of coastal systems, thus capturing all main components of coastal dune mosaic together with their seasonal variation (i.e. vegetation, bare surfaces and water surfaces, Doody 2013), still represents a challenge for delivering more accurate and viable maps.

At present, the availability of remotely sensed data at various spatial, spectral and temporal resolutions, offers a great potential to carry out accurate and cost-effective studies accounting for ecosystem phenology and seasonality (Williams *et al.* 2017, Tonkin *et al.* 2017, Gómez *et al.* 2016), thus reinforcing this research field which traditionally relies on ground-based observations (Senf *et*

al. 2015, Lou *et al.* 2016). The analysis of remotely sensed phenological trends may effectively support land cover classification and mapping (Mannel and Price, 2012, Knight *et al.* 2006). In addition, this potential is steadily growing with the continuous improvement of the temporal resolution of orbiting satellites (Drusch *et al.* 2012, Wulder *et al.* 2015).

The remotely sensed analysis of seasonality, traditionally based on spectral bands (Hill *et al.* 2010, Rapinel *et al.* 2019), has been improved over time by including the time-series analysis of spectral indices (Gómez et al. 2016). Several metrics have been proposed to quantify environmental seasonality and vegetation phenology based on remotely sensed data (Noormets 2009). Such metrics commonly focus on describing the cyclic behavior of spectral indices, intended as the combination of spectral reflectance from two or more bands indicating the relative abundance of features of interest, and on identifying key transition dates (e.g. start, peak, end, and length of seasonal periods, Donohue *et al.* 2009). Additionally, other indices considering the whole array of available bands and used in the past for describing spectral diversity across space, have been recently extended to quantify variations in diversity across time (Rocchini *et al.* 2019, Torresani *et al.* 2019). Among them, the Rao's Q index, borrowed from community and landscape ecology (Ricotta et al. 2000, Ricotta and Moretti, 2011, Ricotta and Carranza, 2013), is able to take into account both the proportion of cells assuming different spectral values and their spectral distance (Rocchini *et al.* 2017). Consequently, extending Rao's Q rationale to the temporal dimension (e.g. comparing spectral values and distances of a given location in a multi-temporal stack), makes it a good candidate to accurately synthesize ecosystems seasonality. The calculation of Rao's Q on a temporal stack generates a new layer of temporal diversity with high or low values indicating seasonal or stable habitats respectively. Several diversity layers summarizing temporal stacks (bands or spectral indices) can be combined instead of the rough spectral values traditionally used on multi-temporal classification (Rocchini *et al.* 2017, Marzialetti et al. 2020). As far as we know, few studies, if any, extending Rao's Q to the spectral temporal diversity for land cover mapping currently exists in transitional systems.

In this context, the present work sets out to provide and test a land cover classification approach specifically designed for coastal landscapes based on the within-year temporal diversity, computed through Rao's Q index. In particular, the within-year diversity will be calculated upon the seasonal behavior of three spectral indices properly describing the main components of the coastal mosaic (i.e. vegetation, bare surfaces and water surfaces). Such behavior will be then classified to provide a map of natural and seminatural land cover types. While accounting for the dynamic/temporal dimension highly characterizing coastal landscape, we expect that such approach will provide a high level of classification accuracy.

3.2. Materials and Methods

3.2.1. Study area

The study was carried out on the Adriatic coast of Central Italy (Molise region, Figure 9). This area, of approximately 9000 km^2, is mainly composed of sandy beaches, few river mouths and channels and, one rocky promontory. Dunes, occupying a narrow strip parallel to the seashore, are low and relatively recent (formed in the Holocene period, Acosta *et al.* 2009, Carranza *et al.* 2008).

Along a sea-to-inland gradient, the typical vegetation zonation ranges from embryonic dunes in the seashore, followed by mobile dunes with perennial herbaceous vegetation, fixed dunes covered by evergreen shrub and small sclerophyllous trees and, in the inner sectors, by wooded dunes covered by coniferous forests (Figure 9, Stanisci *et al.* 2007, Drius *et al.* 2013). The Molise coast hosts several ecosystems of conservation concern in Europe (European Directive 92/43/EEC). For this reason, such area is largely included in the European Natura2000 system (Stanisci *et al.* 2014) and is part of the European LTER monitoring network (Long Term Ecological Research network, Drius *et al.* 2013, Prisco *et al.* 2016).

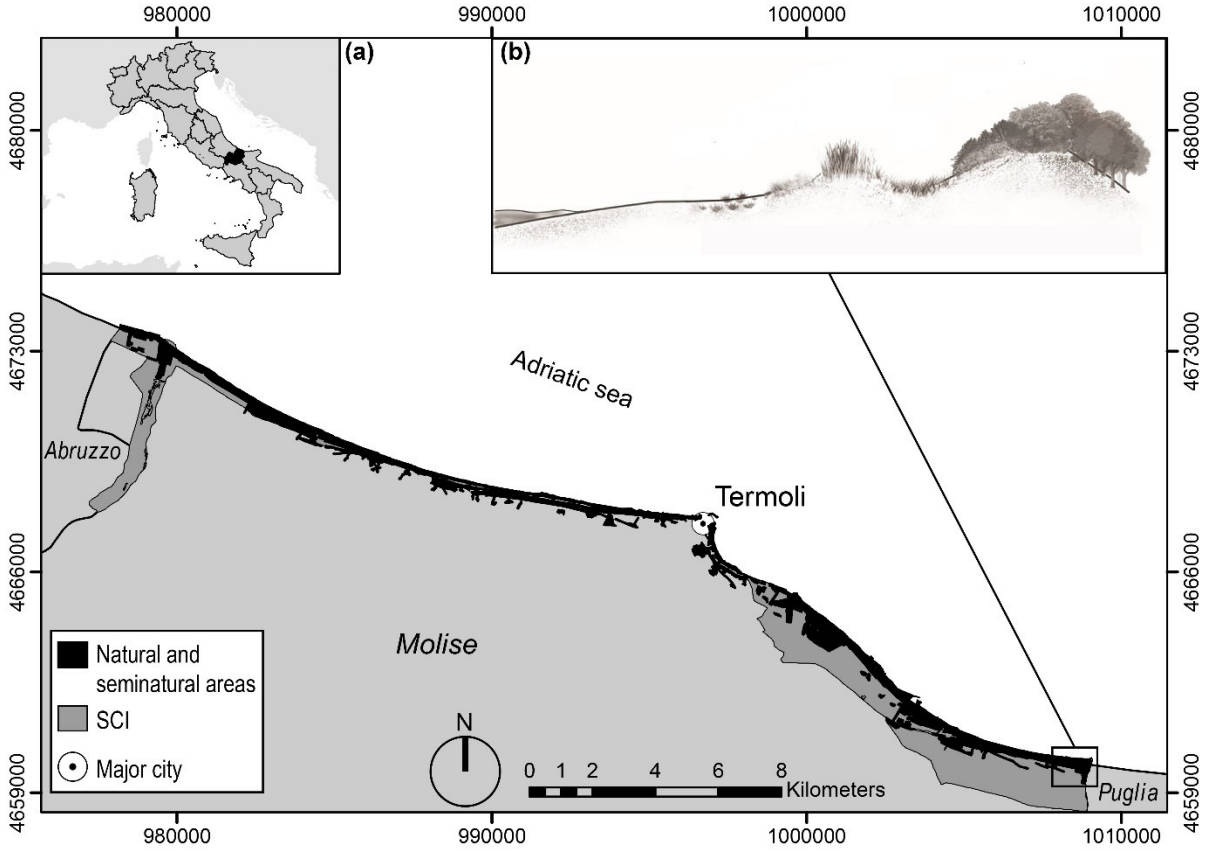

Figure 9. a) In black the study area including the coastal dunes of Molise Region (Italy). Most of the analyzed coastal sectors are included in Sites of European Conservation Concern (SCI, European Directive 92/43/EEC): Foce Trigno-Marina di Petacciato (IT7228221); Foce Biferno-Litorale di Campomarino (IT7222216); Foce Saccione-Bonifica Ramitelli (IT7222217) and belong to the European LTER network. b) An example of coastal zonation. Reference system WGS84 UTM32 (epsg: 32632).

3.2.2. Methodology

We followed an unsupervised approach and classified coastal dune natural and semi-natural land cover types through a hierarchical cluster analysis. The classes identified in the clustering phase were then used as the response variable in a Random Forest (RF) model (an accurate learning method for discriminating differences among classes (Gislason et al. 2006, Pal 2005), in order to quantify their accuracy and to predict their occurrence in the study area. In particular, the procedure was organized in the following steps: (1) Sentinel-2 imagery selection; (2) spectral indices calculation and temporal variability computation; (3) variables selection and classification; (4) accuracy assessment (Figure 10).

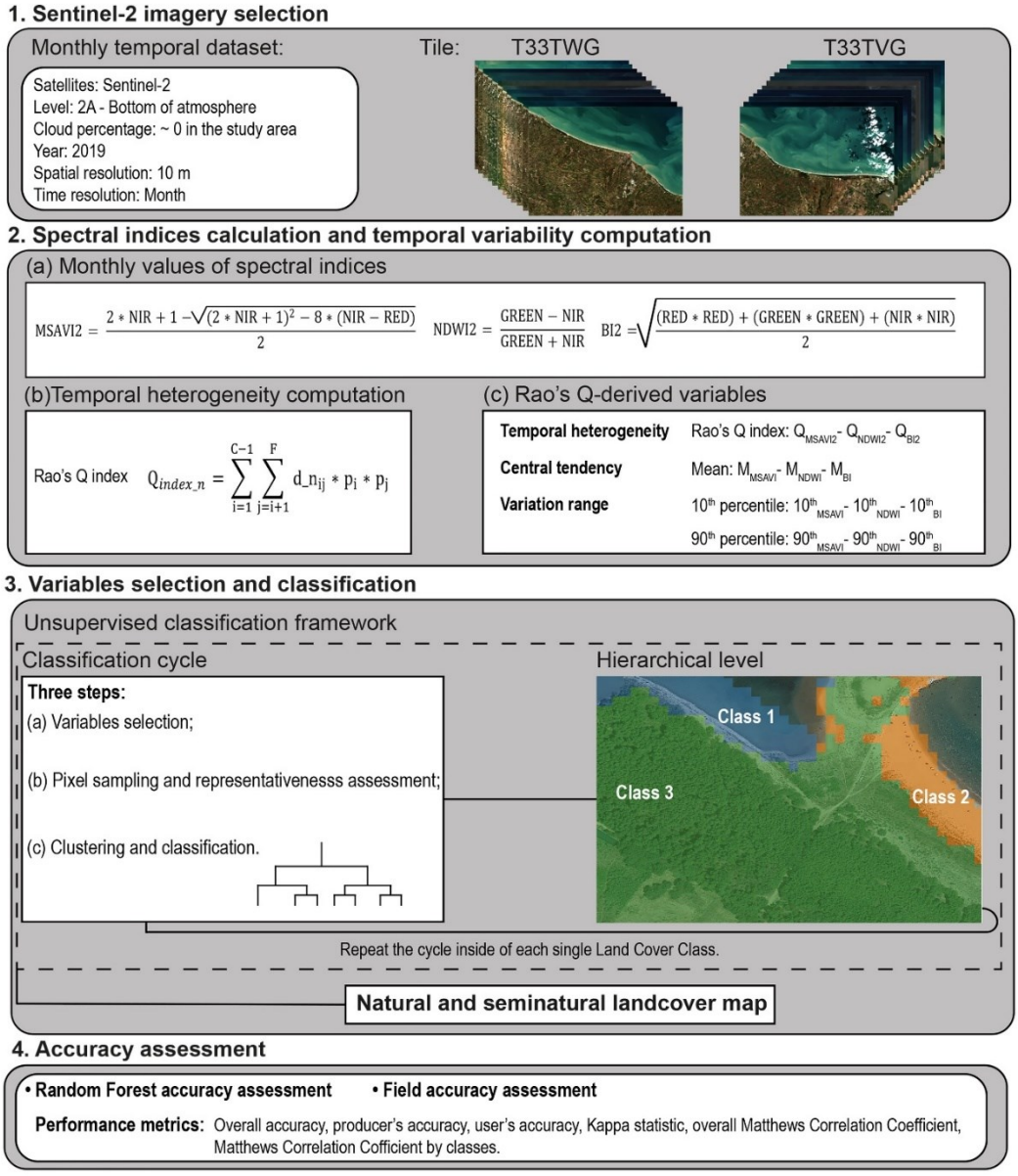

Figure 10. Workflow synthesizing the full mapping procedure of coastal dune Semi-natural and natural cover types with temporal MSAVI2, NDWI2, BI2 series and Random Forest classification approach.

3.2.2.1. Sentinel-2 imagery selection

We used Sentinel-2 mission images as a sound support for land monitoring (Berger *et al.* 2012), with a good spatial (10, 20 or 60 m), temporal (revisit time of 2-3 days at mid-latitudes) and spectral (13 bands ranging from 400 nm to visible to 2400 nm) resolutions (Drusch *et al.* 2012). Multispectral images of Sentinel-2 satellites were downloaded from Copernicus Open Access Hub (https://scihub.copernicus.eu/) at the level of bottom of atmosphere (Level-2A), and used to build a monthly temporal dataset for the year 2019. As the study area falls in two tiles (T33TVG, T33TWG), we selected 24 images (12 for tile) of each month with low cloud coverage (< 5%, Table C1 - Appendix C). All images were atmospherically corrected by ESA through "sen2cor" processor algorithm (Figure 10, box 1, Main-Knorn *et al.* 2017). We specifically used Green band, with wavelength 560 ± 36 nm; Red band, with wavelength 665 ± 31 nm, and NIR band, with wavelength 833 ± 106 nm with 10 meters of resolution.

3.2.2.2. Spectral indices calculation and temporal variability computation

For each image, we calculated three spectral indices: Modified Soil Adjusted Vegetation Index 2 (MSAVI2), Normalized Difference Water Index 2 (NDWI2) and Brightness Index 2 (BI2), as they are good indicators of vegetation biomass, the presence of water surfaces, and bare surfaces, respectively (Figure 10 box 2 a, Table 4).

MSAVI2 is a vegetation index that quantify the photosynthetic biomass based on Red and NIR bands (Table 4). MSAVI2 has been developed for mapping landscapes characterized by high percentages of bare surfaces (Rondeaux *et al.* 1996, Qi *et al.* 1994) and its spatial behavior is a good support for land classification (Wu *et al.* 2016). MSAVI2 ranges from -1 (absence of biomass vegetation) to 1 (maximum of biomass vegetation) with higher values indicating higher percentages of photosynthetic biomass (Qi *et al.* 1994).

NDWI2 is a water index useful to identify water surfaces, exploiting the Green and NIR bands (Table 4). NDWI2 is a remotely sensed index particularly efficient for identifying water surfaces and for mapping water-land transitions (Adam *et al.* 2010, Maglione *et al.* 2014). NIR band and Green band present opposite reflectance values behaviors and NDWI2 values range from -1 to 1 where values greater than 0 indicate water surfaces (McFeeters 1996).

BI2 index is sensitive to soil brightness, hence it quantifies the bare surfaces through the square root of brightness of each pixel (Table 4, Escadafal 1989). BI2 accurately discriminates the bare surfaces from vegetation in heterogeneous environments (Todd et al. 1998, Timm and McGarigal, 2012). The minimum value of BI2 is 0 and indicates the absence of bare surfaces, as growing positive values correspond to increasing percentages of bare surfaces.

We used ESA's Sentinel-2 toolbox—ESA Sentinel Application Platform 7.0 (SNAP) for index calculation.

Table 4. Spectral indices selected for analyzing the temporal diversity, serving as proxies of seasonality in vegetation biomass, presence of water surfaces, and bare surfaces.

Acronym	Name	Formula	index of	References
MSAVI2	Modified Soil Adjusted Vegetation Index 2	$MSAVI2 = \frac{2*NIR+1-\sqrt{(2*NIR+1)^2-8*(NIR-RED)}}{2}$	photosynthetic biomass	Qi *et al.* 1994
NDWI2	Normalized Difference Water Index 2	$NDWI2 = \frac{GREEN-NIR}{GREEN+NIR}$	presence of water surfaces	McFeeters 1996
BI2	Brightness Index 2	$BI2 = \sqrt{\frac{(RED*RED)+(GREEN*GREEN)+(NIR*NIR)}{3}}$	presence of bare surfaces	Escadafal 1989

For each spectral index, we built an annual stack containing the 12 month values (i.e. $MSAVI2_{2019}$, $NDWI2_{2019}$, $BI2_{2019}$), standardized between 0 and 1 to make them comparable (Milligan and Cooper, 1988). To summarize the within-year heterogeneity of ecological conditions (e.g. biomass, water surfaces and bare surfaces yearly variation), we calculated the temporal Rao's Q index for each annual stack (Figure 10 box 2 b). The Rao's Q index has recently been borrowed from functional ecology and successfully applied in remote sensing contexts as an innovative measure of spectral heterogeneity (Rocchini *et al.* 2017). Such proposed version of temporal Rao's Q index accounts for both the relative abundances of the values assumed by a given pixel *n* throughout the temporal stack (e.g. 12 months), and the Euclidean distances among pixel' numerical values.

The Rao's Q diversity index was applied on each annual stack (i.e. $MSAVI2_{2019}$, $NDWI2_{2019}$, and $BI2_{2019}$) according to the following formula (Equation 2, Rocchini *et al.* 2010, Rao 1982):

$$Q_{index\_n} = \sum_{i=1}^{C-1} \sum_{j=i+1}^{F} d\_n_{ij} * p_i * p_j \quad (2)$$

where:

Q_{index_n} = Rao' *Q* quantifying the within-year variability of a spectral index ($MSAVI2_{2019}$, $NDWI2_{2019}$ or $BI2_{2019}$) for the pixel *n*

p = relative abundance of the index value assumed by the pixel *n* within a temporal stack

i = month *i*

j = month *j*

d_n_{ij} = distance between the month i-th and j-th index value of pixel *n* ($d_{ij} = d_{ji}$ and $d_{ii} = 0$)

As similarly done in spectral diversity applications, Rao's Q adapted to detect temporal diversity quantifies the expected dissimilarity between two combinations of pixel values randomly selected

within a pixel temporal stack (Figure 11). Pixels representing highly seasonal cover types (e.g. deciduous or annual formations) are characterized by a pronounced within-year variability of biomass values and bare surfaces cover. Therefore, such pixels should assume high temporal Rao's Q values. On the contrary, pixels representing temporal stable coastal areas (e.g. open sand, pine wood) portraying weak or absent seasonal variations, should score low Rao's Q values. The temporal Rao's Q for each spectral index (Q_{MSAVI2}, Q_{NDWI2}, Q_{BI2}) was computed through R package 'spacetimerao' 0.1 (Bascietto 2018).

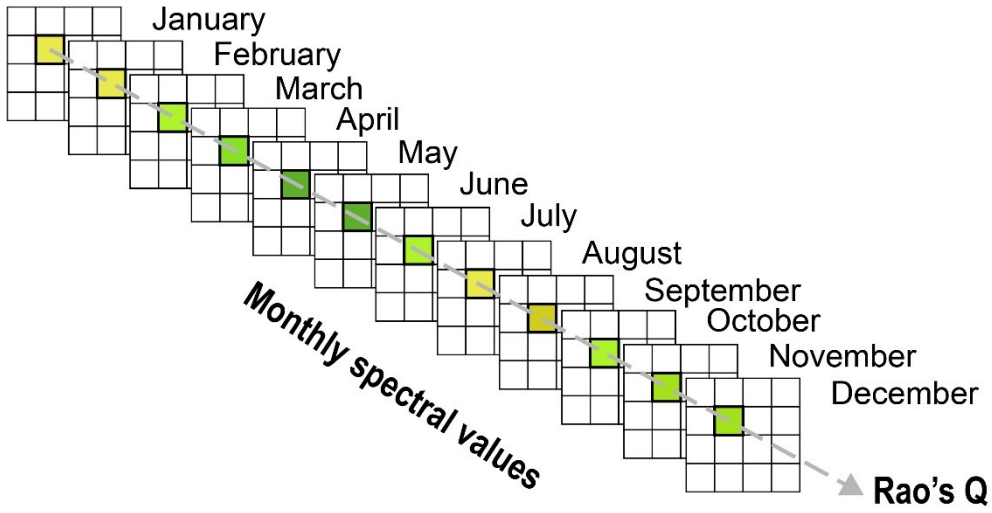

Figure 11. Schematic representation of temporal Rao's Q diversity calculation implemented on year stacks of spectral indices MSAVI2, NDWI2, BI2 to summarize the seasonal behavior of vegetation biomass, water and bare soil surfaces on coastal dunes.

In order to summarize the range of annual variation for each index, we also calculated their mean values (M_{BI2}, M_{MSAVI2}, M_{NDWI2}), along with 10^{th} and 90^{th} percentiles (10^{th}_{BI2}, 10^{th}_{MSAVI2}, 10^{th}_{NDWI2}, 90^{th}_{BI2}, 90^{th}_{MSAVI2}, 90^{th}_{NDWI2}, Figure 10 box 2 c).

3.2.2.3. Variables selection and Classification

The classification phase was implemented through consecutive cycles, each structured into three steps (Figure 10 box 3). Each step consists of a sequence of procedures: a) variables selection, b) pixel sampling and representativeness assessment, c) clustering and classification. As covariates for classification, we used 12 variables, which describe the temporal heterogeneity (Q_{MSAVI2}, Q_{NDWI2}, Q_{BI2}), the central tendency (M_{MSAVI2}, M_{NDWI2}, M_{BI2}), and the variation range (10^{th}_{MSAVI2}, 10^{th}_{NDWI2}, 10^{th}_{BI2}, 90^{th}_{MSAVI2}, 90^{th}_{NDWI2}, 90^{th}_{BI2}) of the three spectral indices (i.e. MSAVI2, NDWI2, BI2).

a) Variables selection

During each cycle, the 12 covariates were checked for their multicollinearity (Graham 2003) using the Variance Inflation Factor (VIF, Figure 10 box 3 a). VIF quantifies the multiple correlation of a variable with respect to all the other variables through linear regressions (Zuur *et al.* 2010). As VIF values greater than 5 indicate multicollinearity problems (Chatterjee and Hadi, 2012), we retained for the analysis the variables with VIF < 5 (Montgomery *et al.* 2012).

b) Pixel sampling and representativeness assessment.

To reduce the computational costs, we run the classification process on a subset of pixels randomly extracted from the study area. In particular, classification was carried out on a 20%-pixel sample and the results were extrapolated throughout the entire study area using RF algorithm. The degree of extrapolation on values of covariates lying outside the RF calibration range was assessed through the Multivariate Environmental Similarity Surface, (MESS, Figure 10 box 3 b, Elith et al. 2010). MESS quantifies the similarity of all the pixels in the study area with respect to the covariates of the extracted 20% sample used for classification. Low MESS values indicate a high similarity between covariate values of calibration and prediction pixels, suggesting a high representativeness of the former. In each classification cycle, we indicated the percentage of highly dissimilarity pixels (MESS value < 0).

c) Clustering and Classification

The random sample of pixels was classified through a hierarchical cluster analysis using the Ward's minimum variance method (Ward 1963), that minimizes the cluster internal variability using the sum-of-squares (Legendre and Legendre, 2012, Murtagh and Legendre, 2014). We used as distance the Bray-Curtis dissimilarity metric (Bray and Curtis, 1957, Goslee 2010) measured as follows (Equation 3)

$$BC_{pq} = \frac{\sum_{i=1}^{n} | x_{pi} - x_{qi} |}{\sum_{i=1}^{n} (x_{pi} + x_{qi})} \quad (3)$$

Where BC_{pq} is the Bray-Curtis dissimilarity between pixels (p, q), x_{pi} are the values of the n selected remote sensed variables (e.g. Q_{MSAVI2}, M_{NDWI2}, 90^{th}_{BI2}) on pixel p and x_{qi} the variables value on pixel q. BC_{pq} ranges from 0 when pixels are identical, and 1 when the pixels are completely different (Ricotta and Podani, 2017).

On each cycle, we identified the optimal number of classes (form from 2 to 10 classes; Table C2 - Appendix C) by calculating three indices (Silhouette index – Kaufman and Rousseeuw, 2015; Calinski-Harabasz index – Calinsky and Harabasz 1974 and Davies-Bouldin index – Davies and

Bouldin, 1979) on the just built hierarchical cluster. The selected indices summarize two cluster characteristics: the compactness of classes (e.g. how closely pixels are grouped inside a class), and the separation between classes (e.g. how the classes are different from each other).

The classes identified in the clustering phase were used as response variable in a RF model (R package 'caret' 6.0-85; Breiman 2001, Breiman *et al.* 1984, Kuhn *et al.* 2020) in order to evaluate their accuracy, to extrapolate the classification throughout all the pixels of the study area, and to evaluate the variables contribution in defining such classes. To optimize RF parameters, we set a high number of uncorrelated decision trees (*Ntree* = 1000, Kattenborn *et al.* 2019, Colditz 2015, Lawrence *et al.* 2006), while testing different combinations of the number of variables randomly selected at each node (*Mtry* parameter) and split rules (Noi and kappas, 2018, Belgiu and Drăgut, 2016, Gastwirth 1972, Geurts *et al.* 2006), then choosing the combination that yielded the highest Kappa statistic value. Specifically, we tested *Mtry* values ranging from 2 to the total number of variables in the cycle based, and Gini index and Extra-Trees algorithm as possible split rules.

Once identified the optimal RF model, it was used to predict the membership of all the study area pixels to one of the classes identified in the clustering phase. Moreover, we estimated the relative variables importance (Cutler *et al.* 2007).

At the end of each cycle, we repeated the three steps (variables selection, pixel sampling and representativeness assessment, clustering and classification) inside the classified land cover classes.

The final classes predicted by the classification phase were then interpreted in terms of coastal cover types through an expert based approach based on field detection and visual interpretation of high resolution aerial images (~1m).

3.2.2.4. Accuracy Assessment

The RF predictive accuracy was assessed by an internal 10-fold cross validation and an independent validation based on 300 random checkpoints. We selected 300 points as to assure a minimum standard number of 20 control points for each land cover class (Congalton and Green, 2009). In the independent accuracy assessment, we compared the assignment of the checkpoints according with the land cover classes obtained by satellite classification with their description obtained from field observations and the visual inspection on Google Earth images. Because of the differences in spatial resolution between Sentinel-2 (10x10 m) and Google Earth images (~1m), we focused our visual inspection on circular buffer areas of 5-meter radius (10 meters' diameter) around each check point (Rwang and Ndambuki, 2017, Matthews 1975, Boughorbel *et al.* 2017, Bekkar *et al.* 2013). In both accuracy assessments, we calculated the same performance metrics. We built a confusion matrix and calculated percentage of overall accuracy, producer's accuracy, user's accuracy and Kappa statistic (Congalton and Green, 2009). Moreover, we calculated the Matthews Correlation Coefficient both

overall and for each land cover class (Dorais and Cardille, 2011). This coefficient is widely used to evaluate the accuracy of classifications (Mohammed and Landry, 2016), as it proved reliable to evaluate the accuracy of classification when the classes have different sizes; its range by -1 to 1 and values close to 1 represents a perfect accuracy (Tilahun and Teferie, 2015).

3.3. Results

3.3.1. Unsupervised Classification

We obtained seven land cover classes after three classification cycles, which are organized in two hierarchical levels, with marked differences in temporal diversity values and in the range of the spectral indices (Figure 12 and 13). During the first classification cycle, we identified the first hierarchical level including three classes (see Table 5, Figure C1 – Appendix C): Water (W), Sand (S), and Vegetation (V, Figure 12, Table 5). The second and third classification cycles established the second hierarchical level in which sand and vegetation clusters were split in two and four classes respectively (see Table 5). Particularly, the second RF cycle applied to Sand class (S) identified two categories (Table 5, Figure C2 – Appendix C): Water Edge (WE) and Open Sand (OS; Figure 12 and 13). The WE class represents the sea-land transition including the inter-tidal area, while OS includes dry sand dunes partially covered by sparse annual vegetation. In the third cycle, RF split the class Vegetation (V) in four categories (Table 5, Figure C3 – Appendix C): Mobile Dune Herbaceous Vegetation (MDHV), Fixed Dune Herbaceous Vegetation with Sparse Shrub (FHVSS), Evergreen Woody Vegetation (EWV), and Deciduous and Humid Herbaceous Vegetation (DHHV, Figure 12 and 13). Since we focused on terrestrial cover types, we did not explore the presence of sub-classes inside Water class (Table 6). For each cycle, RF showed extremely low MESS values, suggesting no extrapolations effect on models predictions throughout the study area. These outcomes evidenced that the selected pixels for each classification cycle are representative of the study area.

Table 5. Description of classification cycles (1°, 2°,3° cycles) in terms of the optimal number of classes (Op. num. classes) according with Silhouette (S), Calinski-Harabasz (CH), Davies-Bouldin (DB) indexes); the MESS values (%); the selected variables according with VIF selection, the variables importance in the definition of classes and the obtained cover classes (Classes). Q_{NDWI2}: temporal Rao of NDWI2, Q_{BI2}: temporal Rao of BI2, Q_{MSAVI2}: temporal Rao of MSAVI2, 10^{th}_{NDWI2}: 10th percentile of NDWI2, 10^{th}_{BI2}: 10th percentile of BI2, 90^{th}_{BI2}: 90th percentile of BI2, 90^{th}_{MSAVI2}: 90th percentile of MSAVI2, M_{MSAVI2}: mean of MSAVI2.

Cycle	**1° cycle**			**2° cycle**			**3° cycle**		
Op. num. classes	S	CH	DB	S	CH	DB	S	CH	DB
	3	3	3	2	2	3	4	4	3
MESS (%)	0.0005			0.0020			0.0003		
Variables	Variable selection	VIF	Variable imp. (%)	Variable selection	VIF	Variable imp. (%)	Variable selection	VIF	Variable imp. (%)
	10^{th}_{NDWI2}	2.30	63	Q_{MSAVI2}	1.73	63	10^{th}_{BI2}	2.89	33
	10^{th}_{BI2}	2.09	22	Q_{BI2}	1.39	26	Q_{MSAVI2}	1.32	32
	Q_{NDWI2}	3.03	11	90^{th}_{BI2}	1.78	11	Q_{BI2}	2.40	26
	Q_{BI2}	2.78	4	90^{th}_{MSAVI2}	1.16	0	Q_{NDWI2}	1.92	9
	Q_{MSAVI2}	1.34	0				M_{MSAVI2}	3.17	0
Classes	Water (W)			Water Edge (WE)			Mobile Dune Herbaceous V. (MDHV)		
	Sand (S)			Open Sand (OS)			Fixed Dune Herbaceous V. with Shrubs (FDHVS)		
	Vegetation (V)						Evergreen Woody V. (EWV)		
							Deciduous and Humid Herbaceous V. (DHHV)		

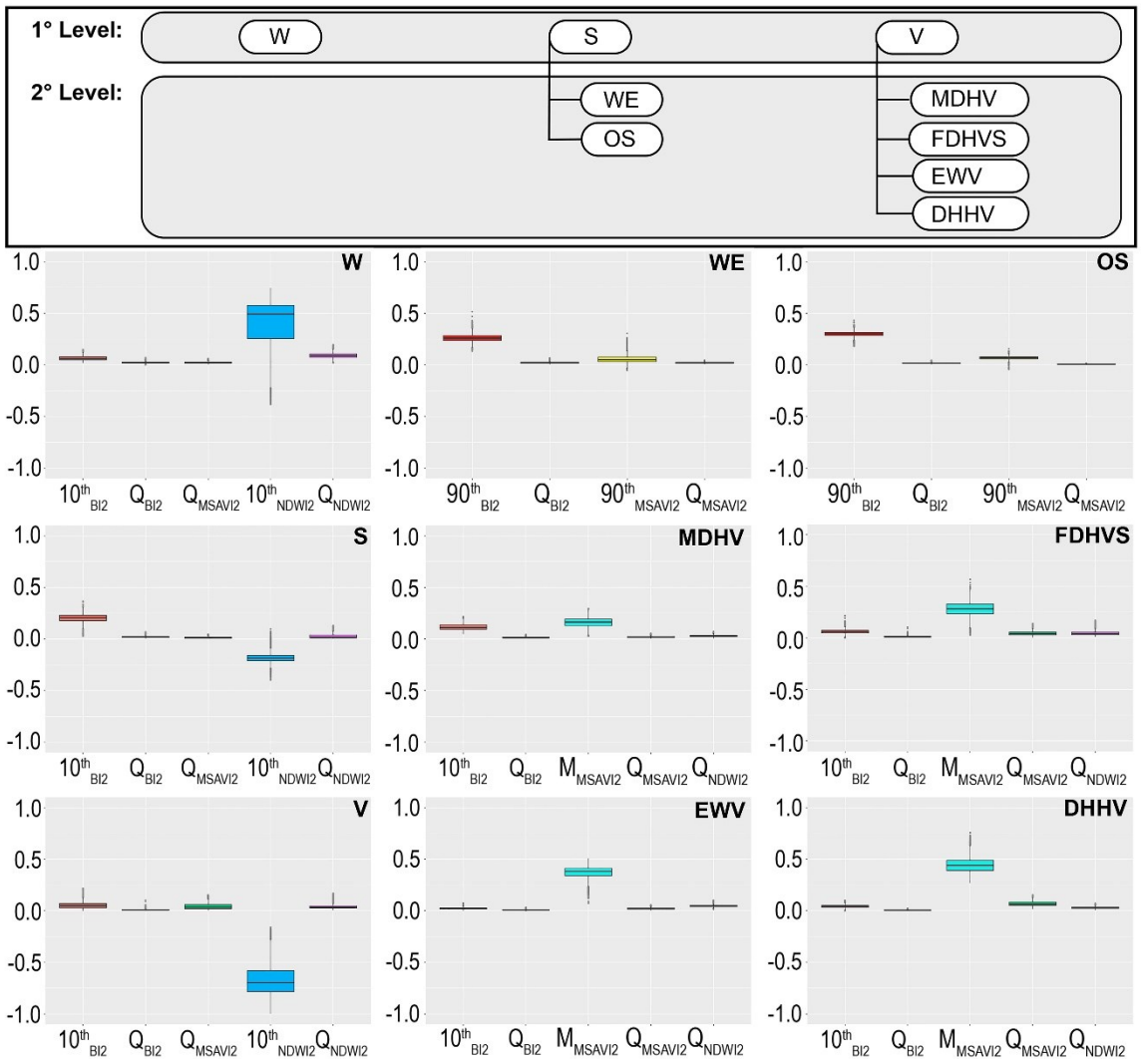

Figure 12. Scheme of the obtained natural and semi-natural cover classes (in the top) along with the respective boxplots showing variables values. Reported variables are those selected by VIF analysis and used for classification on each cycle. Classes are: Water (W), Sand (S), Vegetation (V), Water Edge (WE), Open Sand (OS), Mobile Dune Herbaceous Vegetation (MDHV), Evergreen Woody Vegetation (EWV), Deciduous and Humid Herbaceous Vegetation (DHHV), Fixed Dune Herbaceous Vegetation with Sparse Shrub (FHVSS). Variables are Q_{NDWI2}*:* temporal Rao of NDWI2, Q_{BI2}*:* temporal Rao of BI2, Q_{MSAVI2}*:* temporal Rao of MSAVI2, 10^{th}_{NDWI2}*:* 10th percentile of NDWI2, 10^{th}_{BI2}*:* 10th percentile of BI2, 90^{th}_{BI2}*:* 90th percentile of BI2, 90^{th}_{MSAVI2}*:* 90th percentile of MSAVI2, M_{MSAVI2}*:* mean of MSAVI2.

3.3.2. Accuracy Assessment

In all the three cycles, RF results achieved very high accuracy values according to both cross-validation and field assessments (Table 6).

For the first cycle, the overall accuracy, Kappa statistic and MCC indicate an almost perfect agreement under both assessments (Table 6). Similar results were obtained also by performance metrics by land cover classes. In the field accuracy assessment, both user's and producer's accuracy values in all classes are high, with the Sand class accuracy resulting lower than 90% (Table C3 – Appendix C). The second classification cycle reported cross-validation performances of 99% for overall accuracies, 96% for Kappa statistic, and 0.98 for Matthews Correlation Coefficient, while the performance assessed through the field assessment is slightly lower (overall accuracy: 87%, Kappa

statistic: 72%, Matthews Correlation Coefficient: 0.66, Table 6). All performance metrics by land cover classes calculated through cross-validation indicate an almost perfect agreement, whereas the comparison of the natural and semi-natural land cover map between the field and visual inspection shows a decrement of accuracy (Table C4 – Appendix C). Indeed, the Water Edge class evidences an almost perfect agreement only for the Producer's accuracy, while the agreement of User's accuracy and Matthews Correlation Coefficient show a substantial agreement (Producer's accuracy: 96.67, User's accuracy: 72.22, Matthews Correlation Coefficient: 0.66, Table C4 – Appendix C). The Open sand class displays a higher agreement than the previous class and only for the Matthews Correlation Coefficient the agreement downs to under 0.70 (Table C4 – Appendix C). Finally, the performance of third classification cycle results very high under cross-validation assessment, with all metrics above 95% (overall accuracy: 97%, Kappa statistic: 96%, Matthews Correlation Coefficient: 0.96), while in the field accuracy assessment, the overall metrics show a substantial agreement (Table 6). Similar to the previous cycles, all land cover classes were accurately predicted, as showed by cross-validation results (Table C5 – Appendix C).

Table 6. The percentages of overall accuracy assessment values for three classification cycles, in particular Overall accuracy (O ACC), Kappa statistic (K), overall Matthews Correlation Coefficient (O MCC). In the Random Forest accuracy assessment is indicated the mean values and standard deviation for the overall performance metrics.

1° classification cycle					
Random Forest accuracy assessment					
O ACC (%)	99.61 ± 0.14	K (%)	99.31 ± 0.25	O MCC	0.993 ± 0.002
Field accuracy assessment					
O ACC (%)	96	K (%)	92.47	O MCC	0.925
2° classification cycle					
Random Forest accuracy assessment					
O ACC (%)	99.03 ± 0.05	K (%)	97.95 ± 1.12	O MCC	0.980 ± 0.011
Field accuracy assessment					
O ACC (%)	87.50	K (%)	72.09	O MCC	0.656
3° classification cycle					
Random Forest accuracy assessment					
O ACC (%)	97.38 ± 0.38	K (%)	96.49 ± 0.52	O MCC	0.965 ± 0.005
Field accuracy assessment					
O ACC (%)	82.80	K (%)	76.50	O MCC	0.735

In the field accuracy assessment, the user's accuracy of all classes shows substantially good performances, with the metrics values resulting higher than 75%, especially in Mobile Dune Herbaceous Vegetation class (Table C5– Appendix C). Equally, in the producer's accuracy all classes show a substantial agreement, and the values are higher than 70%, indeed the values range from the minimum of substantial agreement (73%) in Deciduous and Humid Herbaceous Vegetation to the maximum of almost perfect agreement (93%) in Fixed Dune Herbaceous Vegetation with Shrubs (Table C5– Appendix C).

3.3.3. Variables importance

Among the most important variables in the first RF cycle, the 10th percentile of NDWI2 (10^{th}_{NDWI2}) showed a 63% importance, followed by the 10th percentile of BI2 (10^{th}_{BI2}) with 22%, the temporal Rao of NDWI2 (Q_{NDWI2}, 11%), and the temporal Rao of BI2 (Q_{BI2},4%). Water class (W) is characterized by high values of 10^{th}_{NDWI2} and Q_{NDWI2} (Figure 12) and includes the sea, rivers, channels and wetland. In such class, the 10^{th}_{BI2} shows overall low values and variability, while Q_{BI2} and Q_{MSAVI2} are close to zero. These features are also evident inspecting the annual trend of each of the three spectral indices (MSAVI2, NDWI2 and BI2; Figure 13). For the Water class, NDWI2 values are above 0.5 in all months. BI2 and the NDWI2 values are always lower than 0.25 and 0, respectively.

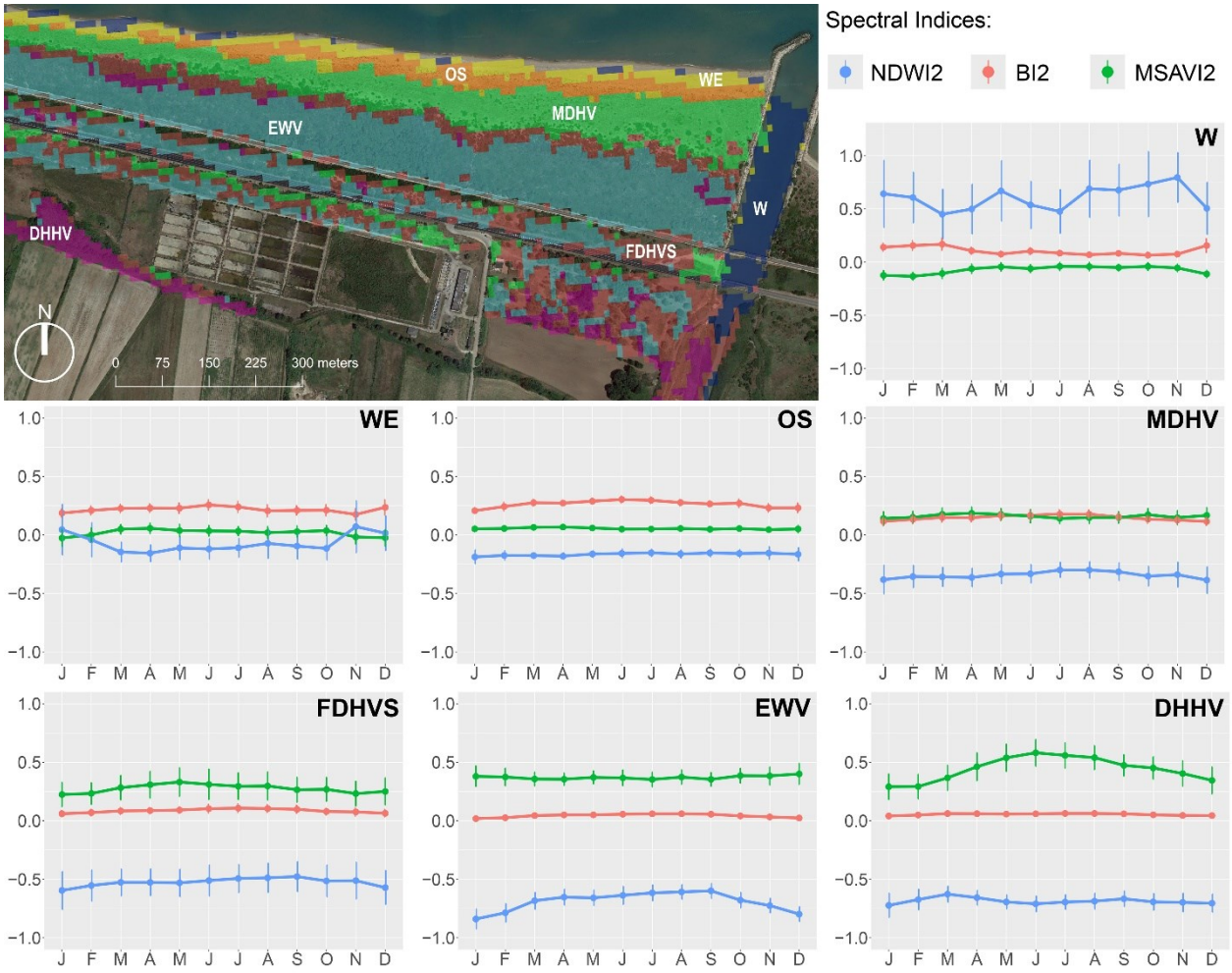

Figure 13. An example of the obtained land cover map reporting classes projected on Google Earth View (on the top) along with monthly average values of NDWI2, BI2, and MSAVI2 ± standard deviation. Water (W), Sand (S), Vegetation (V), Water Edge (WE), Open Sand (OS), Mobile Dune Herbaceous Vegetation (MDHV), Fixed Dune Herbaceous Vegetation with Shrub (FDHVS), Evergreen Woody Vegetation (EWV), Deciduous and Humid Herbaceous Vegetation (DHHV).

The most important variables in the second RF cycle are temporal Rao of MSAVI2 (63%, Q_{MSAVI2}) followed by temporal Rao of BI2 (26%, Q_{BI2}) and the 90th percentile of BI2 (11%, 90^{th}_{BI2}, Table 5).

Water Edge and Open Sand showed similar trends in annual spectral indices (Figure 12, 13), only differing in the upper values of brightness (90^{th}_{BI2}), which is higher in Open Sand. Open Sand shows higher BI2 values in summer (Figure 12), and lower variability in the upper values of biomass (90^{th}_{MSAVI2}, Figure 12).

The most important variables in the third RF cycle are the lower values of bare surfaces (10^{th}_{BI2}, 33%) and the temporal variability of biomass (Q_{MSAVI2}, 32%) and of bare surfaces (Q_{BI2}, 26%, Table 5). Mobile Dune Herbaceous Vegetation (MDHV, Figure 12 and 13) is characterized by high values of bare surfaces (high 10^{th}_{BI2} and low Q_{BI2}) and moderate values of biomass (low M_{MSAVI2} and low Q_{MSAVI2}). The MSAVI2 index profile depicts a mosaic of bare sand with sparse open perennial and annual vegetation that corresponds to coastal herbaceous vegetation referable to mobile dunes (Figure 13). Fixed Dune Herbaceous Vegetation with Shrubs (FDHVS, Figure 12 and 13) is characterized by a strong seasonality (intermediate M_{MSAVI2} and very high Q_{MSAVI2}), intermediate biomass values and moderate presence of bare surfaces (moderate 10^{th}_{BI2} and Q_{BI2}) and water (moderate Q_{NDWI2}). The FDHVS corresponds to herbaceous vegetation with shrubs growing on fixed dunes and dune slacks, more inland respect to the previous class to ruderal vegetation. Evergreen Woody Vegetation (EWV, Figure 12 and 13) is characterized by high biomass values, a low seasonality (intermediate M_{MSAVI2} and very low Q_{MSAVI2}) and almost absent bare surfaces (very low 10^{th}_{BI2} and Q_{BI2}). EWV includes the Mediterranean maquis, pine woods and shrubs and woody evergreen formations. Deciduous and Humid Herbaceous Vegetation class (DHHV, Figure 12 and 13) is characterized by high biomass values and pronounced phenology (very high M_{MSAVI2} and very high Q_{MSAVI2}), as well as moderate bare surfaces occurrence (moderate 10^{th}_{BI2} and Q_{BI2}). The DHHV includes herbaceous and woody vegetation of humid areas close to river mouths, riparian vegetation and residual patches of lowland woods.

3.4. Discussion

In this study, we used information from annual fluctuations of vegetation biomass, water surface, and bare soil combined into the temporal Rao's Q index, in an effort to identify and map seven land cover classes that clearly depicted the sequence of coastal dune natural and semi-natural ecosystems occurring along the sea-inland gradient.

Our modelling approach showed high levels of classification accuracy, substantially confirming the usefulness of time-series analysis for semi-natural and natural land cover mapping (Marzialetti *et al.* 2019, Pesaresi *et al.* 2020, Sun *et al.* 2018). Moreover, we pointed out the high potential of integrating spectral indices as MSAVI2, NDWI2 and BI2 to describe land cover seasonality in heterogeneous environments as those of coastal dunes.

The classification framework allowed to identify and map seven coastal semi-natural cover types organized in two hierarchical levels. For each set of cover types, different variables emerged as the most important for classification. In the first RF cycle implemented on the overall coastal landscape, water surface was split from the other cover classes because of the typical behavior of water-related spectral indices. Specifically, the minimum of NDWI2 (10^{th}_{NDWI2}) and its temporal diversity (Q_{NDWI2}) assumed particularly high values and emerged as the most important variables in the first RF cycle. As previously observed, the spectral response of water and dryland are very different (Chatziantoniou *et al.* 2017, Prajesh *et al.* 2019). Such differences clearly emerged at coarser classification levels on the transition area we analyzed here. However, also the percentage of bare surfaces appeared as an important variable in the first cycle, revealing the presence of open sand and sparse vegetation in the coastal dune mosaic. In the second and third cycles performed on non-water areas, the temporal diversity of biomass (Q_{MSAVI2}) showed an important role in land cover classification, confirming the importance of phenology in coastal landscape mapping (Marzialetti *et al.* 2019). In particular, the second cycle, which focused on open sand and sparse vegetation areas, reported the phenology (Q_{MSAVI2}) along with the annual fluctuations on bare soil (Q_{BI2}) as important variables discriminating bare areas from complex mosaics of pioneer vegetation and sand (Bazzichetto *et al.* 2016, Sciandrello *et al.* 2015). The third RF cycle focused mainly on vegetated areas hosting herbaceous and woody land cover classes, reporting the temporal variability of vegetation biomass (Q_{MSAVI2}) and the low percentages of bare soil ($10th_{BI2}$) as the most important predictors for classification. In addition, low temporal variation on bare soil cover (low Q_{BI2}) helped to discriminate seasonal deciduous formations from the contiguous evergreen vegetation (Carranza *et al.* 2008, Bazzichetto *et al.* 2016).

The classification of Rao's Q temporal diversity measured on spectral indices allowed to identify and map the mosaic characterizing the different sectors of coastal dune zonation with high accuracy levels. However, transition classes as Water Edge and Fixed Dune Herbaceous Vegetation with Shrubs evidenced the lowest values, perhaps due to the spatial dimension of Sentinel-2 images (10 m), which is too coarse to describe this intricate the transition mosaic.

The seven identified classes clearly depicted the sequence of coastal dune natural and semi natural cover classes occurring from the sea to the inland, each characterized by a specific seasonal pattern. Indeed, classes ranged from the Water class including the sea close to the seashore to Deciduous formations and Humid Herbaceous Vegetation growing in the inner dune slacks (Marzialetti *et al.* 2019, Stanisci *et al.* 2014, Pesaresi *et al.* 2020). As for the Water Edge class, it represented the inter-tidal area with higher presence of water during the winter months possibly caused by storms. The Open Sand class included the dry sand beach with the sparse annual vegetation on the drift line, while the embryonic shifting dune formations as Dense Herbaceous Vegetation type represented the mobile

dunes with *Calamagrostis arenaria* subsp. *arundinacea* (see also Marzialetti *et al.* 2019). The Fixed Dune Herbaceous Vegetation with Shrubs class included a fine mosaic of herbaceous and shrub vegetation occurring on transition areas, as well as fuzzy edges between herbaceous and woody vegetation on dune sectors towards sea and shrubs and ruderal formations on inland disturbed areas (Marzialetti *et al.* 2019, Bazzichetto *et al.* 2016). As for the Evergreen Woody Vegetation class, we reported low temporal diversity values of both in vegetation biomass (Q_{MSAVI2}) and bare surfaces (Q_{BI2}), confirming the already known absence of seasonality of this cover class (Marzialetti *et al.* 2019, Bonari *et al.* 2017). The Deciduous and Humid Herbaceous Vegetation class enclosed riparian deciduous woody vegetation and vegetation of humid environments. This class was characterized by a similar seasonality of vegetation biomass and presented two peaks on spring and summer that alternate with lower values in autumn and winter (Zoffoli *et al.* 2008, Fu and Burgerh, 2015).

The results we obtained in this study clearly identified remotely sensed seasonality and Rao's Q temporal diversity as an effective source of information for landscape mapping in coastal areas. Using Sentinel-2 images with accurate spatial, temporal and spectral resolutions (Drusch *et al.* 2012), we derived sound temporal heterogeneity variables for land cover mapping summarizing spectral indices previously implemented separately (e.g. using MSAVI2, or NDWI2, or BI2).

Land cover classification based on multi-temporal remotely sensed data analysis has improved here for landscape mapping on Mediterranean coasts by relying on a set spectral indices rarely analyzed together, as well as by the introduction of Rao's Q for summarizing their temporal variability. Furthermore, the implemented RF classification organized in sequential cycles ensured accurate and ecologically coherent results. For instance, water presence and seasonality evidenced by the yearly behavior of NDWI2 were important variables in the first cycle of classification implemented on overall the coastal area extent which confirmed its potential for discriminating water from emerged areas (Chatziantoniou *et al.* 2017, Prajesh *et al.* 2019) and suggested its role when mapping transition systems between terrestrial and marine realms. Similarly, our results confirmed that biomass and bare soil indexes and their temporal variability are important variables for mapping terrestrial cover classes (Marzialetti *et al.* 2019, Rapinel *et al.* 2019, Pesaresi *et al.* 2020, Grabska *et al.* 2019). Based on our results, it possible to affirm that for remote sensed monitoring and mapping, the inclusion of variables depicting bare soil, water and biomass seasonality are highly advisable.

3.5. Conclusions

The proposed procedure for classifying and mapping natural and semi-natural land cover effectively summarized the dynamic nature of coastal systems, capturing all main components of coastal dune mosaic together with their seasonal variation (i.e. vegetation, bare surfaces and water surfaces) by combining spectral indices rarely used together (MSAVI2, NDWI2, or BI2).

The information provided by Rao's Q offered a sound base for natural and semi-natural land cover monitoring and mapping. In particular, the here proposed implementation of Rao's Q temporal heterogeneity allowed to accurately depict the seasonality of the different cover types conforming the coastal dune mosaic along the sea-inland gradient (e.g. biomass phenology, water seasonality, yearly variation on bare surfaces). Furthermore, the applicability of the proposed framework on the available updated sentinel images emphasized the procedure as a promising tool for cover monitoring and reporting. Even more interestingly, the integration of other remotely sensed data with higher spatial resolution derived by satellite as Planet images, UAV, or LiDAR data, may further improve the classification of coastal zonation.

From an applied perspective, the natural and semi-natural land cover map provided in this study yields a relevant knowledge for coastal monitoring and management; therefore, we hope new studies exploring increasingly larger areas will be analyzed to further test the proposed classification and, at the same time, to provide homogeneous information for coasts in the Mediterranean.

3.6. Appendix C

Table C1: Sentinel-2 dataset indicating for each image the month, day, platform (Sentinel-2A or Sentinel-2B) and the hour of acquisition, the cloud percentage, and the relative tile (T33TVG for Molise north, T33TWF for Molise south).

Month	Day	Cloud (%)	Platform	Hour	Tile
January	23	18.993	S2B	09.53	T33TVG
January	23	13.829	S2B	09.53	T33TWG
February	07	2.022	S2A	09.51	T33TVG
February	07	13.248	S2A	09.51	T33TWG
March	09	5.827	S2A	09.50	T33TVG
March	09	13.563	S2A	09.50	T33TWG
April	18	2.979	S2A	09.50	T33TVG
April	18	2.994	S2A	09.50	T33TWG
May	05	10.568	S2B	09.50	T33TVG
May	05	2.185	S2B	09.50	T33TWG
June	12	0.154	S2B	09.50	T33TVG
June	12	2.500	S2B	09.50	T33TWG
July	07	17.461	S2A	09.50	T33TVG
July	07	18.859	S2A	09.50	T33TWG
August	21	2.016	S2B	09.50	T33TVG
August	21	0.068	S2B	09.50	T33TWG
September	05	1.957	S2A	09.50	T33TVG
September	05	0.898	S2A	09.50	T33TWG
October	15	2.409	S2A	09.50	T33TVG
October	15	2.933	S2A	09.50	T33TWG
November	04	15.429	S2A	09.52	T33TVG
November	04	0.319	S2A	09.52	T33TWG
December	24	0.481	S2A	09.54	T33TVG
December	24	13.969	S2A	09.54	T33TWG

Table C2: The optimal number of classes for each cycle was identified by Silhouette, Calinski-Harabasz, and Davies-Bouldin indices calculated on a specific hierarchical cluster produced through Ward's minimum variance. These three indices identify the optimal number of classes by comparing the intra-class compactness (degree of aggregation between pixels inside each class) and the separation between classes (degree of differences between classes). We fixed as the optimal number of classes, the most frequent output produced by the three indexes.

Index	Compactness	Separation	Optimal number	Reference
Silhouette index	Mean Euclidean distance between pixels intra-class	Mean Euclidean distance between pixels of different classes	Maximum value	Kaufman and Rousseeuw, 2005
Calinski-Harabasz index	Sum of the squares of Euclidean distance between pixels intra-class	Sum of the squares of Euclidean distance between different classes	Maximum value	Calinski and Harabasz, 1974
Davies-Bouldin index	Variance between pixels intra-class calculated by Euclidean distance	Variance of center between different classes calculated by Euclidean distance	Minimum value	Davies and Bouldin, 1979

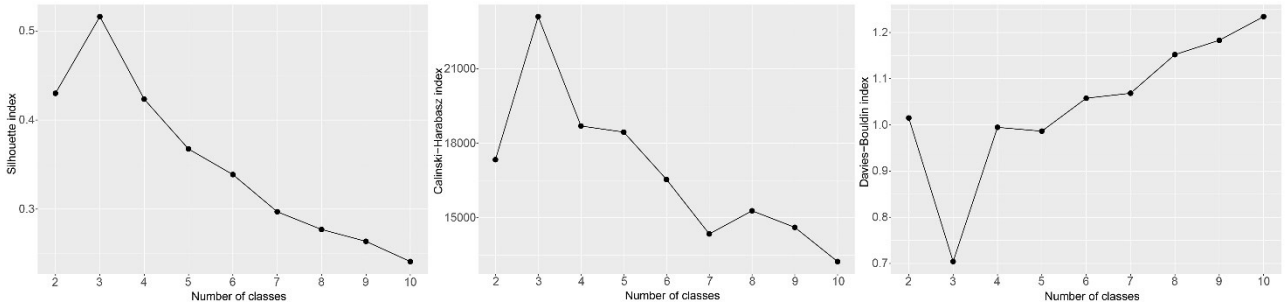

Figure C1: Graphical representation of the Silhouette, Calinski-Harabasz, and Davies-Bouldin indices used for identifying the optimal number of classes in the 1° cycle of Random Forest. All three the indices identified three as the optimal number of classes.

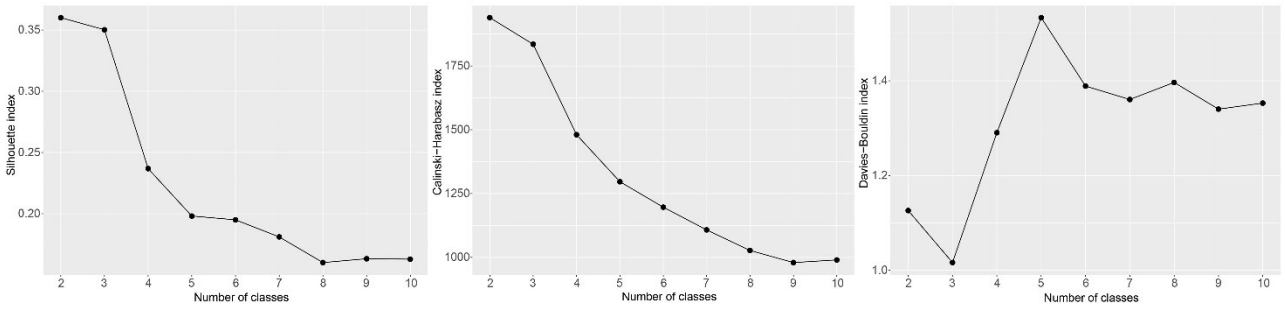

Figure C2: Graphical representation of Silhouette, Calinski-Harabasz, and Davies-Bouldin indices used for identifying the optimal number of classes in the 2° cycle of Random Forest. Two (Silhouette and Calinski-Harabasz) of the three indices have established two as the optimal number classes.

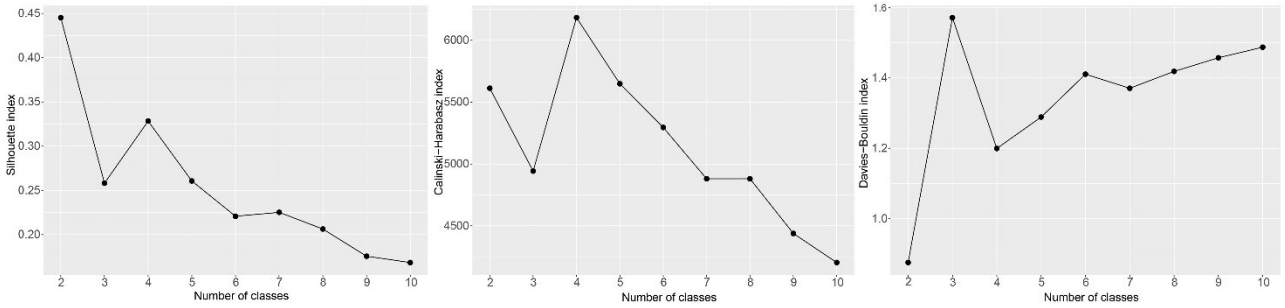

Figure C3: Graphical representation of Silhouette, Calinski-Harabasz, and Davies-Bouldin indices used for identifying the optimal number of classes in the 3° cycle of Random Forest. Two (Silhouette and Calinski-Harabasz) of the three indices suggested four as the optimal number classes.

Table C3: The percentages of accuracy assessment values by land cover classes for first classification cycle: Water (W), Sand (S), Vegetation (V). In particular User's accuracy (U ACC), Producer's accuracy (P ACC), and Matthews Correlation Coefficient (MCC). In the Random Forest accuracy assessment is indicated the mean values and standard deviation for the performance metrics.

1° classification cycle			
Random Forest accuracy assessment. Measures by land cover classes			
Land cover classes	W	S	V
U ACC (%)	98.91 ± 0.59	99.64± 0.26	99.79 ± 0.14
P ACC (%)	99.18 ± 0.51	99.49 ± 0.29	99.77 ± 0.15
MCC	0.989 ± 0.005	0.994 ± 0.003	0.995 ± 0.003
Independent accuracy assessment. Measures by land cover classes			
Land cover classes	W	S	V
U ACC (%)	94.91	94	96.86
P ACC (%)	96.55	88.68	97.88
MCC	0.947	0.895	0.928

Table C4: The percentages of accuracy assessment values by land cover classes for second classification cycle: Water Edge (WE), Open Sand (OS). In particular User's accuracy (U ACC), Producer's accuracy (P ACC), and Matthews Correlation Coefficient (MCC). In the Random Forest accuracy assessment is indicated the mean values and standard deviation for the performance metrics.

2° classification cycle		
Random Forest accuracy assessment. Measures by land cover classes		
Land cover classes	WE	OS
U ACC (%)	98.68 ±1.01	98.77 ± 0.90
P ACC (%)	98.76 ± 1.00	98.63 ± 0.91
MCC	0.980 ± 0.011	0.980 ± 0.11
Independent accuracy assessment. Measures by land cover classes		
Land cover classes	WE	OS
U ACC (%)	72.22	96.67
P ACC (%)	92.86	85.29
MCC	0.656	0.656

Table C5: The percentages of accuracy assessment values by land cover classes for third classification cycle: Dense Herbaceous Vegetation (DHV), Evergreen Woody Vegetation (EWV), Fixed Dune Herbaceous Vegetation with Shrubs (FDHVS), Deciduous and Humid Herbaceous Vegetation (DHHV). In particular User's accuracy (U ACC), Producer's accuracy (P ACC), and Matthews Correlation Coefficient (MCC). In the Random Forest accuracy assessment is indicated the mean values and standard deviation for the performance metrics.

3° classification cycle				
Random Forest accuracy assessment. Measures by land cover classes				
Land cover classes	DHV	EWV	FDHVS	DHHV
U ACC (%)	98.29 ±0.73	98.04 ± 0.75	95.65 ± 0.90	97.91 ± 0.78
P ACC (%)	98.19 ± 0.71	97.57 ± 0.90	96.23 ± 0.94	97.70 ± 0.86
MCC	0.975 ± 0.007	0.972 ± 0.008	0.943 ± 0.009	0.972 ± 0.007
Independent accuracy assessment. Measures by land cover classes				
Land cover classes	DHV	EWV	FDHVS	DHHV
U ACC (%)	88.46	87.50	78.18	80.70
P ACC (%)	92.00	80.77	93.48	73.02
MCC	0.826	0.774	0.632	0.726

Chapter 4: Measuring alpha and beta diversity by field and remote sensing data: A challenge for coastal dunes biodiversity monitoring

4.1. Introduction

Biodiversity loss due to human activities is accelerating with an extraordinary ratio, and several researchers hypothesize that earth life is undergoing to a mass extinction phenomenon (Ceballo *et al.* 2015), which makes continuous ecosystem monitoring a pressing need (Díaz et al. 2015). Still, regular assessment of biodiversity is difficult to undertake via field surveys (Palmer *et al.* 2002).

The economic limitations in many countries restrict the possibilities of implementing monitoring programs based on large-scale fieldwork (Vihervaara *et al.* 2017). Furthermore, collecting extensive and representative data in the field could be hampered by the impossibility to reach some monitoring areas (Petrou *et al.* 2015). Systematically surveying and monitoring complex and dynamic ecosystems (e.g. coastal dunes or river banks) by conventional biodiversity field campaigns might not be possible due to high costs, challenges to access to some sampling sites and lack of historical data. Such crucial limitations hamper implementing statistically sound monitoring schemes that are essential for better understanding and modelling biodiversity in space and time (Rocchini *et al.* 2021).

In contrast to field-based methods, satellite remote sensing (hereafter RS) providing frequent and complete spatial coverages is a cost-effective (free remotely sensed products) and comprehensive support for monitoring several biodiversity features at multiple spatial scales (Rocchini *et al.* 2016, Torresani *et al.* 2019, Torresani *et al.* 2020). Furthermore, combining remotely sensed and in situ field data represents one of the most promising approaches to fill the gaps in biodiversity monitoring (Vihervaara *et al.* 2017).

In 2002, Palmer and coauthors postulated the Spectral Variability Hypothesis (hereafter SVH), stating that the larger the spectral heterogeneity of an environment the higher its biodiversity. Since then, several research efforts have been devoted to explore the relationship between remotely sensed and field-collected data (Rocchini *et al.* 2015, Lausch *et al.* 2020) accounting for both alpha diversity (e.g. within sample/pixel variability, Rocchini 2007a) and beta diversity (e.g. between samples/pixels variability, Rocchini 2007b). The potential of SVH to depict alpha diversity was tested on several ecosystems covering large areas as evergreen forests (Torresani *et al.* 2019), tropical forests (Nagendra *et al.* 2010), wetlands (Heumann *et al.* 2015), grasslands (Hall *et al.* 2012), savannah woodlands (Madonsela et al. 2017). Similarly, SVH was tested to explore beta diversity on Mediterranean shrubs and forests (Rocchini 2007b, Hoffmann *et al.* 2019), tropical forests (Rocchini *et al.* 2009, Féret and Asner, 2014), deciduous forests (Khare *et al.* 2019) and grasslands Gholizadeh *et al.* 2020). However, little attention has been paid to extend SVH applications to more complex and

dynamic landscapes (Schmidtlein and Fassnacht, 2017). In particular, the SVH effectiveness in depicting field and spectral diversity patterns on very dynamic ecosystems such as coastal dunes is still missing.

Coastal dunes environments occur on narrow strips of land interposed between marine and terrestrial realms (Martínez and Psuty 2004, Hesp 1991). The strong influence of continuous sudden changes on abiotic and biotic factors promotes the development of highly specialized biodiversity and a peculiar vegetation mosaic (Acosta *et al.* 2003, Kim and Yu, 2009, Bazzichetto *et al.* 2016). Furthermore, coastal sand dunes are among the most threatened habitats at both global (McLachlan and Brown, 2006, Doody 2013) and European level (Janssen *et al.* 2016, Prisco *et al.* 2020). Therefore, updated monitoring protocols able to summarize its biodiversity trends are urgently needed (Defeo *et al.* 2009). Among multiple threats, coastal landscapes are seriously impinged by alien plant invasions (Chytrý *et al.* 2008, Lazzaro *et al.* 2020, Tordoni *et al.* 2020), whose negative effects on natural ecosystems have been explored using field data or RS independently (Giulio *et al.* 2020, Royiman *et al.* 2019). Field-research gave evidence of alterations of species diversity (Early et al. 2016) and cover (Lambdon *et al.* 2008) in invaded areas, while RS research underlined significant functional traits modifications (Niphadkar and Nagendra, 2016) and niche shifts (Guisan *et al.* 2014). However, an integrated approach summarizing floristic, field–measured, diversity values and spectral RS variability indices in areas with different invasion levels has not been carried out yet. Understanding how plant diversity and spectral variability vary on invaded ecosystems could be crucial for monitoring and management of coastal dunes systems, in order to preserve and improve the conservation status, the functions and the associated ecosystem services (Giulio *et al.* 2020, Drius *et al.* 2019, Viciani *et al.* 2020).

On these bases, the present work sets out to investigate the potential of SVH in linking field collected and remote sensed data in a complex and dynamic ecosystem. Specifically, we explored if spectral diversity provides reliable information to monitor floristic diversity in Mediterranean coastal dunes, as well as the consistency of such information in altered ecosystems due to plant invasions. We analyzed: i) the local diversity (alpha) within sampling units and, ii) the turnover diversity (beta) among sampling units in well preserved and invaded areas, through the simultaneous analysis of field vegetation plots and RS PlanetScope images. We focused on a representative sector of the sea-inland coastal dune mosaic hosting some habitats of conservation concern in Europe (*sensu* 92/43/EEC, Janssen *et al.* 2016, Prisco *et al.* 2020). We followed a standard system of vegetation classification in order to provide specific insights that can help to improve the monitoring strategies claimed by the European conservation directive (Habitats Directive 92/43/EEC). If confirmed for coastal dune

vegetation, SVH will provide an integrative tool for monitoring and management of coastal dune biodiversity, improving and simplifying the assessment of biodiversity in space and time.

4.2. Materials and Methods

4.2.1. Study Area

The study was carried out in a coastal tract representative of the Tyrrhenian dunes in central Italy (Lazio region, Figure 14). The sampled sector, approximately 70 km long, includes low sandy Holocenic dunes with Mediterranean climate (Carranza *et al.* 2008) disposed on a narrow strip along the seashore (< 500 m, Acosta *et al.* 2003). In natural conditions, plant communities on shifting dunes are dominated by few dune-building perennial rhizomatous grasses (e.g. *Thinopyrum junceum*, *Calamagrostis arenaria* subsp. *arundinacea*), which occasionally form monospecific vegetation patches. Plant communities on fixed dunes are characterized by small chamaephytes (e.g. *Crucianella maritima*) intermingled with species-rich therophytic grasslands (e.g. *Cutandia maritima*, *Lagurus ovatus*, Acosta *et al.* 2009, Sperandii *et al.* 2020). As on most of the Mediterranean coasts, the analyzed dunes have undergone persistent human pressure that altered coastal landscape and vegetation (Sperandii *et al.* 2020, Malavasi *et al.* 2016), with several sectors having been invaded by iceplant (*Carpobrotus* spp., Campoy *et al.* 2018, Sarmati *et al.* 2019). *Carpobrotus* spp. is a perennial herb with succulent leaves that develops wide creeping mats (Campoy *et al.* 2018). It is native from South Africa and, along the Italian sand coasts, it preferentially invades herbaceous vegetation of shifting and fixed dunes (Lazzaro *et al.* 2020, Carranza *et al.* 2010, Bazzichetto *et al.* 2018b). Field research evidenced that *Carpobrotus* spp. invasion substantially alters ecosystems diversity (Sarmati *et al.* 2019, Santoro *et al.* 2011) and functioning of invaded areas (Campoy *et al.* 2018, Conser and Connor, 2009), with such variations being also detectable by RS spectral values (Underwood *et al.* 2003, Underwood *et al.* 2007).

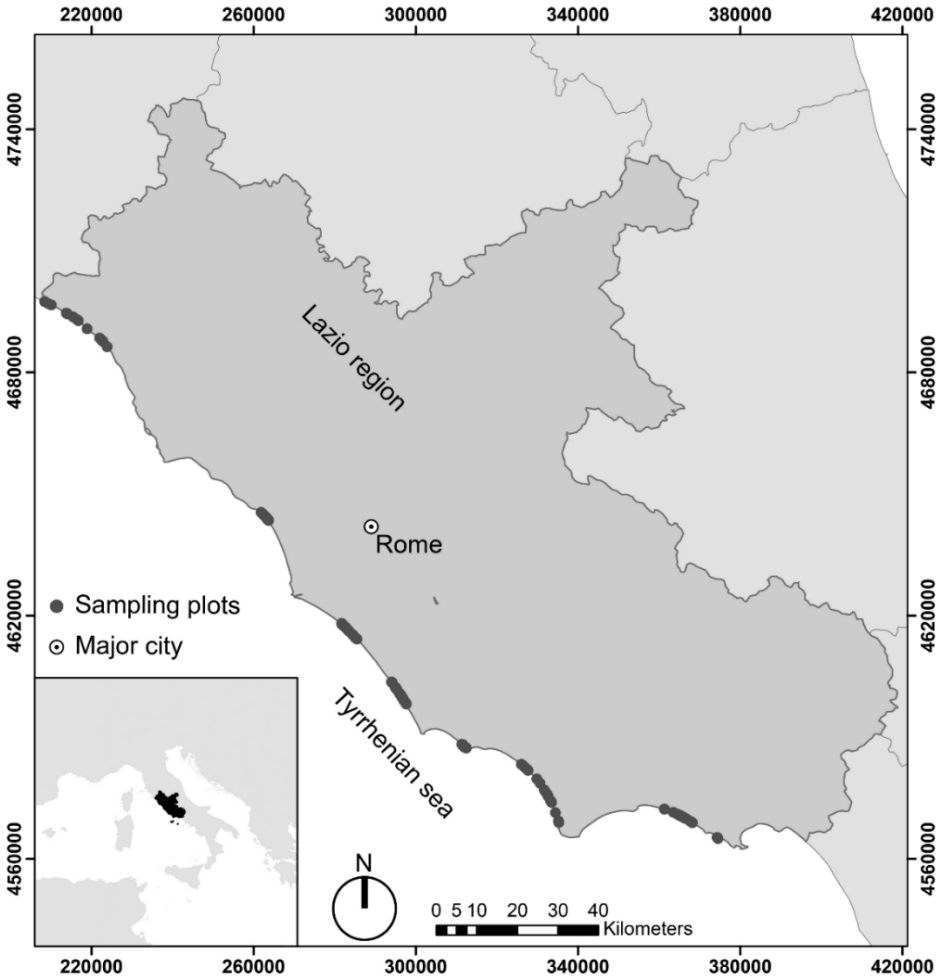

Figure 14. Study area (reference system WGS84 33N, epsg: 32633) along with sampling plots.

4.2.2. Data Analysis

We tested the Spectral Variability Hypothesis (SVH) for alpha and beta diversity in coastal dunes following a sequence of steps schematically reported on Figure 15: (1) Data setting, (2) Alpha diversity analysis, (3) Beta diversity analysis, (4) Spectral Variability Hypothesis test.

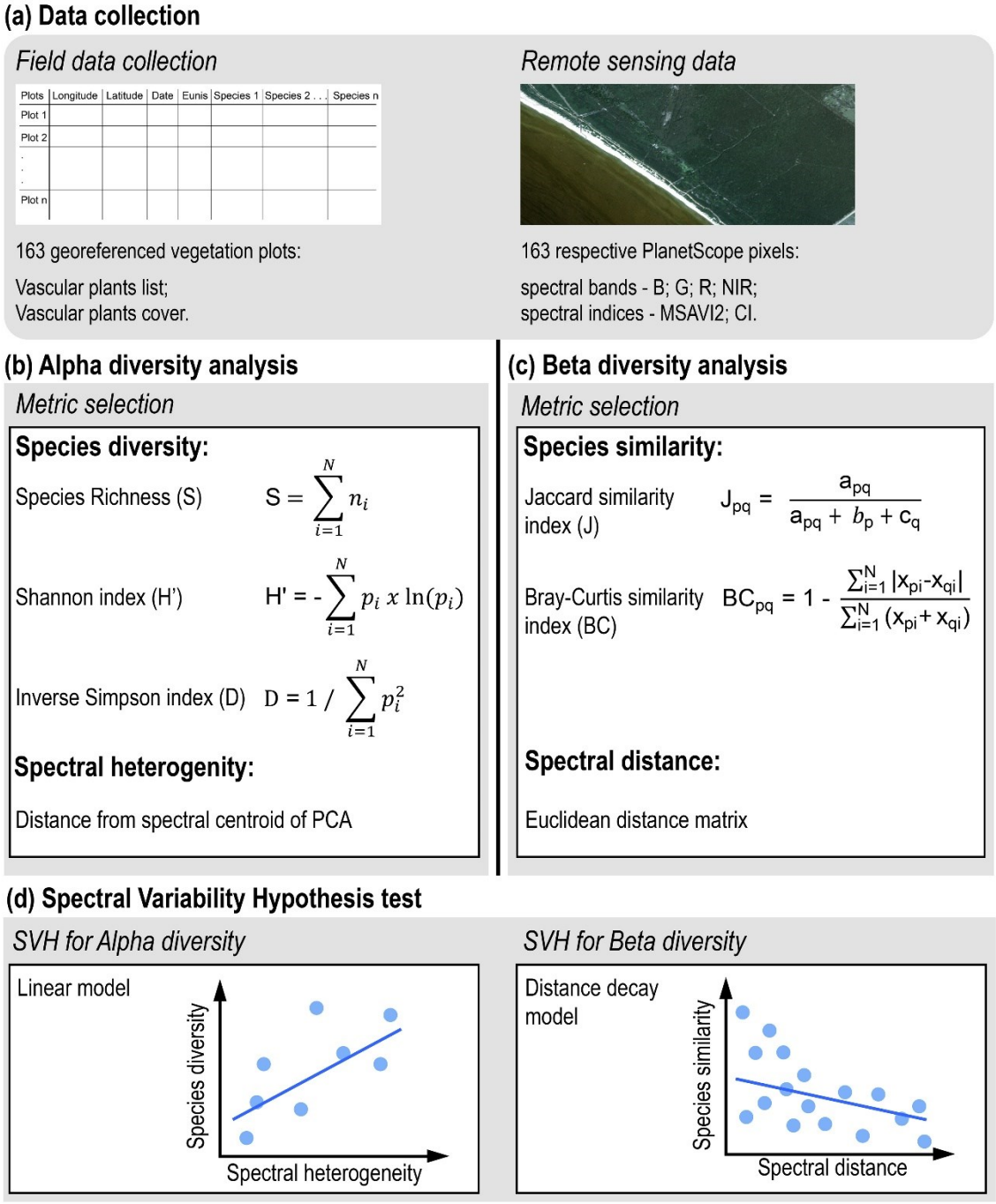

Figure 15. Workflow describing the procedure followed for investigating the potential of Spectral Variability Hypothesis for depicting alpha and beta diversity levels on herbaceous coastal dune vegetation.

4.2.2.1. Data setting

Biodiversity field data were extracted from the "RanVegDunes" database (Sperandii *et al.* 2017), which was built up conforming the European Vegetation Database frame (Chytrý *et al.* 2020). Such data were originally gathered at 163 random vegetation plots (Figure 15, box a, Figure D1) of 2 x 2 m placed on herbaceous shifting and fixed dunes plant communities. We selected those plots that were sampled during the growing seasons (April-May) of the years 2017-2020 for which remote sensed images were available. For each vegetation plot, a complete list of vascular plant species along with their cover in percent was available. Each plot was also assigned to a EUNIS habitat category,

a comprehensive Pan-European classification scheme (Chytrý *et al.* 2020) holding an exact correspondence with European Habitats *sensu* 92/43/EEC (Table 7), which assured the usefulness of our results to develop new habitat-specific monitoring strategies. Overall, the field floristic data include 79 plots collected on shifting coastal dunes (Shifting dunes, EUNIS code N14), 41 plots on fixed coastal dune (Transition dunes, EUNIS code N16) and 43 invaded plots in which *Carpobrotus* spp. covers more than 25 percent (Invaded dunes, Table 7).

Table 7. Description of herbaceous dune communities referred to EUNIS categories, along with their correspondent EU habitat (ex Annex I 92/43/EEC) and the respective number of sampling plots. Coastal dune vegetation with the presence *Carpobrotus spp.* covering more than 25 percent are also reported.

Acronym/ Vegetation categories	Description and correspondence with EU habitats (ex Annex I 92/43/EEC)	Number of plots
Shifting dunes/ EUNIS-N14	Mobile coastal sand ridges including embryonic dunes characterized by *Thinopyrum junceum* and semi-permanent dune systems dominated by *Calamagrostis arenaria* subsp. *arundinacea* (EU habitat code: 2110, 2120).	79
Transition dunes/ EUNIS-N16	Fixed dune grasslands including chamaephytic communities of the inland dunes dominated by *Crucianella maritima* and annual species-rich communities colonizing dry interdunal depressions. (EU habitat code: 2210, 2230).	41
Invaded dunes	Herbaceous vegetation with the presence *Carpobrotus* spp. covering more than 25 percent.	43

Spectral data was derived from PlanetScope (PS) satellite images. We used 12 cloud-free PS satellite images (zenith angle view < 10°) covering the same geographic area and time period of the field data (https://www.planet.com/explorer/, Table D1 – Appendix D). These images have a daily temporal resolution and a pixel size of 3 meters. We used the surface reflectance of the orthorectified PS images (level 3B).

We used for the analysis four spectral bands: Blue (B, 455-515 nm), Green (G, 500-590 nm), Red (R, 590-670 nm), Near Infrared (NIR, 780-860, Cooley *et al.* 2017) and two spectral indices: e. Modified Soil-Adjusted Vegetation Index 2 (MSAVI2) and Coloration Index (CI, Table 8). The selected spectral indices are particularly appropriate for describing and mapping heterogeneous landscapes where vegetation and bare surfaces are intermingled (Marzialetti *et al.* 2020) as is the case of well-preserved and altered coastal dunes invaded by *Carpobrotus* spp. (Underwood *et al.* 2003, Underwood *et al.* 2007). MSAVI2 is especially useful for quantifying the photosynthetic biomass in landscapes characterized by high percentages of bare surfaces (Marzialetti *et al.* 2020, Qi *et al.* 1994, Wu *et al.* 2016). It ranges from −1 (absence of vegetation biomass) to 1 (maximum of vegetation biomass), with higher values indicating higher percentages of photosynthetic biomass (Qi *et al.* 1994, Rondeaux *et al.* 1996). CI is a color soil index used to characterize soil conditions (Mathieu *et al.* 1998) and to reveal the organic content in arid soils by the green−red reflectance ratio (Bachaoui *et*

al. 2014). This index ranges from −1 to 1, with higher values indicating darker coloration (Escadafal 1993).

We built up the spectral dataset (Figure 15, box a) by extracting for each vegetation plot the respective pixel PS value of Blue, Green, Red and Nir spectral bands, and of the derived MSAVI2, and CI spectral indices (Table 8). Pixels were classified according with their respective field plot EUNIS (e.g. "Shifting dunes" - EUNIS-N14, "Transition dunes" - EUNIS-N16) or altered ("Invaded dunes") category.

Table 8. Spectral variables selected for analyzing alpha and beta spectral diversity along with their related bandwidth/ equation, index proxy and references.

Acronym	Name	Bandwidth / Equation	Index of	Reference
B	Blue band	455–515 nm	–	[59]
G	Green band	500–590 nm	–	[59]
R	Red band	590–670 nm	–	[59]
NIR	Near Infrared band	780–860 nm	–	[59]
MSAVI2	Modified Soil Adjusted Vegetation Index 2	$\frac{2*NIR+1-\sqrt{(2*NIR+1)^2-8*(NIR-RED)}}{2}$	photosynthetic biomass	[61]
CI	Colouration index	$\frac{RED - GREEN}{RED + GREEN}$	organic content level in soil	[64]

4.2.2.2. Alpha diversity analysis

Alpha diversity summarizes the variability within sampling units and can be expressed as richness (i.e. the number of item types) and evenness (i.e. items' relative abundance, Whitaker 1960, Whitaker 1972). As sampling units, we considered the vegetation plots for field dataset and the corresponding pixels for spectral information.

We analyzed alpha diversity from field data using three indices (Figure 15, box b; Table 9): Species Richness (S), Shannon (H') and Inverse Simpson index (D, Magurran 2004), through the "BiodiversityR" R package (function *diversityresult*, Kindt and Coe 2005). Species Richness quantifies the count of species inside plots (Fisher *et al.* 1943), while Shannon diversity (H') accounts for the number of species and their relative evenness (Madonsela *et al.* 2017, Shannon 1948, Oldeland *et al.* 2010). Shannon index varies from 0 in plots with one dominant species to an undetermined maximum in plots with equally abundant species (Magurran 2004). Simpson index, also called "dominance index", summarizes species richness and dominance. The Inverse Simpson index (D) is the reciprocal of the Simpson index, and ranges from one in plots with only one species to an undetermined maximum in plots with all individuals belonging to different species (Magurran 2004, Peet 1974, Jost 2007).

Table 9. Alpha diversity indices used for analyzing field vegetation data along with the formula and references. N = total number of species; n_i= each species; p_i = abundance value of i-species.

Acronym	Name	Formula	References
S	Species Richness	$\sum_{i=1}^{N} n_i$	Fisher *et al.* 1943
H'	Shannon index	$-\sum_{i=1}^{N} p_i \times \ln(p_i)$	Shannon 1948
D	Inverse Simpson index	$1 / \sum_{i=1}^{N} p_i^2$	Oldeland *et al.* 2010

We expressed the RS alpha diversity as the Distance from the Spectral Centroid index (Figure 15, box b, Rocchini *et al.* 2016, Rocchini 2007a). Specifically, we calculated the mean distance of all the sampled pixels from the Principal Component Analysis (PCA) centroid built on pixels' spectral values (B, G, R, NIR, MSAVI2 and CI, Rocchini 2007a, Oldeland *et al.* 2010). Higher values of the distance from the spectral centroid index indicates higher pixel spectral heterogeneity (Rocchini 2007a). The PCA of the spectral dataset, the identification of the spectral centroid and the calculation of the Euclidean distance from the spectral centroid, were performed using R package "pracma" (function *distmat*, Borchers 2019).

4.2.2.3. Beta diversity analysis

Beta diversity depicts the variation among sampling units in both composition and abundance values (Whitaker 1960, Whitaker 1972). For beta diversity analysis, we considered as sampling units the vegetation plots (species presence and abundance) and the corresponding pixels (spectral bands and indices values).

Beta diversity in field data was analyzed using two different pairwise measures: the Jaccard similarity matrix using plant occurrence (presence/absence data), and the Bray-Curtis similarity matrix based on abundance values (species cover). Jaccard similarity index (J) quantifies the pairwise similarity between vegetation plots as the ratio between the number of species in common and the number of species that are unique to each plot. J values scoring as zero indicate total inequality among plots, while the total equality is identified by J values of one (Table 10, Jaccard 1901, Wildi 2010). Bray-Curtis similarity index (BC) depicts the vegetation plots pairwise differences using quantitative species cover data (Magurran 2004, Bray and Curtis, 1957). The BC dissimilarity is defined as the ratio between the difference of abundance values and the sum of abundance values for each species. We calculated the similarity values by subtracting the dissimilarity values to one (Table 10). BC ranges from zero when the plots are completely different to one when the species composition of two plots is identical (Pavoine and Ricotta, 2019).

Table 10. Beta diversity indices used for analyzing field floristic data along with the formula and references. In the Jaccard similarity between plots (p, q), a = number of species shared between p and q vegetation plots, b = number of unique species in the p vegetation plot, c = number of unique species in q plot. In the Bray-Curtis similarity between plots (p, q), x_{pi} = the abundance value of the i-species on plot p and x_{qi} the abundance value of the i-species on plot q.

Acronym	Name	Formula	References
J	Jaccard similarity index	$\frac{a_{pq}}{a_{pq} + b_p + c_q}$	Jaccard 1901
BC	Bray-Curtis similarity index	$1 - \frac{\sum_{i=1}^{n} \lvert x_{pi} - x_{qi} \rvert}{\sum_{i=1}^{n} (x_{pi} + x_{qi})}$	Bray and Curtis, 1957

Spectral beta diversity was calculated as the pairwise multivariate Euclidean distance of the pixel spectral values (Rocchini 2007b, Hoffmann *et al.* 2019, Rocchini *et al.* 2009). The Euclidean distance measured the shortest possible distance between two pixels, with higher Euclidean distance values corresponding to higher differences between two pixels in RS bands and spectral indices values (Rocchini *et al.* 2016). All the spectral dataset variables were standardized to zero mean and unit variance, before moving toward the subsequent analytical steps (Hoffmann *et al.* 2019).

4.2.2.4. Spectral Variability Hypothesis test

To test the SVH for alpha diversity, we analyzed the relationship between alpha diversity per plot and spectral heterogeneity for the respective pixels using linear regressions. Specifically, we included in turn plots diversity indices (i.e. Species Richness, Shannon index and Inverse Simpson index) as response variables and the respective pixels' distance from the spectral centroid index, along with dune well preserved and invaded categories (Shifting, Transition and Invaded dunes, Table 7), as explanatory variables. Goodness-of-fit was evaluated through R^2 (Figure 15, box d, Rocchini *et al.* 2016, Madonsela *et al.* 2017, Oldeland *et al.* 2010). Since alpha diversity indices are not normally distributed, we fit linear regressions where coefficients significance was evaluated by randomly permuting observations in the data. This approach has the substantial advantage of relaxing the normality assumption of linear regression (Anderson and Robinson, 2001), thus resulting particularly appropriate in our analytical context. Permutational marginal regressions were calculated using the R package "permuco" (function *lmperm*), allowing 5000 random permutations among observations (Frossard and Renaud, 2019). Moreover, the Shannon index vs. Distance to centroid and Inverse Simpson index vs. Distance models to centroid showed not constant variance of residuals. In order to assure homoscedasticity, we rectified the values of Shannon and Inverse Simpson indices using Box-Cox transformation flowed by the Breush-Pagan test and Non-constant Variance Score test (NCV test, Legendre and Legendre, 2012, Breusch and Pagan 1979, Cook and Weisberg 1983). Appling the Box-Cox transformation to the Shannon index vs. Distance to centroid ($\lambda = 1.596$) and Inverse Simpson index vs. Distance to centroid ($\lambda = 0.586$) models, the results of Breush-Pagan test and NCV

test show absence of heteroscedasticity with p-values always above 0.05. In particular, in order to applied the Box-Cox transformation in the Shannon index, we eliminated the monospecific plots.
To test SVH for Beta diversity, we carried out a Distance Decay Model (DDM, Cade and Noon 2003). In particular, we fit linear regressions and quantile regressions among the floristic Jaccard and Bray-Curtis similarities and the between-pixels Euclidean distances (Rocchini *et al.* 2009). We tested SVH using both approaches because linear regressions model can be less accurate when based on matrices with a high amount of zeroes, as in our case. The quantile regressions can overcome this limitation and allow to characterize the relationship of SVH by focusing on specific quantiles (Cade and Noon, 2003, Henning *et al.* 2005). We calculated the quantile regressions using four upper quantiles (τ = 0.99, 0.95, 0.90, 0.75) according to the hypothesis that maximum decay modelling allows to characterize the maximum beta diversity value (Rocchini 2007b). Moreover, a higher slopes of Distance Decay Model indicate higher Beta diversity values between samples (Rocchini *et al.* 2015). Finally, we calculated coefficients confidence intervals for both linear and quantile regressions through a bootstrapping approach (number of iterations: 1000, Rocchini *et al.* 2009). We computed the quantile regressions and their confidence intervals using R package "quantreg" (function *rq* and *boot.rq* respectively, Koenker 2020).

4.3. Results

4.3.1. SVH Alpha diversity

We observed a significant, positive relationship between species diversity indices and spectral heterogeneity (Figure 16, Table 11) depicting that species diversity values per plot increase toward higher values of spectral heterogeneity per pixel. Among the analyzed alpha diversity indices, Species Richness scored the highest goodness-of-fit (R^2 = 0.383), followed by Inverse Simpson index (R^2 = 0.337) and Shannon index (R^2 = 0.325, Table 11). The interaction effects suggested that the abovementioned positive relationship is true for all the analyzed vegetation types (Shifting, Transition and Invaded dunes, Figure 16). The regression model for Species Richness showed a highly significant relationship, with positive coefficients for all three vegetation categories (Table 11). Similarly, the model for Inverse Simpson and Shannon indices reported significant relationships for the three analyzed vegetation categories (Table 11). Permutation regressions confirmed significant relationships for all the considered alpha diversity indices (Table D2 – Appendix D).
In the Cartesian space, the Shifting coastal dune vegetation (EUNIS-N14) regression line was below the other categories with significant lower values for species richness (S_{N14}= 1 – 13), Shannon index (H'_{N14}= -0.592 – 1.674) and Inverse Simpson index (D_{N14}= 0.000 – 3.797, Figure 16). The regression lines for transition fixed dunes (EUNIS-N16) and invaded vegetation (Invaded dunes) showed similar

trends and ranges, slightly differentiating only in species numbers (S_{N16} = 2 – 15; S_I = 4 – 18, Figure 16), whereas in both Shannon index and Inverse Simpson index the trends and ranges resulted almost identical (H'_{N16}= -0.315 – 2.043, H'_I = 0.079 – 2.081, D_N16= 0.725 – 5.233, D_I= 0.942 – 4.562).

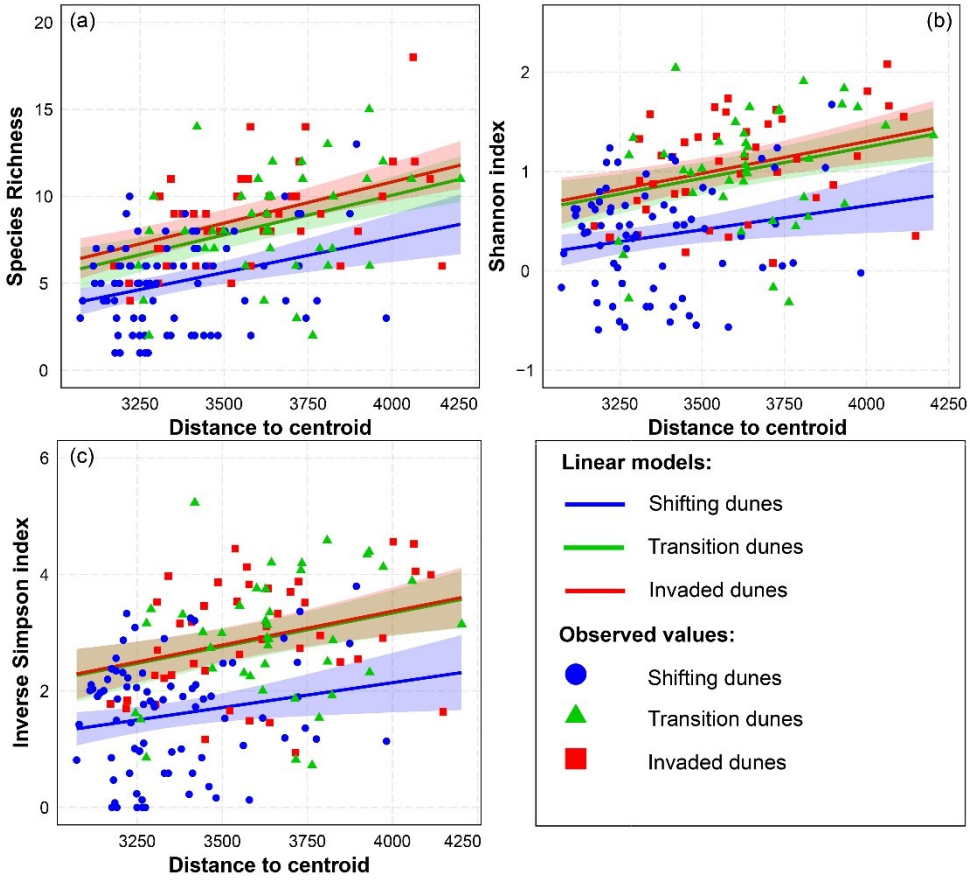

Figure 16. Linear regression models of alpha floristic diversity (Species Richness, Shannon and Inverse Simpson) vs. spectral heterogeneity (mean distance from spectral PCA centroid). Shifting dunes: N14 EUNIS category; Transition dunes: N16 EUNIS category: Invaded dunes: coastal dune vegetation with the presence *Carpobrotus* sp. covering more than 25 percent.

Table 11. Summary of linear regressions for alpha floristic diversity (Species Richness, Shannon and Inverse Simpson) vs. spectral heterogeneity (distance from spectral centroid index). Shifting dunes: N14 EUNIS category; Transition dunes: N16 EUNIS category: Invaded dunes: coastal dune vegetation with the presence *Carpobrotus* sp. covering more than 25 percent. P-value: * < 0.05; ** < 0.01; *** < 0.001.

Species Richness – Distance to centroid	**R^2 = 0.383**		
Linear Model with interactions	estimate	std. error	p-value
Distance to centroid: Shifting dunes	3.937×10^{-3}	9.512×10^{-4}	5.362×10^{-5}***
Distance to centroid: Transition dunes	4.554×10^{-3}	8.794×10^{-4}	6.666×10^{-7}***
Distance to centroid: Invaded dunes	4.746×10^{-3}	8.903×10^{-4}	3.311×10^{-7}***
Shannon Index – Distance to centroid	**R^2 = 0.325**		
Linear Model with interactions	estimate	std. error	p-value
Distance to centroid: Shifting dunes	4.805×10^{-4}	1.914×10^{-4}	0.013*
Distance to centroid: Transition dunes	6.284×10^{-4}	1.773×10^{-4}	5.229×10^{-4}***
Distance to centroid: Invaded dunes	6.423×10^{-4}	1.800×10^{-4}	4.644×10^{-4}***
Inverse Simpson Index – Distance to centroid	**R^2 = 0.337**		
Linear Model with interactions	estimate	std. error	p-value
Distance to centroid: Shifting dunes	8.535×10^{-4}	3.552×10^{-4}	0.017*
Distance to centroid: Transition dunes	1.152×10^{-3}	3.283×10^{-4}	5.85×10^{-4}***
Distance to centroid: Invaded dunes	1.160×10^{-3}	3.324×10^{-4}	6.271×10^{-4}***

4.3.2. SVH Beta diversity

The distance decay models fit with both linear and quantile regressions evidenced negative and significant decay rates (Figure 17, Table 12) for all the categories (i.e. Jaccard floristic similarities vs Euclidean spectral distance and Bray-Curtis floristic similarities vs. Euclidean spectral distance). Accordingly, the similarity among floristic plots were significantly higher when the respective pixels were spectrally closer.

In the DDM based on Jaccard floristic similarity vs Euclidean spectral distance, the decay rates showed the lower slope values for linear regression, with slopes increasing until the 0.95 quantile. The slope of 0.99 quantile instead resulted lower than the 0.95 one (Figure 17, Table 12).

The DDM based on Bray-Curtis floristic similarity vs Euclidean spectral distance showed most intense decay rates at intermediate quantiles (0.90 and 0.95), and the lower rate for the linear regression. The decay rates of the 0.75 and 0.99 quantile showed a intermediate trends respect the others quantiles (Figure 17, Table 12).

In both DDMs, the intercepts of all five regressions indicated significant values with higher values respect to the linear regression to 0.99 quantile (Figure 17, Table 12). This increasing intercept values confirmed that plots with higher similarity values correspond to pixels with lower spectral distance.

The distribution of fitted values in the DDM (Jaccard floristic similarities vs. Euclidean distance and Bray-Curtis floristic similarities vs. Euclidean distance) differed. Even if the two similarity matrices showed comparable variation ranges (0.000-0.937 for Jaccard similarities matrix, 0.000-0.968 for Bray-Curtis similarities matrix), the measures of central tendency diverged. Indeed, the Jaccard similarity matrix resulted closer to zero (mean: 0.107, median: 0.083, standard deviation: 0.106) than the Bray-Curtis one (mean: 0.179, median: 0.154. standard deviation: 0.157).

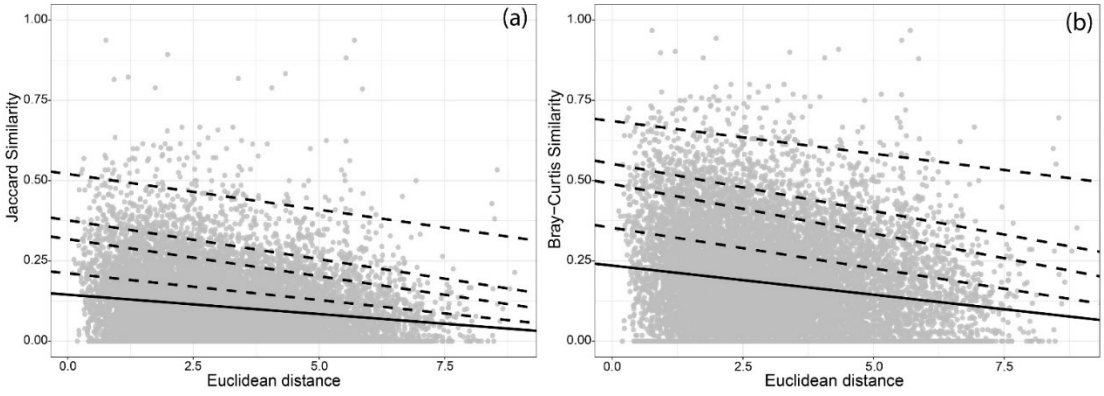

Figure 17. Distance Decay Models of Jaccard (**a**) and Bray-Curtis (**b**) species similarity versus spectral distance (spectral pairwise Euclidean distance). The linear regression is described by solid line, the quantile regressions considering four different τ (from upper to lower lines: 0.99, 0.95, 0.90, 0.75) are reported by dashed lines. Gray dots represent the sampling plots.

Table 12. Results of Distance Decay Models calculated by linear and quantile regressions at four different τ values (from upper to lower lines: 0.99, 0.95, 0.9, 0.75). P-value: * < 0.05; ** < 0.01; *** < 0.001.

Jaccard similarities – Euclidean distance					
Regression type	τ	Intercept	Intercept boundaries (99%)	decay rate (10^{-2})	decay rate (10^{-2}) boundaries (99%)
Linea regression	–	0.145***	0.138 – 0.152	-1.207***	-1.405 – -1.009
Quantile regressions	0.75	0.211***	0.202 – 0.220	-1.665***	-1.892 – -1.412
	0.90	0.318***	0.306 – 0.330	-2.312***	-2.655 – -2.009
	0.95	0.377***	0.361 – 0.393	-2.426***	-2.83 – -1.927
	0.99	0.521***	0.491 – 0.564	-2.226***	-3.208 – -0.849
Bray-Curtis similarities – Euclidean Distance					
Regression type	τ	Intercept	Intercept boundaries (99%)	decay rate (10^{-2})	decay rate (10^{-2}) boundaries (99%)
Linear regression	–	0.235***	0.207 – 0.257	-1.814***	-2.106 – -1.522
Quantile	0.75	0.353***	0.339 – 0.367	-2.529***	-2.867 – -2.200
	0.90	0.489***	0.473 – 0.505	-3.082***	-3.529 – -2.614
	0.95	0.552***	0.533 – 0.573	-2.938***	-3.581 – -2.206
	0.99	0.686***	0.659 – 0.726	-2.030***	-3.123 – -0.699

When analyzing the DDM separately for the dunes category, the results showed different trends. The significance of decay rates in Shifting dunes (EUNIS-N14) partially confirmed SVH. Examining the Jaccard floristic similarities vs. Euclidean distance the relationships are preserved for the linear regression, 0.75 and 0.90 quantiles, whereas only the decay rate of 0.75 quantile is negative and significant in the Bray-Curtis floristic similarities vs. Euclidean distance models (Table D3, Figure D1 – Appendix D). In the transitional Gray dunes (EUNIS-N16) and in the Invaded dunes, the Bray-Curtis floristic similarities vs. Euclidean distance models confirmed the SVH for all regressions with negative and significant decay rates, whereas in Jaccard floristic similarities vs. Euclidean distance models these two categories showed different trends (see Table D4, Table D5, Figure D2, Figure D3 – Appendix D). The transition Gray dunes verified the SVH only for the linear regression, 0.95 and 0.99 quantiles, and the Invaded dunes registered negative and significant decay rates for all models (see Table D4, Table D5, Figure D2, Figure D3 – Appendix D).

4.4. Discussion

In this study, we provided a first assessment of the relationship between floristic and spectral RS diversity in a highly dynamic landscape, such as coastal dunes. The SVH analysis, suggested the potential of RS spectral data in providing reliable information concerning floristic alpha and beta diversity in well preserved Mediterranean coastal vegetation (Shifting dunes and Transition dunes) and also on altered dunes invaded by *Carpobrotus* spp..

The relation between floristic indices of Richness, Shannon and Inverse Simpson with spectral diversity (Distance from the Spectral Centroid) gave evidence of the potential RS data for monitoring alpha biodiversity (Rocchini 2007a, Warren *et al.* 2014) on heterogeneous and fine grained

landscapes as Mediterranean dunes. As observed in other ecosystems as the savannah (Madonsela *et al.* 2017, Oldeland *et al.* 2010) and the evergreen (Torresani *et al.* 2019) and temperate forests (Meng *et al.* 2016), we have registered a positive relation between species and spectral diversity. As noticed by Nagendra *et al.* 2010 on a markedly different environment as dry tropical forests, species richness on coastal vegetation resulted strongly related with spectral variability. Furthermore, the observed link of Inverse Simpson index and Shannon index with spectral diversity values extended the field of application of SVH beyond the previous results reported for coarse and homogeneous vegetation types as forests (Torresani *et al.* 2019) and gave new evidence of the benefit of using RS for monitoring tiny dynamic mosaics as coastal dunes. Similarly, to which was registered by Madonsela *et al*, 2017 on savannah woodlands, also on coastal dunes we observed a similar relation of Inverse Simpson index and Shannon values with spectral diversity. Such results suggest that both: evenness and dominance, have a comparable weight in determining the field vs RS variability relationship.

Some studies have characterized alpha spectral diversity analyzing pixel values of single bands or indices, losing outstanding information supplied by RS images (Nagendra *et al.* 2010, Heumann *et al.* 2015, Arekhi *et al.* 2017). The use of multivariate spectral distance (Madonsela *et al.* 2017, Gholizadeh *et al.* 2020) had allowed to capitalize PlanetScope images information for describing coastal landscape variability and to relate it with species diversity. Moreover, the use of spectral bands combined with the estimates of biomass (MSAVI2) and soil organic matter content (CI, Warren *et al.* 2014) supported the potential of SVH for depicting coastal dune vegetation diversity. The consistency of vegetation plots dimension with PlanetScope pixel size, as well as the chosen indices of plant diversity and spectral variability (Rocchini *et al.* 2011, Schmidtlein and Fassnacht, 2017), have further enabled the present application on coastal dune landscapes. Concerning the observed weak goodness-of-fit of linear regressions we considered that as observed by Schmidtlein and Fassnacht (2017) also in our case it should be likely due to the low spectral resolution of RS (4 spectral bands, and 2 spectral indices).

Concerning beta diversity, the analyzed distance decay models disclosing floristic similarities (Jaccard and Bray-Curtis) and spectral Euclidean distance, showed significant relationships in all quantile regressions and linear regression considering all dunes categories. Our results gave evidence of the effectiveness of the distance decay model to describe coastal landscape beta diversity on natural as well as on invaded dunes. Increasing values in spectral distance concomitant with decreasing floristic similarity were observed in other ecosystems characterized by coarser scales (grain and extent) as temperate (Arekhi *et al.* 2017), tropical (Draper *et al.* 2018), and Mediterranean (Rocchini 2007b) forests. The observed weak decay rates in the linear regression model compared to the quantile regressions is probably related with the high number of zeros in the similarity matrix (Rocchini *et al.*

2009). It should be noted that the relation among RS spectral Euclidean distances and floristic similarities computed with species abundance are stronger than those computed with presence/absence data. The moderate decay rate of 0.99 quantile regressions in both distance decay models is probably due to minor errors on spatial matching between RS PlanetScope images and the field georeferenced plots (Rocchini *et al.* 2009, Xu *et al.* 2009). Analyzing beta diversity separately for each dune habitat, we observed a robust distance decay model on habitat types characterized by continuous vegetation cover (e.g. transition dunes - EUNIS-N16 and Invaded vegetation), whereas in the Shifting dunes (EUNIS-N14) it is weak. This weak decay trend is probably related with the intrinsic characteristics of shifting dunes given in the field by monospecific or floristically poor plots (low beta diversity) and in RS images by pixels with different degrees of bare soil and sparse vegetation (high between pixel distance). Similar to what was reported by Wang *et al.* 2018 on natural grasslands, the PlanteScope RS spatial resolution seemed too coarse to discriminate some tinny monospecific formations on shifting dunes, thus the RS beta diversity included the variability of reflectance values of pixels hosting Shifting dunes communities with different levels of vegetation cover and bare soil (Wang *et al.* 2018).

The SVH analysis for alpha and beta diversity evidenced a similar behavior of Herbaceous vegetation with the presence *Carpobrotus* spp. and natural dune vegetation (Shifting and Transition coastal dune vegetation). The relation of spectral alpha and beta diversity on *Carpobrotus* spp. invaded plots is included in the general pattern of the analyzed herbaceous coastal vegetation mosaic (Figure 15, Table 11, see also Table D5, Figure D3). These general biodiversity trends are most likely related with the coastal dune vegetation gradient that, on well preserved plots, ranges from monospecific formations (Acosta *et al.* 2007) to chamaephytic vegetation intermingled with species-rich therophytic grasslands and on invaded areas to different invasion strengths (Campoy *et al.* 2018, Carranza *et al.* 2010, Santoro *et al.* 2011).

Our results underlined the effectiveness of the Spectral Variability Hypothesis for depicting both alpha and beta diversity levels, thus supporting the application of RS data for estimating and monitoring diversity on coastal landscapes. The RS assessment of biodiversity based on Spectral Variability Hypothesis, which was already proposed for monitoring other ecosystems (Heumann *et al.* 2015, Féret and Asner, 2014, Hernández-Stefanoni *et al.* 2012), can now be extended to highly heterogeneous and dynamic mosaics as coastal dunes even on altered conditions due to plant invasions.

The observed relationship between spectral and floristic diversity in natural and invaded dune vegetation is certainly a first applied outcome of the SVH and support it as a valid approach to better

exploring variations in alpha and beta diversity and to improve the early warning system needed to prevent the biodiversity loss.

4.5. Conclusions

In this study, we provided a first assessment of the relationship between floristic and spectral RS diversity in Mediterranean coastal dunes' herbaceous vegetation, extending the applicability of the SVH also in these dynamic landscapes. Such relationship was analyzed for well-preserved European habitats (sensu 92/43/EEC) and on invaded ecosystems, providing useful insights for improving the biodiversity monitoring and reporting obligations required by the Habitats Directive and supporting field surveys. This research extended the field of applicability of RS for alpha and beta diversity assessment on coastal dunes, as well as gave evidence of the potential of using spectral bands combined with spectral indices to better depict ground biodiversity. This results had been made possible by the support of multispectral PlanetScope satellite images (https://www.planet.com/explorer/) which free access have increased the opportunities of monitoring the coastal biodiversity at low cost. Further analysis using RS images with higher spectral resolution (e.g. the open PRISMA data funded by Italian Space Agency ASI), could enhance the potential for discriminating different species (Rocchini *et al.* 2015, Rocchini 2007a), reinforcing the observed alpha field vs spectral RS diversity relationship.

4.6. Appendix D

Figure D1. Photos reporting some examples of the random vegetation plots (2x2 m) carried out in the analyzed coastal areas. A) Shifting dune plot - EUNIS code N14; b) Transition dune – EUNIS code N16, and c) an Invaded plots with *Carpobrotus* spp.

Table D1. PlanetScope images selected accounting of the geographic and temporal distribution of field collected vegetation plots. For each image we reported: the satellite, the date and the hour of acquisition, the product level, the cloud percentage, the zenith angle of acquisition, the coordinate of the center of each multispectral image, the name of cities and geographic area covered and the administrative Province in brackets (RM: Rome; LT: Latina; VT: Viterbo).

Satellite	Date	Hour	Level	Cloud (%)	Zenith angle	Coordinate of center	Cities and geographic area
0e2f	27/05/2017	09.19	3B	0	3.785	12.1936675271 41.9379571084	Passoscuro – Fiumicino, (RM)
102d	31/05/2017	09.07	3B	1	9.172	13.3541468572 41.2546364732	Terracina – Sperlonga (LT)
1001	02/05/2017	09.10	3B	1	7.728	12.4889034354 41.5776757004	Tor San Lorenzo – Ardea (RM)
1001	02/05/2017	09.10	3B	1	7.854	12.469110219 41.5104592855	Tor San Lorenzo – Ardea (RM)
1033	20/05/2018	09.25	3B	0	1.751	12.6713729304 41.5264322048	Tor San Lorenzo – Ardea (RM)
1024	26/05/2018	09.30	3B	0	1.274	11.5377771274 42.3621860846	Montalto di Castro – Tarquinia (VT)

1024	26/05/2018	09.30	3B	0	1.385	11.5180971353 42.2968474549	Montalto di Castro – Tarquinia (VT)
1035	04/05/2020	09.41	3B	0	4.390	12.431300301 41.6706456578	Castel Porziano – Torvaianica (RM)
1025	22/05/2020	09.37	3B	0	2.147	12.6736592396 41.4095091625	Astura – Nettuno (LT)
1040	31/05/2020	09.40	3B	5	5.516	13.0277337974 41.3654442532	San Felice Circeo – Sabaudia (LT)
1040	31/05/2020	09.40	3B	5	5.503	13.0085585357 41.3000635355	San Felice Circeo – Sabaudia (LT)
1040	31/05/2020	09.40	3B	0	5.504	12.9888313645 41.234645998	San Felice Circeo – Sabaudia (LT)

Table D2. Results of permutation marginal regressions, indicating the significance of estimates in all three linear regression (Species Richness – Distance to Centroid, Shannon Index – Distance to centroid, Inverse Simpson Index – Distance to Centroid) after 5000 permutations. P-value: * < 0.05; ** < 0.01; *** < 0.001.

Species Richness – Distance to centroid	p-value after 5000 permutations
Distance to centroid: Shifting dunes	0.0001***
Distance to centroid: Transition dunes	0.0001***
Distance to centroid: Invaded dunes	0.0001***
Shannon Index – Distance to centroid	**p-value after 5000 permutations**
Distance to centroid: Shifting dunes	0.0212*
Distance to centroid: Transition dunes	0.0006***
Distance to centroid: Invaded dunes	0.0010**
Inverse Simpson Index – Distance to centroid	**p-value after 5000 permutations**
Distance to centroid: Shifting dunes	0.0086*
Distance to centroid: Transition dunes	0.0004***
Distance to centroid: Invaded dunes	0.0004***

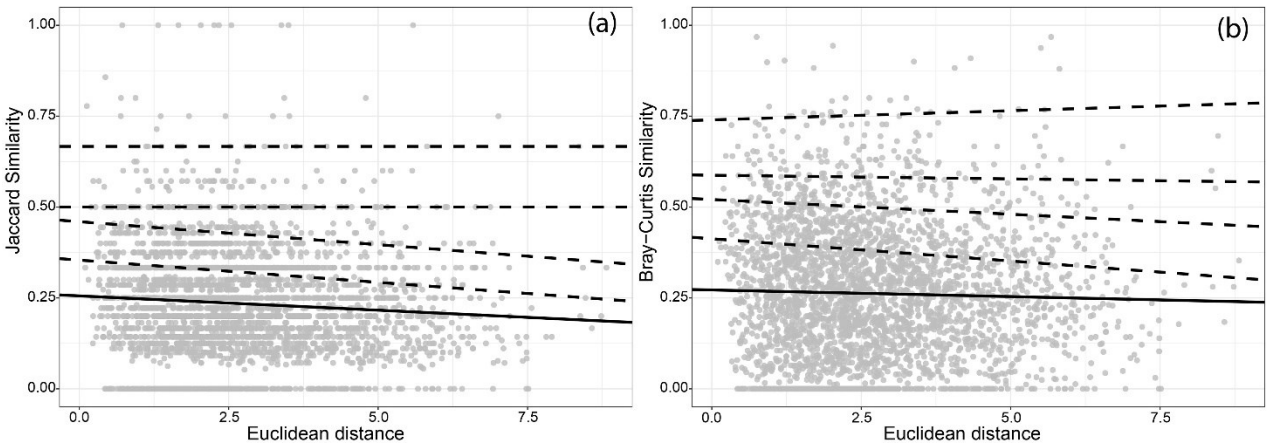

Figure D1. Distance Decay Models of species similarity, Jaccard (**a**) and Bray-Curtis (**b**), versus spectral distance (spectral pairwise Euclidean distance) considering Shifting dunes (N14 EUNIS category). The linear regression is described by solid line, the quantile regressions considering four different τ (from upper to lower lines: 0.99, 0.95, 0.90, 0.75) are reported by dashed lines. Gray dots represent the sampling plots.

Table D3. Results of Distance Decay Models calculated by linear regression model and quantile regression at four different τ values (from upper to lower lines: 0.99, 0.95, 0.9, 0.75), considering the vegetation plots and the pixels of Shifting dunes (N14 EUNIS category). P-value: * < 0.05; ** < 0.01; *** < 0.001.

Jaccard similarities – Euclidean distance

Regression type	τ	Intercept	Intercept boundaries (99%)	decay rate	decay rate boundaries (99%)
Linear regression	–	0.256***	0.238 – 0.275	-0.049***	-0.084 – -0.013
Quantile	0.75	0.353***	0.333 – 0.371	-0.073***	-0.106 – 0.000
	0.90	0.463***	0.435 – 0.505	-0.082***	-0.160 – -0.033
	0.95	0.500***	0.500 – 0.568	0.000	-0.156 – 0.000
	0.99	0.667***	0.631 – 0.854	0.000	-0.262 – 0.123

Bray-Curtis similarities – Euclidean Distance

Regression type	τ	Intercept	Intercept boundaries (99%)	decay rate (10^{-2})	decay rate (10^{-2}) boundaries (99%)
Linear regression	–	0.272***	0.250 – 0.295	-0.365	-1.081 – 0.351
Quantile	0.75	0.413***	0.386 – 0.440	-1.222***	-1.963 – -0.379
	0.90	0.521***	0.484 – 0.564	-0.810	-2.245 – 0.481
	0.95	0.587***	0.555 – 0.648	-0.201	-2.048 – 1.047
	0.99	0.740***	0.688 – 0.796	0.505	-1.202 – 4.509

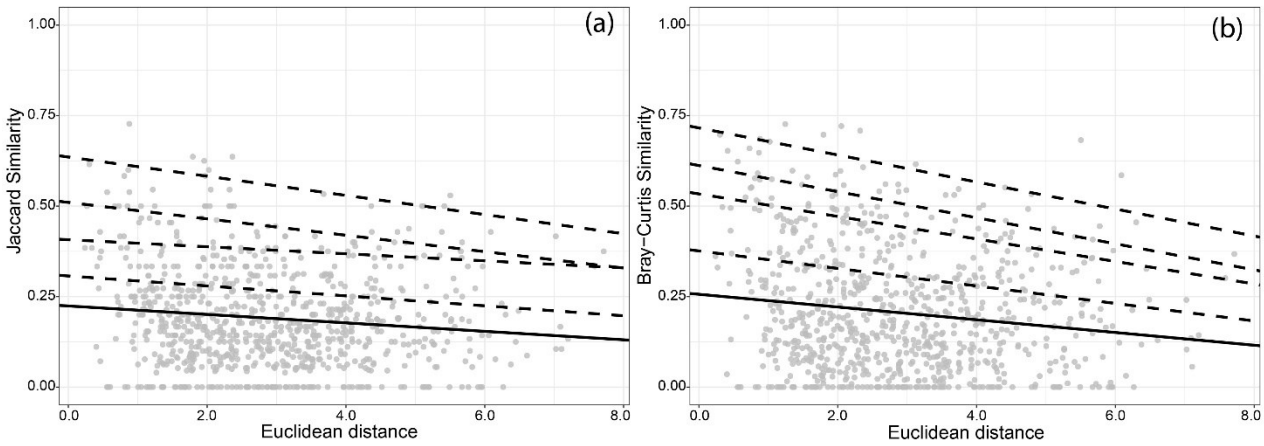

Figure D2. Distance Decay Models of species similarity, Jaccard (**a**) and Bray-Curtis (**b**), versus spectral distance (spectral pairwise Euclidean distance) considering the vegetation plots and the pixels of Transition dunes (N16 EUNIS category. The linear regression is described by solid line, the quantile regressions considering four different τ (from upper to lower lines: 0.99, 0.95, 0.90, 0.75) are reported by dashed lines. Gray dots represent the sampling plots.

Table D4. Results of Distance Decay Models calculated by linear regression model and quantile regression at four different τ values (from upper to lower lines: 0.99, 0.95, 0.9, 0.75), considering the vegetation plots and the pixels of Transition dunes (N16 EUNIS category). P-value: * < 0.05; ** < 0.01; *** < 0.001.

Jaccard similarities – Euclidean distance

Regression type	τ	Intercept	Intercept boundaries (99%)	decay rate (10^{-2})	decay rate (10^{-2}) boundaries (99%)
Linear regression	–	0.224***	0.189 – 0.260	-1.168***	-2.268 – -0.067
Quantile	0.75	0.307***	0.267 – 0.364	-1.374	-3.022 – 0.127
	0.90	0.407***	0.357 – 0.509	-0.973	-4.031 – 0.403
	0.95	0.510***	0.430 – 0.573	-2.267***	-3.911 – -0.276
	0.99	0.635***	0.576 – 0.749	-2.649**	-4.132 – -0.374

Bray-Curtis similarities – Euclidean Distance

Regression type	τ	Intercept	Intercept boundaries (99%)	decay rate (10^{-2})	decay rate (10^{-2}) boundaries (99%)
Linear regression	–	0.256***	0.214 – 0.299	-1.759***	-3.082 – -0.436
Quantile	0.75	0.376***	0.316 – 0.452	-2.417***	-4.427 – -0.441
	0.90	0.534***	0.491 – 0.594	-3.108***	-4.892 – -1.718
	0.95	0.612***	0.535 – 0.673	-3.602***	-5.302 – -1.646
	0.99	0.716***	0.658 – 0.804	-3.73*	-5.459 – 0.581

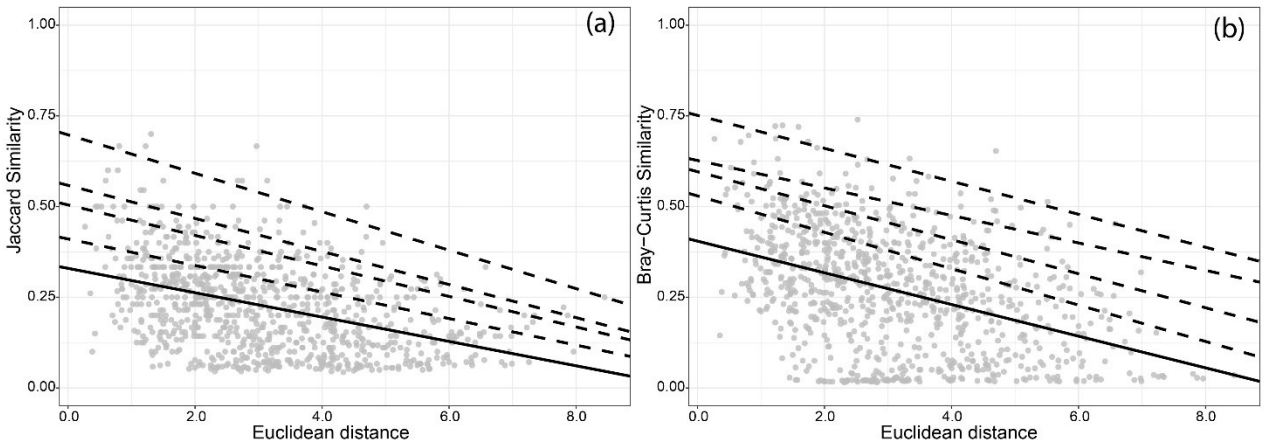

Figure D3. Distance Decay Models of species similarity, Jaccard (**a**) and Bray-Curtis (**b**), versus spectral distance (Euclidean distance) considering the vegetation plots and the pixels invaded by *Carpobrotus* spp., Invaded category. The linear regression is described by solid line, the quantile regressions considering four different τ (from upper to lower lines: 0.99, 0.95, 0.90, 0.75) are reported by dashed lines. Gray dots represent the sampling plots.

Table D5. Results of Distance Decay Models calculated by linear regression model and quantile regression at four different τ values (from upper to lower lines: 0.99, 0.95, 0.9, 0.75), considering the vegetation plots and the pixels invaded by *Carpobrotus* spp., Invaded category. P-value: * < 0.05; ** < 0.01; *** < 0.001.

Jaccard similarities – Euclidean distance					
Regression type	τ	Intercept	Intercept boundaries (99%)	decay rate (10^{-2})	decay rate (10^{-2}) boundaries (99%)
Linear regression	–	0.330***	0.301 – 0.358	-3.357***	-3.018 – -3.577
Quantile	0.75	0.411***	0.383 – 0.445	-3.657***	-4.560 – -2.815
	0.90	0.505***	0.460 – 0.525	-4.204***	-4.943 – -3.078
	0.95	0.558***	0.503 – 0.609	-4.557***	-5.571 – -3.126
	0.99	0.698***	0.626 – 0.791	-5.299***	-6.832 – -2.232
Bray-Curtis similarities – Euclidean Distance					
Regression type	τ	Intercept	Intercept boundaries (99%)	decay rate (10^{-2})	decay rate (10^{-2}) boundaries (99%)
Linear regression	–	0.405***	0.368 – 0.441	-4.367***	-5.421 – -3.313
Quantile	0.75	0.529***	0.484 – 0.564	-5.016***	-6.131 – -3.679
	0.90	0.596***	0.551 – 0.639	-4.688***	-6.027 – -2.938
	0.95	0.627***	0.562 – 0.721	-3.788***	-6.789 – -1.964
	0.99	0.751***	0.717 – 0.820	-4.544***	-6.344 – -2.105

Conclusions and Future Perspectives

This research presented some examples depicting the great potential of some free RS data to develop innovative monitoring tools on coastal dune landscapes. Different uses of RS data and objective processing procedures offering support to environmental monitoring and decision-making are proposed and tested. The thesis gave evidence of the appropriateness of the spatial, temporal and spectral resolution of some free RS data (e.g. Sentinel-2, PlanetScope, LiDAR) to analyze dynamic and heterogeneous landscapes. Specifically, new procedures are proposed aimed at reducing the gap of RS applications on coastal dunes that being distributed on narrow strips hosting tinny complex and dynamic ecosystems were hardly detectable by the old satellite missions.

The first chapter, dealing with the statistical analysis and modeling of *A saligna* invasion on coastal dunes, gave evidence of the usefulness of RS data on determining the drivers of invasion and on predicting the areas in which invasion is most likely to occur.

The thesis also proposed and tested new approaches using semi-automatic and automatic procedures and based on spectral indices depicting the main components the mosaic (vegetation, bare surfaces and water) which resulted particularly effective for mapping coastal dune environments. The availability of free daily/weekly multispectral satellite images effectively supported the analysis of RS biomass phenology and of the temporal variability of vegetation, soil and water (described in second and third chapters) which effectively supported coastal dune landscape analysis and monitoring.

The last chapter dealt with the application of RS data for ecosystem biodiversity monitoring. Specifically, the observed relationship between the field measured plant diversity and the RS spectral variability on coastal dunes, gave new evidence of the potential of RS for biodiversity analysis and monitoring on coastal dunes.

However, the spatial and spectral resolution of the actual free RS data, are still too coarse to fully describe the complexity of coastal dune environments. The semi-automatic and automatic classification of RS satellite data on these ecosystems gave poor results on some herbaceous dune habitats. Similarly, the observed relationship between field measured and RS biodiversity for some ecosystems resulted weak suggesting the need of further research and finer scale RS instruments.

The new RS instruments currently in design or testing phase should foster in the near future the new applications of RS data for environmental monitoring. For instance, the new hyperspectral PRISMA satellites launched by the Agenzia Spaziale Italiana (ASI) on 22/03/2019 and the EnMAP hyperspectral satellite planned by the German Aerospace Center (DLR) and the German Research

Centre for Geosciences (GFZ) in collaboration with European Space Agency (ASI) will offer free satellite images with over 200 spectral bands and improved spatial and temporal resolutions.
Furthermore, the increasing utilization of Unmanned Aerial Vehicle (UAV) gave new possibilities for local photogrammetric analysis using several instruments (e.g. RGB, multispectral sensor, LiDAR, etc.). UAVs offer new possibilities for exploring small areas of interest with very high spatial resolutions (up to 1 cm).

Acknowledgments

I acknowledge the colleagues and professors for their consistent collaboration and constructive exchanges which help me to develop the different steps of the present PhD thesis.
In particular I acknowledge for the collaboration in chapter 1: Manuele Bazzichetto, Marco Malavasi, Silvia Giulio, the professor Angela Stanisci and in particular the two tutors, the professors Alicia Teresa Acosta and Maria Laura Carranza.
I acknowledge for the collaboration in chapter 2: Silvia Giulio, Marco Malavasi, Marta Gaia Sperandii and the two tutors, the professors Alicia Teresa Acosta and Maria Laura.
I acknowledge for the collaboration in chapter 3: Mirko Di Febbraro, Marco Malavasi, Silvia Giulio and the two tutors, the professors Alicia Teresa Acosta and Maria Laura Carranza.
I acknowledge for the collaboration in chapter 4: Silvia Cascone, Mirko Di Febbraro, Ludovico Frate and the two tutors, the professors Alicia Teresa Acosta and Maria Laura Carranza.
I acknowledge my colleagues of the Vegetation Science laboratory in University of Roma 3 and of the EnvixLab in University of Molise.

References

Abd El-Gawad AM, El-Amier YA (2015) Allelopathy and potential impact of invasive *Acacia saligna* (Labill.) Wendl. on plant diversity in the Nile delta coast of Egypt. *Int. J. Environ. Res.* 9:923–932.

Acosta ATR, Blasi C, Carranza ML, Ricotta C, Stanisci A (2003) Quantifying ecological mosaic connectivity and hemeroby with a new topoecological index. *Phytocoenologia* 33, 623-631. https://10.1127/0340-269X/2003/0033-0623

Acosta ATR, Carranza ML, Izzi F (2005) Combining Land cover mapping of coastal dunes with vegetation analyses. *App. Veg. Sci.* 8, 133-138. https://doi.org/10.1111/j.1654-109X.2005.tb00638.x

Acosta ATR, Ercole V, Stanisci A, De Patta Pillar V, Blasi C (2007) Coastal vegetation zonation and dune morphology in some Mediterranean ecosystems. *J. Coastal Res.* 23(6), 1518-1524. https//doi.org/10.2112/05-0589.1

Acosta ATR, Carranza ML, Izzi CF (2009) Are there habitats that contribute best to plant species diversity in coastal dunes? *Biodivers. Conserv.* 18, 1087-1098. http://doi.org/ 10.1007/s10531-008-9454-9

Adam E, Mutanga O, Rugege D (2010) Multispectral and hyperspectral remote sensing for identification and mapping of wetland vegetation: a review. *Wetl. Ecol. Manag*. 18, 281-296. https://doi.org/10.1007/s11273-009-9169-z

Adamo M, Tarantino C, Tomaselli V, Veronico G, Nagendra H, Blonda, P. (2016) Habitat mapping of coastal wetlands using expert knowledge and Earth observation data. *J. Appl. Ecol.* 53, 1521-1532. http://doi.org/10.1111/1365-2664.12695

Anderson MJ, Robinson J (2001) Permutation Tests for Linear Models. *Aust. Nz. J. Stat.* 43, 75-88. https//doi.org/10.1111/1467-842X.00156

Arekhi M, Yilmaz OY, Yilmaz H, Akyüz YF (2017) Can tree species diversity be assessed with Landsat data in a temperate forest? *Environ. Monit. Assess.* 189(11), 586. https//doi.org/10.1007/s10661-017-6295-6

Arévalo JR, Delgado JD, Otto R, Naranjo A, Salas M, Fernández-Palacios M (2005) Distribution of alien vs. native plant species in roadside communities along an altitudinal gradient in Tenerife and Gran Canaria (Canary Islands). *Perspect. Plant Ec.* 7, 185–202. https://doi.org/10.1016/j.ppees.2005.09.003

Bachaoui B, Bachaoui EM, Maimouni S, Lhissou R, El Harti A, El Ghmari A (2014) The use of spectral and geomorphometric data for water erosion mapping in El Ksiba region in the central High Atlas Mountains of Morocco. *Applied Geomatics* 6, 159-169. https/doi.org/10.1007/s12518-014-0130-3

Bajocco S, Ferrara C, Alivernini A, Bascietto M, Ricotta C Remotely-sensed phenology of Italian forest: going beyond the species. *Int. J. Appl. Earth Obs.* 2019, 74, 314–321. https://doi.org/10.1016/j.jag.2018.10.003

Bar Kutiel P, Cohen O, Shoshany M (2004) Invasion rate of the alien species *Acacia saligna* within coastal sand dune habitats in Israel. *Isr. J. Plant Sci.* 52, 115–124. https://dx.doi.org/10.1560/8BK5-GFVT-NQ9J-TLN8

Bartolucci F, Peruzzi L, Galasso G, Albano A, Alessandrini A, Ardenghi N M G, Astuti G, Bacchetta G, Ballelli S, Banfi E, et al. (2018) An updated checklist of the vascular flora native to Italy. *Plant Biosyst.* 152(2), 179-303. https://doi.org/10.1080/11263504.2017.1419996

Bascietto M (2018) Compute Rao's diversity index on numeric vectors and matrices. R package version 0.1.0. https://github.com/mbask/spacetimerao/.

Bazzichetto M, Malavasi M, Acosta ATR, Carranza ML (2016) How does dune morphology shape coastal EC habitats occurrence? A remote sensing approach using airborne LiDAR on the Mediterranean coast. *Ecol. Indic.* 71, 618-626. http://dx.doi.org/10.1016/j.ecolind.2016.07.044

Bazzichetto M, Malavasi M, Barták V, Acosta ATR, Moudrý V, Carranza ML (2018a) Modeling plant invasion on Mediterranean coastal landscapes: an integrative approach using remotely sensed data. *Landscape Urban Plan.* 171, 98-106. https//doi.org/10.1016/j.landurbplan.2017.11.006

Bazzichetto M, Malavasi M, Bartak V, Acosta ATR, Rocchini D, Carranza ML (2018b) Plant invasion risk: a quest for invasive species distribution modeling in managing Natura 2000 sites. *Ecol. Indic.* 95, 311–319. https://doi.org/10.1016/j.ecolind.2018.07.046

Bekkar M, Djemaa HK, Alitouche TA (2013) Evaluation measures for models assessment over imbalanced data set. *Journal of Information Engineering and Applications* 3(10), 27-39.

Belgiu M, Csillik O (2018) Sentinel-2 cropland mapping using pixel-based and object-based time-weighted dynamic time warping analysis. *Remote Sens. Environ.* 204, 509–523. http://dx.doi.org/10.1016/j.rse.2017.10.005

Bell DT, Plummer JA, Taylor SK (1993) Seed germination ecology in southwestern Western Australia. *Bot. Rev.* 59(1), 24–73. https://doi.org/10.1007/BF02856612

Bellard C, Leroy B, Thuiller W, Rysman JF, Courchamp F (2016) Major drivers of invasion risks throughout the world. *Ecosphere* 7, 1–14. https://doi.org/10.1002/ecs2.1241

Berger M, Moreno J, Johannessen JA, Levelt PF, Hanssen RF (2012) ESA's sentinel missions in support of Earth system science. *Remote Sens. Environ.* 120, 84-90. https://doi.org/10.1016/j.rse.2011.07.023

Bertini F, Brand O, Carlier S, Del Bello U, Drusch M, Duca R, Fernandez V, Ferrario C, Ferreira MH, Isola C, et al. (2012) Sentinel-2 ESA's Optical High-Resolution Mission for GMES Operational Services. Noordwjik, Netherlands: ESA Communications,pp. 1–70.

Bertoni R (2012) La Rete Italiana per la ricerca ecologica a lungo termine (LTER-Italia). Roma: Aracne Editrice pp. 99–107.
Bonari G, Acosta ATR, Angiolini C (2017) Mediterranean coastal pine forest stands: Understorey distinctiveness or not? *Forest Ecol. Manag.* 391: 19 - 28. https://doi.org/10.1016/j.foreco.2017.02.002.
Bonari G, Acosta ATR, Angiolini C (2018) EU priority habitats: rethinking Mediterranean coastal pine forests. *Rendiconti Lincei. Scienze Fisiche e Naturali* 29: 295 - 307. https://doi.org/10.1007/s12210-018-0684-9
Borchers HW pracma: Pratical numerical math functions, R Package Version 2.2.9. 2019. https://cran.r-project.org/web/packages/pracma/index.html.
Boughorbel S, Jarray F, El-Anbari M (2017) Optimal classifier for imbalanced data using Matthews Correlation Coefficient metric. *PloS One* 12(6), 1-17. https://doi.org/10.1371/journal. pone.0177678
Brauner N, Shacham M (1998) Role of Range and Precision of the Independent Variable in Regression of Data. *AIChE J.* 44, 603–611. https://doi.org/10.1002/aic.690440311
Bray JR, Curtis JT (1957) An ordination of the upland forest communities of Southern Wisconsin. *Ecol. Monogr.* 27(4), 325 – 349. https//doi.org/10.2307/1942268
Breiman L, Friedman JH, Olshen RA, Stone CJ (1984) Classification and regression trees, 3rd ed, Boca Ration, Florida, USA: Chapman & Hall, pp. 1–358.
Breiman L (2001) Random Forests. *Mach. Learn.* 45, 5–32. https://doi.org/10.1023/A:1010933404324
Breusch T S, Pagan AR (1979) A simple test for heteroscedasticity and random coefficient variation. *Econometrica* 47, 1287-1294. https://doi.org/10.2307/1911963
Brothers TS, Spingarn A (1992) Forest fragmentation and alien plant invasion of central Indiana old- growth forests. *Conserv. Biol.* 6, 91–100. https://doi.org/10.1046/j.1523-1739.1992.610091.x
Brown SC, Lester RE, Versace VL, Fawcett J, Laurenson L (2014) Hydrologic landscape regionalization using deductive classification and random forests. *PLoS ONE* 9, 1–20. https://doi.org/10.1371/journal.pone.0112856
Burnham KM, Lee TD (2010) Canopy gaps facilitate establishment, growth, and reproduction of invasive *Frangula alnus* in a *Tsuga canadensis* dominated forest. *Biol. Invasions* 12, 1509–1520. htpps://doi.org/10.1007/s10530-009-9563-8
Cade BS, Noon BR (2003) A gentle introduction to quantile regression for ecologists. *Front. Ecol. Environ.* 1(8), 412-420. https//doi.org/10.1890/1540-9295(2003)001[0412:AGITQR]2.0.CO;2
Calabrese V, Frate L, Iannotta F, Prisco I, Stanisci A (2017) *Acacia saligna*: an invasive species on the coast of Molise (southern Italy). *Foresta - Journal of Silviculture and Forest Ecology* 14, 28–33. htpps://doi.org/10.3832/efor2211-013
Calinski T, Harabasz J (1974) A dendrite method for cluster analysis. *Commun. Stat*. 3(1), 1-27.
Campbell JB, Wynne RH (2011) Introduction to Remote Sensing, 5th ed, New York: the Guilford Press, pp. 1 – 622.
Campoy JG, Acosta ATR, Affre L, Barreiro R, Brundu G, Buisson E, González L, Buisson E, González L, Lema M (2018) Monographs of invasive plants in Europe: Carpobrotus. *Botany Letters* 165(3-4), 440-475. https//doi.org/10.1080/23818107.2018.1487884
Carboni M, Carranza ML, Acosta ATR (2009) Assessing conservation status on coastal dunes: a multiscale approach. *Landscape Urban Plan.* 91, 17-25. https://10.1016/j.landurbplan.2008.11.004
Carone MT, Guisan A, Cianfrani C, Simoniello T, Loy A, Carranza ML (2014). A multi-temporal approach to model endangered species distribution in Europe: the case of the Eurasian otter in Italy. *Ecol. Model.* 274: 21–28. https://doi.org/10.1016/j.ecolmodel.2013.11.027
Carranza ML, Acosta ATR, Stanisci A, Pirone G, Ciaschetti G (2008) Ecosystem classification for EU habitat distribution assessment in sandy coastal environments: An application in central Italy. *Environ. Monit. Assess.* 140, 99 – 107. https://doi.org/10.1007/s10661-007-9851-7
Carranza ML, Carboni M, Feola S, Acosta ATR (2010) Landscape-scale patterns of alien plant species on coastal dune: the case of iceplant in central Italy. *Appl. Veg. Sci.* 13, 135-145. https://doi.org/10.1111/j.1654-109X.2009.01065.x
Carranza ML, Frate L, Paura B (2012) Structure, ecology and plant richness patterns in fragmented beech forests. *Plant Ecol. Divers.* 5(4), 541-551. https://doi.org/10.1080/17550874.2012.740509
Catford JA, Jansson R, Nilsson C (2009) Reducing redundancy in invasion ecology by integrating hypotheses into a single theoretical framework. *Divers. Distrib.* 15, 22-40. https://doi.org/10.1111/j.1472-4642.2008.00521.x
Ceballos G, Ehrlich PR, Barnosky AD, García A, Pringle RM, Palmer TM (2015) Accelerated modern human–induced species losses: Entering the sixth mass extinction. *Sci. Adv.* 1(5), e1400253. htpps://doi.org/10.1126/sciadv.1400253
Celesti-Grapow L, Pretto F, Carli E, Blasi C (2010) Flora vascolare alloctona e invasive delle regioni d'Italia. Roma: Casa Editrice Università La Sapienza, pp. 1-208.
Chatterjee S, Hadi AS Regression analysis by example, 5nd ed, Hoboken, New Jersey, USA: John Wiley & Sons, Inc., pp. 248-251.
Chatziantoniou A, Petropoulos GP, Psomiadis E (2017) Co-orbital Sentinel 1 and 2 for LULC mapping with emphasis on wetlands in a Mediterranean setting based on machine learning. *Remote Sens.* 9, 1259. https//doi.org/10.3390/rs9121259

Chytrý M, Tichý L, Hennekens SM, Knollová I, Janssen JAM, Rodwell JS, Peterka T, Marcenò C, Landucci F, Danihelka J, et al. (2020) EUNIS habitat classification: expert system, characteristic species combinations and distribution maps of European habitats. *Appl. Veg. Sci.* 00, 1-28 https//doi.org/10.1111/avsc.12519

Cohen O, Riov J, Katan J, Gamliel A, Bar Kutiel P (2008) Reducing Persistent Seed Banks of Invasive Plants by Soil Solarization—The Case of *Acacia saligna*. *Weed Sci.* 56, 860–865. https://doi.org/10.1614/WS-08-073.1

Cohen O, Bar Kutiel P (2017) The impact of *Acacia saligna* invasion on the indigenous vegetation in various coastal habitats in Israel and its implication for nature conservation. *Isr. J. Plant Sci.* 1–11. https://doi.org/10.1080/07929978.2016.1275362

Colditz RR (2015) An evaluation of different training sample allocation schemes for discrete and continuous land cover classification using decision tree-based algorithms. *Remote Sens.* 7, 9655-9681. https://doi.org/10.3390/rs70809655

Congalton RG, Green K (2009) Assessing the accuracy of remotely sensed data. Principles and practices, 2nd ed, Boca Raton, FL, USA: CRC Press Taylor & Francis Group, pp. 1–183.

Conser C, Connor EF (2009) Assessing the residual effects of *Carpobrotus edulis* invasion, implications for restoration. *Biol. Invasions* 11(2), 349-358. https//doi.org/10.1007/s10530-008-9252-z

Cook RD, Weisberg S (1983) Diagnostic for heteroscedasticity in regression. *Biometrika* 70, 1-10. https://doi.org/10.2307/2335938

Cooley SW, Smith LC, Stepan L, Mascaro J (2017) Tracking dynamic northern surface water changes with high-frequency Planet CubeSat imagery. *Remote Sens.* 9, 1306. https//doi.org/10.3390/rs9121306

Couch C, Leontidou L, Petschel-Held G (2007) Urban Sprawl in Europe: landscapes, Land-use Change and Policy, 1st ed., Oxford: Wiley-Blackwell, pp. 1-294.

Colautti RI, Grigorovich IA, MacIsaac HJ (2006) Propagule pressure: A null model for biological invasions. *Biol. Invasions* 8, 1023–1037. https://doi.org/10.1007/s10530-005-3735-y

Cori B (1999) Spatial dynamics of Mediterranean coastal regions. *J. Coast. Conserv.* 5, 105-112. https://doi.org/10.1007/BF02802747

Cutler DR, Edwards TC Jr, Beard KH, Cutler A, Hess KT, Gibson J, Lawler JJ (2007) Random forests for classification in ecology. *Ecology* 88, 2783–2792. https://doi.org/10.1890/07-0539.1

Davies D, Bouldin D (1979) A cluster separation measure. *IEEE T. Pattern Anal*. 1(4), 224.227.

Del Vecchio S, Acosta A, Stanisci A (2013) The impact of *Acacia saligna* invasion on Italian coastal dune EC habitats. *C. R. Biol* 336, 364–369. https//doi.org/10.1016/j.crvi.2013.06.004

Díaz S, Demissew S, Carabias J, Joly C, Lonsdale M, Ash N, Larigauderie A, Adhikari JR, Arico S, Báldi A, et al. (2015) The IPBES conceptual framework—connecting nature and people. *Curr. Opin. Env. Sust.* 14, 1–16. https//doi.org/10.1016/j.cosust.2014.11.002

Díaz-Delgado R, Lucas R, Hurford C (2017) The roles of remote sensing in nature conservation. A pratical guide and case studies, 1st ed, Cham, Switzerland: Springer, pp. 1-318.

Donohue RJ, McVicar TR, Roderick ML (2009) Climate-related trends in Australian vegetation cover as inferred from satellite observations, 1981–2006. *Glob. Change Biol.* 15, 1025–1039. https://doi.org/10.1111/j.1365-2486.2008.01746.x

Doody JP (2013) Sand dune conservation, management and restoration, 1st ed, Dordrecht: Springer, pp. 201-235 (in Netherlands).

Dorais A, Cardille J (2011) Strategies for incorporating high-resolution Google Earth databases to guide and validate classifications: Understanding deforestation in Borneo. *Remote Sens.* 3, 1157–1176. https://doi.org/10.3390/rs3061157

Drius M, Malavasi M, Acosta ATR, Ricotta C, Carranza ML (2013) Boundary-based analysis for the assessment of coastal dune landscape integrity over time. *Appl. Geo.* 45:41–48. https://doi.org/10.1016/j.apgeog.2013.08.003

Drius M, Jones L, Marzialetti F, De Francesco MC, Stanisci A, Carranza ML (2019) Not just a sandy beach. The multi-service value of Mediterranean coastal dunes. *Sci. Total Environ.* 668, 1139-1155. https://doi.org/10.1016/j.scitotenv.2019.02.364

Drusch M, Del Bello U, Carlier S, Colin O, Fernandez V, Gascon F, Hoersch B, Isola C, Labertini P, Martimort P, et al. (2012) Sentinel-2: ESA's optical high-resolution mission for GMES operational services. *Remote Sens. Environ.* 120, 25–36. https://doi.org/10.1016/j.rse.2011.11.026

Dudley KL, Dennison PE, Roth KL, Roberts DA, Coates AR (2015) A multi-temporal spectral library approach for mapping vegetation species across spatial and temporal phenological gradients. *Remote Sens. Environ.* 167, 121 – 134. http://dx.doi.org/10.1016/j.rse.2015.05.004

Elith J, Leathwick JR (2009) Species Distribution Models: Ecological Explanation and Prediction Across Space and Time. *Annu. Rev. Ecol. Evol. S.* 40(1), 677–697. https://doi.org/10.1146/annurev.ecolsys.110308.120159

Elith J, Kearney M, Philips S (2010) The art of modelling range-shifting species. *Methods Ecol. Evol*. 1: 330-342. https://doi.org/10.1111/j.2041-210X.2010.00036.x

Eppstein MJ, Molofsky J (2007) Invasiveness in plant communities with feedbacks. *Ecol. Lett.* 10, 253–263. https://doi.org/10.1111/j.1461-0248.2007.01017.x

Escadafal R (1993) Remote sensing of soil color: principles and applications. *Remote Sensing Reviews* 7, 261-279. https//doi.org/10.1080/02757259309532181

Estes LD, Reillo PR, Mwangi AG, Okin GS, Shugart HH (2010) Remote sensing of structural complexity indices for habitat and species distribution modeling *Remote Sens. Environ.* 114, 792-804. https://doi.org/10.1016/j.rse.2009.11.016

Evans D (2006) The habitats of the European Union Habitats directive. *Biol. Environ.* 106B(3), 167-173. https//doi.org/10.3318/BIOE.2006.106.3.167

Feagin RA, Sherman DJ, Grant WE (2005) Coastal erosion, global sea-level rise, and the loss of sand dune plant habitats. *Front. Ecol. Environ.* 3, 359–364. https://doi.org/10.1890/1540-9295(2005)003[0359:CEGSRA]2.0.CO;2

Falcucci A, Maiorano L, Boitani L (2007) Changes in land-use/land-cover patterns in Italy and their implications for biodiversity conservation. *Landscape Ecol.* 22, 617–631. https://doi.org/10.1007/s10980-006-9056-4

Féret JB, Asner GP (2014) Mapping tropical forest canopy diversity using high-fidelity imaging spectroscopy. *Ecol. Appl.* 24(6), 1289-1296. https//doi.org/10.1890/13-1824.1

Fisher RA, Corbet AS, Williams CB (1943) The relation between the number of species and the number of individuals in a random sample of an animal population. *J. Anim. Ecol.* 12(1), 42-58. https://doi.org/10.2307/1411

Flory SL, Clay K (2006) Invasive shrub distribution varies with distance to roads and stand age in eastern deciduous forests in Indiana, USA. *Plant Ecol.* 184:131–141. https://doi.org/10.1007/s11258-005-9057-4

Forey E, Lortie CJ, Michalet R (2009) Spatial patterns of association at local and regional scales in coastal sand dune communities. *J. Veg. Sci.* 20, 916–925. https://doi.org/10.1111/j.1654-1103.2009.01095.x

Franklin J (2010) Mapping species distributions: spatial inference and prediction, 1st ed. New York: Cambridge University Press, pp. 1 - 320.

Frossard J, Renaud O (2019) permuco: Permutation Tests for Regression, (repeated measures) ANOVA / ANCOVA and comparison of signals, R Package Version 1.1.0. https://cran.r-project.org/web/packages/permuco/index.html

Fu B, Burgher I (2015) Riparian vegetation NDVI dynamics and its relationships with climate, surface water and groundwater. *J. Arid Environ*. 113, 59-68. http://dx.doi.org/10.1016/j.jaridenv.2014.09.010

Galasso G, Conti F, Peruzzi L, Ardengi N M G, Banfi E, Celesti-Grapow L, Albano A, Alessandrini A, Bacchetta G, Ballelli S, et al. (2018) *Plant Biosyst.* 152(2), 179-303. https://doi.org/10.1080/11263504.2018.1441197

Gallien L, Carboni M, Münkemüller T (2014) Identifying the signal of environmental filtering and competition in invasion patterns - a contest of approaches from community ecology. *Methods Ecol. Evol.* 5, 1002–1011. https://doi.org/10.1111/2041-210X.12257

Gastwirth JL (1972) The estimation of the Lorenz curve and Gini index. *Rev. Econ. Stat* 54(3), 306-316.

Gehlhausen SM, Schwartz MW, Augspurger CK (2000) Vegetation and microclimatic edge effects in two mixed-mesophytic forest fragments. *Plant Ecol.* 147, 21–35. https://doi.org/10.1023/A:1009846507652

Genovesi P, Carboneras C, Vilà M, Walton P (2015) EU adopts innovative legislation on invasive species: a step towards a global response to biological invasions? *Biol Invasions* 17,1307–1311. https://doi.org/10.1007/s10530-014-0817-8

Geurts P, Ernest D, Wehenkel L (2006) Extremely randomized trees. *Machine Learning* 63, 3-42. https://doi.org/10.1007/s10994-006-6226-1

Gillespie TW, Foody GM, Rocchini D, Giorgi AP, Saatchi S (2008) Measuring and modelling biodiversity from space *Prog. Phys. Geog.* 32(2), 203-221. https://doi.org/10.1177/0309133308093606

Gislason PO, Benediktsson JA, Sveinsson JR (2006) Random forests for land cover classification. *Pattern Recognit. Lett.* 27, 294-300. https//doi.org/10.1016/j.patrec.2005.08.011

Ghimire B, Rogan J, Miller J (2010) Contextual land-cover classification: incorporating spatial dependence in land-cover classification models using random forests and the Getis statistic. *Remote Sens. Lett.* 1, 45–54. https://doi.org/10.1080/01431160903252327

Gholizadeh H, Gamon JA, Helzet CJ, Cavender-Bares J (2020) Multi-temporal assessment of grassland α- and β-diversity using hyperspectral imaging. *Ecol. Appl.* 30(7), e02145. https//doi.org/10.1002/eap.2145

Goslee SC (2010) Correlation analysis of dissimilarity matrices. *Plant Ecol.* 206, 279-286. https://doi.org/10.1007/s11258-009-9641-0

Grabska E, Hostert P, Pflugmacher D, Ostapowicz K (2019) Forest stand species mapping using the Sentinel-2 time series. *Remote Sens.* 11, 1197-1221. https//doi.org/10.3390/rs11101197

Gray AN (2005) Eight nonnative plants in western Oregon forests: Associations with environment and management. *Environ. Monit. Assess.* 100, 109–127. https://doi.org/10.1007/s10661-005-7060-9

Guisan A, Thuiller W (2005) Predicting species distribution: Offering more than simple habitat models. *Ecol. Lett.* 8,993–1009. https://doi.org/10.1111/j.1461-0248.2005.00792.x

Gutierres F, Gil A, Reis E, Lobo A, Neto C, Calado H, Costa JC (2011) Acacia saligna (Labill.) H. Wendl in the Sesimbra County: invaded habitats and potential distribution modeling. *J. Coast. Res.* 64, 403–407.

Izzi CF, Acosta A, Carranza ML, Ciaschetti G, Conti F, Di Martino L, D'Orazio, Frattaroli A, Pirone G, Stanisci A (2007) Sampling the vascular flora in coastal dune ecosystems of Central Italy. *Fitosociologia* 44(1), 129-137.

Hadjikyriakou G, Hadjisterkotis E (2002) The adventive plants of Cyprus with new records of invasive species. *Z. Jagdwiss* 48:59–71. https://doi.org/10.1007/BF02192393

Hakkenberg CR, Peet RK, Urban DL, Song C (2018) Modeling plant composition as community continua in a forest landscape with LiDAR and hyperspectral remote sensing. *Ecol. Appl.* 28, 177–190. https//doi.org/10.1002/eap.1638

Hall K, Reitalu T, Sykes MT, Prentice HC (2012) Spectral heterogeneity of QuickBird satellite data is related to fine-scale plant species spatial turnover in semi-natural grasslands. *Appl. Veg. Sci.* 15, 145 – 157. https://doi.org/10.1111/j.1654-109X.2011.01143.x

Helman D, Lensky IM, Tessler N, Osem Y (2015) A phenology-based method for monitoring woody and herbaceous vegetation in Mediterranean forests from NDVI time series. *Remote Sens.* 7, 12314-12335. https://doi.org/ 10.3390/rs70912314

Henning SK, Estrup HA, Kathrin K (2005) Rejecting the mean: estimating the response of fen plant species to environmental factors by non-linear quantile regression. *J. Veg. Sci.* 16, 373-382. https//doi.org/10.1111/j.1654-1103.2005.tb02376.x

Hernández-Stefanoni JL, Gallardo-Cruz JA, Meave JA, Rocchini D, Bello-Pineda J, López-Martínez JO (2012) Modeling α- and β-diversity in a tropical forest from remotely sensed and spatial data. *Int. J. Appl. Earth Obs.* 19, 359-368. https//doi.org/10.1016/j.jag.2012.04.002

Herold M, Woodcock CE, di Gregorio A, Mayaux P, Belward AS, Latham J, Schmullius CC (2006) A joint initiative for harmonization and validation of land cover datasets. *IEEE Trans. Geosci. Remote Sens.* 44, 1719–1727. https//doi.org/10.1109/TGRS.2006.871219

Heumann BW, Hackett RA, Monfils AK (2015) Testing the spectral diversity hypothesis using spectroscopy data in a simulated wetland community. *Ecol. Inform.* 25, 29-34. https//doi.org/10.1016/j.ecoinf.2014.10.005

Hill RA, Wilson AK, George M, Hinsley SA (2010) Mapping tree species in temperate deciduous woodland using time-series multi-spectral data. *App. Veg. Sci.* 13, 86-99. https://doi.org/10.1111/j.1654-109X.2009.01053.x

Hijmans RJ (2012) Cross-validation of species distribution models : removing spatial sorting bias and calibration with a null model. *Ecology* 93, 679–688. https//doi.org/10.1890/11-0826.1

Hoffmann S, Schmitt TM, Chiarucci A, Irl SDH, Rocchini D, Vetaas OR, Tanase MA, Stéphane M, Bouvet A, Beierkuhnlein C (2019) Remote sensing of β-diversity: evidence from plant communities in a semi-natural system. *Appl. Veg. Sci.* 22, 13-26. https://doi.org/10.1111/avsc.12403

Honeck E, Castello R, Chatenoux B, Richard JP, Lehmann A, Giuliani, G (2018) From a vegetation index to a sustainable development goal indicator: forest trend monitoring using three decades of earth observations across Switzerland. *Int. J. Geo-Inf.* 7, 1 -13. https://doi.org/ 10.3390/ijgi7120455

Hosmer DW, Lemeshow S (2000) Interpretation of the fitted logistic regression model. In: Hosmer DW, Lemeshow S (Eds) *Applied logistic regression*. John Wiley & Sons, 47–90 (in New York).

Huete AR (2012) Vegetation indices, remote sensing and forest monitoring. *Geogr. Compass* 6, 513 – 532. https://doi.org/10.1111/j.1749-8198.2012.00507.x

Hulme PE, Pyšek P, Nentwig W, Vilà M (2009) Will threat of biological invasions unite the European Union? *Science* 324, 40–41. https://doi.org/10.1126/science.1171111

Jaccard P (1901) Étude comparative de la distribution florale dans une portion des Alpes et du Jura. *Bulletin de la Société vaudoise des sciences naturelles* 37, 547-579.

Janssen JAM, Rodwell JS, García Criado M, Gubbay S, Haynes T, Nieto A, Sanders N, Landucci F, Loidi J, Ssymank A, et al. (2016) European red list of habitats. Part 2. Terrestrial and freshwaters habitats, 1st ed, Luxemburg: European Union, pp. 1-38.

Jolicoeur S, O'Carroll S (2007) Sandy barriers, climate change and long-term planning of strategic coastal infrastructures, Îles-de-la-Madeleine, Gulf of St. Lawrence (Québec, Canada). *Landscape Urban Plan.* 81, 287 – 298. https://doi.org/10.1016/j.landurbplan.2007.01.011

Jones L, Sowerby A, Williams DL, Jones RE (2008) Factors controlling soil development in sand dunes: evidence from a coastal dune soil chronosequence. *Plant Soil* 307, 219-234. https://doi.org/10.1007/s11104-008-9601-9

Jones G, Bunting P, Hurford C (2017) Mapping Coastal Habitats in Wales. In Díaz-Delgado R, Lucas R, Hurford C (Eds) *The Roles of Remote Sensing in Nature*. *A practical guide and case studies*, 1st ed, Gewerbestrasse, Switerland: Springer, pp. 91–120.

Jørgensen RH, Kollmann J (2009) Invasion of coastal dunes by the alien shrub *Rosa rugosa* is associated with roads, tracks and houses. *Flora Morphology Distribution Functional Ecology of Plants* 204, 289–297. https//doi.org/10.1016/j.flora.2008.03.002

Jost L (2007) Partitioning diversity into independent alpha and beta components. *Ecology* 88(10), 2427-2439. https//doi.org/10.1890/06-1736.1

Kattenborn T, Lopatin J, Förster M, Braun AC, Fassnacht FE (2019) UAV data as alternative to field sampling to map woody invasive species based on combined Sentinel-1 and Sentinel-2 data. *Remote Sens. Environ.* 227, 61-73. https://doi.org/10.1016/j.rse.2019.03.025

Kaufman L, Rousseeuw PJ (2005) Finding Groups in Data, 10rd ed, New York., USA: John Wiley & Sons, pp. 1-342.

Khare S, Latifi H, Rossi S (2019) Forest beta-diversity analysis by remote sensing: how scale and sensors affect the Rao's Q index. *Ecol. Indic.* 106, 105520. https//doi.org/10.1016/j.ecolind.2019.105520

Kindt R, Coe R (2005) Tree diversity analysis. A manual and software for common statistical methods for ecological and biodiversity studies, 1st ed, Nairobi, Kenya: World Agroforestry Centre (ICRAF), pp. 31-70.

Koenker R (2020) Quantreg: quantile regression, R package version 5.73. https://cran.r-project.org/web/packages/quantreg/index.html

Kosmidou V, Petrou Z, Bunce RGH, Mücher CA, Jongman RHG, Bogers MMB, Lucas RM, Tomaselli V, Blonda P, Padoa-Schioppa E, et al. (2014) Harmonization of the Land Cover Classification System (LCCS) with the General Habitat Categories (GHC) classification systems. *Ecol. Indic.* 36, 290–300. http://dx.doi.org/10.1016/j.ecolind.2013.07.025

Kuhn M, Wing J, Weston S, Williams A, Keefer C, Engelhardt A, Cooper T, Mayer Z, Kenkel B, Benesty M (2020) Classification and Regression Training. R package version 6.0-85. https://github.com/topepo/caret/

Lasaponara R (2006) On the use of principal component analysis (PCA) for evaluating interannaual vegetation anomalies from SPOT/VEGETATION NDVI temporal series. *Ecol. Model.* 194, 429-434. https://doi.org/10.1016/j.ecolmodel.2005.10.035

Lausch A, Heurich M, Magdon P, Rocchini D, Schulz K, Bumberger J, King DJ (2020) A Range of Earth Observation Techniques for Assessing Plant Diversity. In Cavender-Bares J, Gamon J, Townsend P (Eds) *Remote Sensing of Plant Biodiversity*, 1st ed, Cham: Springer Nature, 309 – 348 (in Switzerland)

Lawrence RL, Wood SD, Sheley RL (2006) Mapping invasive plans using hyperspectral imagery and Breiman Cutler classifications (RandomForest). *Remote Sens. Environ.* 100, 356-262. https://doi.org/10.1016/j.rse.2005.10.014

Lazzaro L, Bolpagni R, Buffa G, Gentili R, Lonati M, Stinca A, Acosta ATR, Adorni M, Aleffi M, Allegrezza M, et al. (2020) Impact of invasive alien plants on native plant communities and Natura 2000 habitats: state of the art, gap analysis and perspectives in Italy. *J. Environ. Manage.* 274, 111140. https//doi.org/10.1016/j.jenvman.2020.111140

Le Dell, E. Petersen, M. van der Laan M (2015) Computationally efficient confidence intervals for cross- validated area under the ROC curve estimates. *Electron. J. Stat.* 9(1), 1173–1178. https://doi.org/10.1126/science.1249098.Sleep

Legendre P, Legendre L (2012) Numerical Ecology, 3nd ed, Oxford, UK: Elsevier, pp. 46-367.

Le Maitre D, van Wilgen BW, Chapman RA (2004) Alien plant invasions in South Africa: driving forces and the human dimension. *South African Journal Science* 100,103-112.

Le Maitre DC (2004) Predicting Invasive Species Impacts on Hydrological Processes : The Consequences of Plant Physiology for Landscape Processes. *Weed Technol.* 18, 1408–1410. https://doi.org/10.1614/0890-037X(2004)018[1408:PISIOH]2.0.CO;2

Le Maitre DC, Gaertner M, Marchante E, Ens EJ, Holmes PM, Pauchard A, O'Farrell PJ, Rogers AM, Blanchard R, Blignaut J, Richardson DM (2011) Impacts of invasive Australian acacias: Implications for management and restoration. *Diverss Distrib.* 17, 1015–1029. https://doi.org/10.1111/j.1472-4642.2011.00816.x

Lloyd DA (1990) Phenological classification of terrestrial vegetation cover using shortwave vegetation index imagery. *Int. J. Remote Sens.* 11, 2269-2279. https://doi.org/10.1080/01431169008955174

Lobo JM, Jiménez-valverde A, Real R (2008) AUC: A misleading measure of the performance of predictive distribution models. *Global Ecol. Biogeogr* 17, 145–151. https://doi.org/10.1111/j.1466-8238.2007.00358.x

Lockwood JL, Cassey P, Blackburn T (2005) The role of propagule pressure in explaining species invasions. *Trends Ecology & Evolution* 20, 223–228. https//doi.org/10.1016/j.tree.2005.02.004

Lucas NS, Shanmugam S, Barnsley M (2002) Sub-pixel habitat mapping of a costal dune ecosystem. *Appl. Geogr.* 22, 253–270. https//doi.org/10.1016/S0143-6228(02)00007-3

Luis J, Debaecker V, Pflug B, Main-Knorn M, Bieniarz J, Mueller-Wilm U, Cadau E, Gascon F (2016) Sentinel-2 Sen2cor: L2A processor for users. In Proceedings of the Living Planet Symposium, Prague, Czech Republic, 9–13 May 2016.

Machín AM, Marcello J, Hernández-Cordero AI, Abasolo JM, Eugenio F (2018) Vegetation species mapping in a coastal-dune ecosystem using high resolution satellite imagery. *GISci. Remote Sens.* 56, 210–232. https://doi.org/10.1080/15481603.2018.1502910

Madonsela S, Cho MA, Ramoelo A, Mutanga O (2017) Remote sensing of species diversity using Landsat 8 spectral variables. *ISPRS J. Photogramm.* 133, 116-127. https://doi.org/ 10.1016/j.isprsjprs.2017.10.008

Maglione P, Parente C, Vallario A (2014) Coastline extraction using high resolution WorldView-2 satellite imagery. *Eur. J. Remote Sen*. 47, 685-699. https://doi.org/10.5721/EuJRS20144739

Magurran AE (2004) Measuring biological diversity, 1st ed, Maden, USA: Blackwell Science, pp. 100-185.

Main-Knorn M, Pflug B, Louis J, Debaecker V, Müller-Wilm U, Gascon F (2017) Sen2Cor for Sentinel-2. In Image and Signal Processing for Remote Sensing XXIII, Proceedings of Spie Remote Sensing, Warsaw, Poland, 21-24 September; Bruzzone, L; Bovolo, F; Publisher: SPIE, Bellingham, WA

Malavasi M, Santoro R, Cutini M, Acosta ATR, Carranza ML (2013) What has happened to coastal dunes in the last half century? A multitemporal coastal landscape analysis in Central Italy. *Landscape Urban Plan.* 119, 54-63. http://dx.doi.org/10.1016/j.landurbplan.2013.06.012

Malavasi M, Carboni M, Cutini M, Carranza ML, Acosta ATR (2014) Land use legacy, landscape fragmentation and propagule pressure promote plant invasion on coastal dunes. A patch based approach. *Landsc. Ecol.* 29, 1541–1550. https//doi.org/10.1007/s10980-014-0074-3

Malavasi M, Santoro R, Cutini M, Acosta ATR, Carranza ML (2016) The impact of human pressure on landscape patterns and plant species richness in Mediterranean coastal dunes. *Plant Biosyst.* 150, 73–82. https://doi.org/10.1080/11263504.2014.913730

Malavasi M, Acosta ATR, Carranza ML, Bartolozzi L, Basset A, Bassignana M, Campanaro A, Canullo R, Caruggio F, Cavallaro V, et al. (2018a) Plant invasions in Italy: An integrative approach using the European LifeWatch infrastructure database. *Ecol. Indic.* 91, 182–188. https//doi.org/10.1016/j.ecolind.2018.03.038

Malavasi M, Bartak V, Carranza ML, Simova P, Acosta ATR (2018b) Landscape pattern and plant biodiversity in Mediterranean coastal dune ecosystems: do habitat loss and fragmentation really matter? *J. Biogeogr.* 45, 1367–1377. https://doi.org/10.1111/jbi.13215

Mannel S, Price M (2012) Comparing classification results of multi-seasonal TM against AVIRIS imagery – seasonality more important than number of bands. *PFG* 5, 603–612. https//doi.org/10.1127/1432-8364/2012/0142

Marzialetti F, Giulio S, Malavasi M, Sperandii MG, Acosta ATR, Carranza ML (2019) Capturing coastal dune natural vegetation types using a phenology-based mapping approach: the potential of Sentinel-2. *Remote Sens.* 11, 1506. https//doi.org/10.3390/rs11121506

Marzialetti F, Di Febbraro M, Malavasi M, Giulio S, Acosta ATR, Carranza ML (2020) Mapping coastal dune landscape through spectral Rao's Q temporal diversity. *Remote Sens.* 12, 2315. https//doi.org/10.3390/rs12142315

Mathieu R, Pouget M, Cervelle B, Escadafal R (1998) Relationships between satellite-based radiometric indices simulated using laboratory reflectance data and typic soil colour of an arid environment. *Remote Sens. Environ.* 66(1), 17-28. https//doi.org/10.1016/S0034-4257(98)00030-3

McFadden D (1973) Conditional logit analysis of qualitative choice behavior. In: Zarembka P (Eds.) *Frontiers in Econometrics*. New York: Wiley, pp. 105–142.

McFeeters SK (1996) The use of the Normalized Difference Water Index (NDWI) in the delineation of open water features. *Int. J. Remote Sens.* 17(7), 1425-1432. https://doi.org/10.1080/01431160600589179

McGarigal, K. Cushman, SA Ene E (2012) FRAGSTATS v4: Spatial Pattern Analysis Program for Categorical and Continuous Maps. http//www.umass.edu/landeco/research/fragstats/fragstats.html.

Mehta S. 2000. The Invasion of South African Fynbos by an Australian Immigrant: The story of *Acacia saligna*.

Meng J, Li S, Wang W, Liu Q, Xie S, Ma W (2016) Estimation of forest structural diversity using the spectral and textural information derived from SPOT-5 satellite images. *Remote Sens.*8, 125. https//doi.org/10.3390/rs8020125

Midgley SJ, Turnbull JW (2003) Domestication and use of Australian acacias: Case studies of five important species. *Aust. Syst. Bot.* 16:89–102. https://doi.org/10.1071/SB01038

Millar MA, Byrne M, O'Sullivan W (2011) Defining entities in the *Acacia saligna* (Fabaceae) species complex using a population genetics approach. *Aust. J. Bot.* 59, 137–148. https://doi.org/10.1071/BT10327

Miller J (2010) Species Distribution Modeling *Geography Compass* 4/6, 490-509. https://doi.org/10.1111/j.1749-8198.2010.00351.x

Milligan GW, Cooper MC (1988) A study of standardization of variables in cluster analysis. *Journal of Classification* 5, 181-204.

Milton SJ, Hall A V. (1981) Reproductive biology of Australian acacias in the south-western cape province, South Africa. *Transactions of the Royal Society of South Africa* 44, 465–487. https://doi.org/10.1080/00359198109520589

Mitchell CE, Agrawal AA, Bever JD, Gilbert GS, Hufbauer RA, Klironomos JN, Maron JL, Morris WF, Parker IM, Power AG, et al. (2006) Biotic interactions and plant invasions. *Ecol. Lett.* 9(6), 726-740. https://doi.org/10.1111/j.1461-0248.2006.00908.x

Mohammed NZ, Landry R Jr (2017) Assessing horizontal positional accuracy of Google Earth imagery in the city of Montreal, Canada. *Geod. Cartogr.* 43, 55–65. https://doi.org/10.3846/20296991.2017.1330767

Montgomery DC, Peck EA, Vining G (2012) Introduction to linear regression analysis, 5nd ed, Hoboken, New Jersey, USA: John Wiley & Sons Inc., pp. 1-645.

Murtagh F, Legendre P (2014) Ward's hierarchical agglomerative clustering method: which algorithms implement ward's criterion? *Journal of Classification* 31, 274-295. https//doi.org/10.1007/s00357-014-9161-z

Nagendra H, Rocchini D, Ghate R, Sharma B, Pareeth S (2010) Assessing plant diversity in a dry tropical forest: comparing the utility of Landsat and Ikonos satellite images. *Remote Sens.* 2, 478-496. https://doi.org/10.3390/rs2020478

Nagendra H, Lucas R, Honrado JP, Jongman RHG, Tarantino C, Adamo M, Mairota P (2013) Remote sensing for conservation monitoring: assessing protected areas, habitat extent, habitat condition, and threats. *Ecol. Indic.* 33, 45–49. http://dx.doi.org/10.1016/j.ecolind.2012.09.014

Noi PT, Kappas M (208) Comparison of Random Forest, k-Nearest Neighbor and Support Vector Machine classifiers for land cover classification using Sentinel-2 imagery. *Sensors* 18(18), 1-20. https//doi.org/10.3390/s18010018

Noormets A (2009) Phenology of Ecosystem Processes. Applications in global change research, 1st ed, New York: Springer, pp. 1-275.

Nsikani MM, Novoa A, van Wilgen BW, Keet JH, Gaertner M (2017) *Acacia saligna*'s soil legacy effects persist up to 10 years after clearing: Implications for ecological restoration. *Austral Ecol.* 42, 880–889. https//doi.org/10.1111/aec.12515

Oldeland J, Wesuls D, Rocchini D, Schmidt M, Jürgens N (2010) Does using species abundance data improve estimates of species diversity from remotely sensed spectral heterogeneity? *Ecol. Indic.* 10, 390-396. https//doi.org/10.1016/j.ecolind.2009.07.012

Pal M (2005) Random forest classifier for remote sensing classification. *Int. J. Remote Sens.* 26, 217–222. https://doi.org/10.1080/01431160412331269698

Palmer MW, Earls PG, Hoagland BW, White PS, Wohlgemuth T (2002) Quantitative tools for perfecting species lists. *Environmetrics* 13, 121-137. https//doi.org/10.1002/env.516

Parendes L, Jones J (2000) Role of light availability and dispersal in exotic plant invasion along roads and streams in the H.J. Andrews experimental forest, Oregon. *Conservat. Biol.* 14, 64–75. https://doi.org/10.1046/j.1523-1739.2000.99089.x

Pavoine S, Ricotta C (2019) Measuring functional dissimilarity among plots: adapting old methods to new questions. *Ecol. Indic.* 97, 67-72. https//doi.org/10.1016/j.ecolind.2018.09.048

Pearce J, Ferrier S (2000) Evaluating the predictive performance of habitat models developed using logistic regression. *Ecol. Model.* 133, 225–245. https://doi.org/10.1016/S0304-3800(00)00322-7

Peet RK (1974) The measurement of species diversity. *Annu. Rev. Ecol. Syst.* 5, 285-307. https//doi.org/10.1146/annurev.es.05.110174.001441

Pesaresi S, Mancini A, Quattrini G, Casavechia S (2020) Mapping mediterranean forest plant associations and habitats with functional principal component analysis using Landsat 8 NDVI time series. *Remote Sens.* 12, 1132. https://doi.org/10.3390/rs12071132

Pettorelli N, Vik JO, Mysterud A, Gaillard JM, Tucker CJ, Stenseth NC (2005) Using the satellite-derived NDVI to assess ecological responses to environmental change. *Trends Ecol. Evol.* 20, 503 – 510. https://doi.org/10.1016/j.tree.2005.05.011

Petrou ZI, Manakos I, Stathaki T (2015) Remote sensing for biodiversity monitoring: a review of methods for biodiversity indicator extraction and assessment of progress towards international targets. *Biodivers. Conserv.* 24, 2333 – 2363. https://doi.org/10.1007/s10531-015-0947-z

Prajesh PJ, Kannan B, Pazhanivelan S, Kumaraperumal R, Ragunath KP (2019) Monitoring and mapping of seasonal vegetation trend in Tamil Nadu using NDVI and NDWI imagery. *Journal of Applied and Natural Science*. 2019, 11(1), 54-61. https://doi.org/10.31018/jans.v11i1.1964

Prisco I, Stanisci A, Acosta ATR (2016) Mediterranean dunes on the go: evidence from a short term study on coastal herbaceous vegetation. *Estuar. Coast. Shelf S* 182(A), 40-46. https://doi.org/10.1016/j.ecss.2016.09.012

Prisco I, Angiolini C, Assini S, Buffa G, Gigante D, Marcenó C, Sciandrello S, Villani M, Acosta ATR (2020) Conservation status of Italian coastal dune habitats in the light of the 4th monitoring report (92/43/EEC Habitats directive). *Plant Sociology* 57(1), 55-64. https//doi.org/10.3897/pls2020571/05

Qi J, Chehbouni A, Huete AR, Kerr YH, Sorooshian SA (1994) A modified soil adjusted vegetation index. *Remote Sens. Environ.* 48, 118-126. https//doi.org/10.1016/0034-4257(94)90134-1

Qin Y, Xiao X, Dong, Zhang G, Roy PS, Joshi PK, Gilani H, Murthy MSR, Jin, C., Wang J, et al. (2016) Mapping forests in monsoon Asia with ALOS PALSAR 50-m mosaic images and MODIS imagery in 2010. *Sci. Rep.* 6, 1–10. https//doi.org/10.1038/srep20880

Rao CR (1982) Diversity and dissimilarity coefficients: a unified approach. *Theor. Popul. Biol.* 21, 24-43. https://doi.org/10.1016/0040-5809(82)90004-1

Rapinel S, Clément B, Magnanon S, Sellin V, Hubert-Moy L (2014) Identification and mapping of natural vegetation on a coastal site using a Worldview-2 satellite image. *J. Environ. Manage.* 144, 236 – 246. http://dx.doi.org/10.1016/j.jenvman.2014.05.027

Rapinel S, Mony C, Lecoq L, Clénìment B, Thomas A, Hubert-Moy L (2019) Evaluation of Sentinel-2 time-series for mapping floodplain grassland plant communities. *Remote Sens. Environ* 223, 115-129. https://doi.org/10.1016/j.rse.2019.01.018

Recanatesi F, Giuliani C, Ripa MN (2018) Monitoring Mediterranean Oak decline in a peri-urban protected area using the NDVI and Sentinel-2 images: the case study of Castelporziano State Natural Reserve. *Sustainability* 10, 1-10. http://doi.org/10.3390/su10093308

Richardson DM, Pyšek P (2006) Plant invasions: Merging the concepts of species invasiveness and community invasibility. *Prog. Phy. Geog.* 30, 409–431. https://doi.org/10.1191/0309133306pp490pr

Richardson DM, Rejmánek M (2011) Trees and shrubs as invasive alien species - a global review. *Divers Distrib* 17,788–809. https//doi.org/10.1111/j.1472-4642.2011.00782.x

Richardson DM, Carruthers J, Hui C, Impson FA, Miller JT, Robertson MP, Rouget M, Le Roux JJ, Wilson JRU (2011) Human-mediated introductions of Australian acacias - a global experiment in biogeography. *Divers. Distrib.* 17:771–787. https://doi.org/10.1111/j.1472-4642.2011.00824.x.

Ricotta C, Carranza ML, Avena G, Blasi C (2000) Quantitative comparison of the diversity of landscapes with actual vs. potential natural vegetation. *App. Veg. Sci.* 3(2), 157-162. https://doi.org/10.2307/1478994

Ricotta C, Moretti M (2011) CWM and Rao's quadratic diversity: a unified framework for functional ecology. *Oecologia*. 167, 181–188. https://doi.org/10.1007/s00442-011-1965-5

Ricotta C, Carranza ML (2013) Measuring scale-dependent landscape structure with Rao's quadratic diversity. *ISPRS Int. J. Geo-Inf.* 2, 405-412. https://doi.org/10.3390/ijgi2020405

Ricotta C, Podani J (2017) On some properties of the Bray-Curtis dissimilarity and their ecological meaning. *Ecol. Complex.* 31, 201-205. http://dx.doi.org/10.1016/j.ecocom.2017.07.003

Rocchini D (2007a) Effects of spatial and spectral resolution in estimating ecosystem α-diversity by satellite imagery. *Remote Sens. Environ.* 111, 423-434. https://doi.org/ 10.1016/j.rse.2007.03.018

Rocchini D (2007b) Distance decay in spectral space in analyzing β-diversity. *Int. J. Remote Sens.* 28(11), 2635-2644. https://doi.org/10.1080/01431160600954712
Rocchini D, Nagendra H, Ghate R, Cade BS (2009) Spectral distance decay: assessing species beta-diversity by quantile regression. *Photogramm. Eng. Rem. S.* 75(10), 1225-1230. https://doi.org/0099-1112/09/7510–1225/$3.00/0
Rocchini D, Hernández-Stefanoni JL, He KS (2015) Advancing species diversity estimate by remotely sensed proxies: a conceptual review. *Ecol. Inform.* 25, 22-28. https://doi.org/10.1016/j.ecoinf.2014.10.006
Rocchini D, Boyd DS, Féret JB, Foody GM, He KS, Lausch A, Nagendra H, Wegmann M, Pettorelli N (2016) Satellite remote sensing to monitor species diversity: potential and pitfalls. *Remote Sensing in Ecology and Conservation* 2(1), 25-36. https://doi.org/10.1002/rse2.9
Rocchini D, Marcantonio M, Ricotta C (2017) Measuring Rao's Q diversity index from remote sensing: an open source solution. *Ecol. Indic.*72, 234-238. http://dx.doi.org/10.1016/j.ecolind.2016.07.039
Rocchini D, Marcantonio M, Da Re D, Chirici G, Galluzzi M, Lenoir J, Ricotta C, Torresani M, Ziv G (2019) Time-lapsing biodiversity: An open source method for measuring diversity changes by remote sensing *Remote Sens. Environ.* 231, 111192. https//doi.org/10.1016/j.rse.2019.05.011
Rocchini D, Salvatori N, Beierkuhnlein C, Chiarucci A, de Boissieu F, Förster M, Garzon-Lopez CX, Gillespie TW, Hauffe HC, He KS, et al. (2021) From local spectral species to global spectral communities. a benchmark for ecosystem diversity estimate by remote sensing. *Ecol. Inform.* 61, 101195. https//doi.org/10.1016/j.ecoinf.2020.101195
Rodriguez-Galiano VF, Ghimire B, Rogan J, Chica-Olmo M, Rigol-Sanchez JP (2012) An assessment of the effectiveness of a random forest classifier for land-cover classification. *ISPRS J. Photogramm. Remote Sens.* 67, 93–104. https//doi.org/10.1016/j.isprsjprs.2011.11.002
Romano B, Zullo F (2014) The urban transformation of Italy's Adriatic coastal strip: Fifty years of unsustainability. *Land Use Policy* 38, 26–36. https://doi.org/10.1016/j.landusepol.2013.10.001
Rondeaux G, Steven M, Baret F (1996) Optimization of soil-adjusted vegetation indices. *Remote Sens. Environ.* 55, 55-107. https/7doi.org/10.1016/0034-4257(95)00186-7
Rouse JW, Haas RH, Schell JA, Deering DW (1973) Monitoring vegetation systems in the Great Plains with ERTS. In Proceedings of the Third ERTS Symposium, NASA: Washington, DC, USA, 10–14 NASA SP-351; pp. 309–317.
Rwanga SS, Ndambuki JM (2017) Accuracy assessement of land use/land cover classification using remote sensing and GIS. *International Journal of Geosciences* 8, 611-622. https://doi.org/10.4236/ijg.2017.84033
Santoro R, Jucker T, Carranza ML, Acosta ATR (2011) Assessing the effects of *Carpobrotus* invasion on coastal dune soils. Does the nature of the invaded habitat matter? *Community Ecol.* 12, 234-240. https://doi.org/10.1556/ComEc.12.2011.2.12
Santoro R, Jucker T, Prisco I, Carboni M, Battisti C, Acosta ATR (2012) Effects of trampling limitation on coastal dune plant communities. *Environ. Manag.* 49, 534–542. https//doi.org/10.1007/s00267-012-9809-6
Sarmati S, Conti L, Acosta ATR (2019) *Carpobrotus acinaciformis* vs *Carpobrotus edulis*: are there any differences in their impact on coastal dune plant biodiversity? *Flora* 257, 151422. https://doi.org/10.1016/j.flora.2019.151422
Schlacher T, Dugan J, Schoeman DS, Lastra M, Jones A, Scapini F, McLachlan A, Defeo O (2007) Sandy beaches at the brink. *Divers. Distrib.* 13, 556-560. https://doi.org/10.1111/j.1472-4642.2007.00363.x
Schmidtlein S, Fassnacht FE (2017) The spectral variability hypothesis does not hold across landscapes. *Remote Sens. Environ.* 192, 114-125. https://doi.org/10.1016/j.rse.2017.01.036
Sciandrello S, Tomaselli G, Minissale P (2015) The role of natural vegetation in the analysis of the spatio-temporal changes of coastal dune system: a case study in Sicily. *J. Coast. Conserv*. 19, 199-212. https:/doi.org/10.1007/s11852-015-0381-0
Selmants PC, Knight DH (2003) Understory plant species composition 30-50 years after clearcutting in southeastern Wyoming coniferous forests. *Forest Ecol. Manag* 185, 275–289. https://doi.org/10.1016/S0378-1127(03)00224-X
Shannon CE (1948) A mathematical theory of communication. *Bell Syst. Tech. J.* 23, 379-423. https//doi.org/10.1002/j.1538-7305.1948.tb01338.x
Simberloff D, Martin JL, Genovesi P, Maris V, Wardle DA, Aronson J, Courcham F, Galil B, García-Berthou, Pascal M, Pyšek P, Sousa R, Tabacchi E, Vilá M (2013) Impacts of biological invasions: What's what and the way forward. *Trends in Ecology & Evolution* 28(1), 58–66. https://doi.org/10.1016/j.tree.2012.07.013
Simpson EH (1949) Measurement of diversity. *Nature* 163, 688.
Sitzia T, Campagnaro T, Kowarik I, Trentanovi G (2016) Using forest management to control invasive alien species: helping implement the new European regulation on invasive alien species. *Biol. Invasions* 18, 1–7. https://doi.org/10.1007/s10530-015-0999-8
Spellerberg I (1998) Ecological effects of roads and traffic: a literature review. *Global Ecol. Biogeogr.* 7, 317-333. https://doi.org/10.1046/j.1466-822x.1998.00308.x
Sperandii MG, Prisco I, Stanisci A, Acosta ATR (2017) RanVegDunes-A random plot database of Italian coastal dunes. *Phytocoenologia* 47(2), 231-232. https//doi.org/10.1127/phyto/2017/0198
Sperandii MG, Prisco I, Acosta ATR (2018) Hard times for Italian coastal dunes: insights from a diachronic analysis base on random plots. *Biodivers. Conserv.* 27, 633–646. https://doi.org/10.1007/s10531-017-1454-1
Sperandii MG, Bazzichetto M, Gatti F, Acosta ATR (2019) Back into the past: Resurveying random plots to track community changes in Italian coastal dunes. *Ecol. Indic.* 96, 572-578. https://doi.org/10.1016/j.ecolind.2018.09.039

Sperandii MG, Barták V, Acosta ATR (2020) Effectiveness of the Natura 2000 network in conserving Mediterranean coastal dune habitats. *Biol. Conserv.* 248, 108689. https//doi.org/10.1016/j.biocon.2020.108689

Stanisci A, Acosta ATR, Carranza ML, Feola S, Giuliano M (2007) Gli habitat di interesse comunitario sul litorale molisano e il loro valore naturalistico su base floristica. Fitosociologia. 44(2), 171-175.

Stanisci A, Acosta ATR, Carranza ML, de Chiro M, Del Vecchio S, Di Martino L, Frattaroli AR, Fusco S, Izzi CF, Pirone G, Prisco I (2014) EU habitats monitoring along the coastal dunes of the LTER sites of Abruzzo and Molise (Italy). *Plant Sociology* 51, 51–56. https://doi.org/10.7338/pls2014512S1/07

Stoms DM, Hargrove WW (2000) Potential NDVI as a baseline for monitoring ecosystem functioning. *Int. J. Remote Sens.* 21, 401-407. https://doi.org/10.1080/014311600210920

Strydom M, Esler KJ, Wood AR (2012) *Acacia saligna* seed banks: Sampling methods and dynamics, Western Cape, South Africa. *S. Afr. J. Bot.* 79:140–147. https//doi.org/10.1016/j.sajb.2011.10.007

Sun C, Fagherazzi S, Liu Y (2018) Classification mapping of salt marsh vegetation by flexible monthly NDVI time-series using Landsat imagery. *Estuar. Coast. Shelf. Sci.* 213, 61 – 80. https://doi.org/10.1016/j.ecss.2018.08.007 (

Thompson SD, Gergerl S (2008) Conservation implications of mapping rare ecosystems using high spatial resolution imagery: recommendations for heterogeneous and fragmented landscapes. *Landsc. Ecol.* 23, 1023–1037. https//doi.org/10.1007/s10980-008-9263-2

Thuiller W, Richardson DM, Pyšek P, Midgley GF, Hughes GO, Rouget M (2005) Niche-based modelling as a tool for predicting the risk of alien plant invasions at a global scale. *Glob. Change Biol.* 11, 2234–2250. https//doi.org/10.1111/j.1365-2486.2005.01018.x

Tilahun A, Teferie B (2015) Accuracy assessment of land use land cover classification using Google Earth. *AJEP*, 4, 193–198. https//doi.org/10.11648/j.ajep.20150404.14

Timm BC, McGarigal K (2012) Fine-scale remotely-sensed cover mapping of coastal dune and salt marsh ecosystems at Cape Cod National Seashore using Random Forests. *Remote Sens. Environ.* 127, 106-117. https://doi.org/10.1016/j.rse.2012.08.033

Todd SW, Hoffer RM, Milchunas DG (1998) Biomass estimation on grazed and ungrazed rangelands using spectral indices. *Int. J. Remote Sens.* 19(3), 427-438. https://doi.org/10.1080/014311698216071

Tomaselli V, Adamo M, Veronico G, Sciandrello S, Tarantino C, Dimopoulos P, Medagli P, Nagendra H, Blonda P (2017) Definition and application of expert knowledge on vegetation pattern, phenology, and seasonality for habitat mapping, as exemplified in a Mediterranean coastal site. *Plant Biosyst.* 151, 887-899. https://doi.org/10.1080/11263504.2016.1231143

Torresani M, Rocchini D, Sonnenschein R, Zebisch M, Marcantonio M, Ricotta C, Tonon G (2019) Estimating tree species diversity from space in an alpine conifer forest: the Rao's Q diversity index meets the spectral variation hypothesis. *Ecol. Inform.* 52, 26-34. https://doi.org/10.1016/j.ecoinf.2019.04.001

Torresani M, Rocchini D, Sonnenschein R, Zebisch M, Hauffe HC, Heym M, Pretzsch H, Tonon G (2020) Height variation hypothesis: a new approach for estimating forest species diversity with CHM LiDAR data. *Ecol. Indic.* 117, 106520. https://doi.org/10.1016/j.ecolind.2020.106520

Tucker CJ (1979) Red and photographic infrared linear combinations of monitoring vegetation. *Remote Sens. Environ.* 8, 127 – 150. https://doi.org/10.1016/0034-4257(79)90013-0

Tulloch AIT, Sutcliffe P, Naujokaitis-Lewis I, Tingley R, Brotons L, Ferraz KM, Possingham H, Guisan A, Rhodes JR (2016) Conservation planners tend to ignore improved accuracy of modelled species distributions to focus on multiple threats and ecological processes. *Biol. Conserv.* 199, 157–171. https://doi.org/10.1016/j.biocon.2016.04.023

Underwood E, Ustin SL, Di Pietro D (2003) Mapping nonnative plants using hyperspectral imagery. *Remote Sens. Environ.* 86, 150-161. https//doi.org/10.1016/S0034-4257(03)00096-8

Underwood E, Ustin SL, Ramirez CM (2007) A comparison of spatial and spectral image resolution for mapping invasive plants in coastal California. *Environ. Manage.* 39, 63-83. https//doi.org/10.1007/s00267-005-0228-9

Valentini E, Taramelli A, Filipponi F, Giulio S (2015) An effective procedure for EUNIS and Natura 2000 habitat type mapping in estuarine ecosystems integrating ecological knowledge and remote sensing analysis. *Ocean Coast. Manage.* 108, 52 – 64. http://dx.doi.org/10.1016/j.ocecoaman.2014.07.015

van der Maarel E (2003) Some remarks on the functions of European coastal ecosystems. *Phytocoenologia* 33, 187-202. https://doi.org/10.1127/0340-269X/2003/0033-0187

Vihervaara P, Auvinen AP, Mononen L, Törmä M, Ahlroth P, Anttila S, Böttcher K, Forsius M, Heino J, Heliola J, et al. (2017) How essential biodiversity variables and remote sensing can help national biodiversity monitoring. *Global Ecology and Conservation*, 10, 43–59. https//doi.org/10.1016/j.gecco.2017.01.007

Vrieling A, Meroni M, Darvishzadeh R, Skidmore AK, Wang T, Zurita-Milla R, Oosterbeek K, O'Connor K, Paganini M (2018) Vegetation phenology from Sentinel-2 and field cameras for a Dutch barrier island. *Remote Sens. Environ.* 215, 517-529. https://doi.org/10.1016/j.rse.2018.03.014

Wang R Gamon JA, Cavender-Bares V, Townsend PA, Zygielbaum A (2018). The spatial sensitivity of the spectral diversity-biodiversity relationship: an experimental test in a prairie grassland. *Ecol. Appl.* 28(2), 541-556. https//doi.org/10.1002/eap.1669

Ward JH (1963) Hierarchical grouping to optimize and objective function. *J. Am. Stat. Assoc.* 58, 236-244. https://doi.org/10.2307/2282967

Warren SD, Alt M, Olson KD, Irl SDH, Steinbauer MJ. Jentsch A (2014) The relathionship between the spectral diversity of satellite imagery habitat heterogeneity, and plant species richness. *Ecol. Inform.* 24, 160-168. https//doi.org/10.1016/j.ecoinf.2014.08.006

Weiher E, Keddy PA (1995) Assembly Rules, Null Models, and Trait Dispersion: New Questions from Old Patterns. *Oikos* 74(1), 159-164. https://doi.org/10.2307/3545686

Whitaker RH (1960) Vegetation of the Siskiyou Mountains, Oregon and California. *Ecol. Monogr.* 30(3), 279-338. https//doi.org/10.2307/1943563

Whitaker RH (1972) Evolution and measurement of species diversity. *Taxon* 21(2/3), 213.251. https//doi.org/10.2307/1218190

Wildi O (2010) Data analysis in vegetation ecology, 1st ed, Chichester, UK: John Wiley & Sons, pp. 25-34.

Wilson JRU, Gairifo C, Gibson MR, Arianoutsou M, Bakar BB, Baret S, Celesti-Grapow L, DiTomaso JM, Dufour-Dror JM, Kueffer C, et al. (2011) Risk assessment, eradication, and biological control: Global efforts to limit Australian acacia invasions. *Divers. Distrib.* 17, 1030–1046. https//doi.org/10.1111/j.1472-4642.2011.00815.x

Witkowski ETF (1994) Growth of seedlings of the invasives, *Acacia saligna* and *Acacia cyclops*, in relation to soil Phosphorus. *Aust. J. Ecol.* 19, 290–296. https://doi.org/10.1111/j.1442-9993.1994.tb00492.x

Wu, J. (2004) Effects of changing scale on landscape pattern analysis: scaling relations. *Landsc. Ecol.* 19, 125–138. https//doi.org/10.1023/B:LAND.0000021711.40074.ae

Wu W, Zhou Y, Tian B (2017) Coastal wetlands facing climate change and anthropogenic activities: a remote sensing analysis and modelling application. *Ocean Coast. Manage.* 138, 1 -10. http://dx.doi.org/10.1016/j.ocecoaman.2017.01.005

Wu Z, Velasco M, McVay, J, Middleton B, Vogel J, Dye D (2016) MODIS derived vegetation index for drought detection on the San Carlos Apache reservation. *International Journal of Advanced Remote Sensing and GIS* 5, 1524-1538. https//doi.org/10.23953/cloud.ijarsg.44

Xie Y, Sha Z, Yu M (2008) Remote sensing imagery in vegetation mapping: a review *J. Plant Ecol.* 1, 9-23. http://doi.org/10.1093/jpe/rtm005

Xu Y, Dickson BG, Hampton HM, Sisk TD, Palumbo JA, Prather JW (2009) Effects of mismatches of scale and lo-cation between predictor and response variables on forest structure mapping. *Photogramm. Engin. Rem. S.* 75(3), 313-322. https//doi.org/0099-1112/09/7503–0313/$3.00/0

Yelenik SG, Stock WD, Richardson DM (2004) Ecosystem level impacts of invasive *Acacia saligna* in the South African fynbos. *Restor. Ecol.* 12, 44–51. https://doi-org/10.1111/j.1061-2971.2004.00289.x

Zhang L, Baas ACW (2012) Mapping functional vegetation abundance in a coastal dune environment using a combination of LSM and MLC: a case study at Kenfig NNR, Wales. *Int. J. Remote Sens.* 33, 5043 – 5071. https://doi.org/10.1080/01431161.2012.657369

Zoffoli ML, Kandus P, Madanes N, Calvo DH (2008) Seasonal and interannual analysis of wetlands in South America using NOAA-AVHRR NDVI time series: the case of the Parana delta region. *Landscape Ecol*. 23(7), 833-848. https://doi.org/10.1007/s10980-008-9240-9

Zuur AF, Ieno EN, Elphick CS (2010) A protocol for data exploration to avoid common statistical problems. *Methods Ecol. Evol.* 1(1), 3-14. https://doi.org/10.1111/j.2041-210X.2009.00001.x

List of papers (published, Journal, DOI, or submitted).

Marzialetti F, Bazzichetto M, Giulio S, Acosta ATR, Stanisci A, Malavasi M, Carranza ML (2019) Modelling Acacia saligna invasion on the Adriatic coastal landscape: An integrative approach using LTER data. *Nat. Conserv.*- 34, 127-144. https://doi.org/10.3897/natureconservation.34.29575

Marzialetti F, Giulio S, Malavasi M, Sperandii MG, Acosta ATR, Carranza ML (2019) Capturing Coastal Dune Natural Vegetation Types Using a Phenology-Based Mapping Approach: The Potential of Sentinel-2. *Remote Sens.* 11, 1506. https//doi.org/10.3390/rs11121506

Marzialetti F, Di Febbraro M, Malavasi M, Giulio S, Acosta ATR, Carranza ML (2020) Mapping Coastal Dune Landscape through Spectral Rao's Q Temporal Diversity *Remote Sens.* 12, 2315. https//doi.org/10.3390/rs12142315

Marzialetti F, Cascone S, Frate L, Di Febbraro M, Acosta ATR, Carranza (2021) Measuring alpha and beta diversity by field and remote sensing data: A challenge for coastal dunes biodiversity monitoring. *Remote Sens.* 13, 1928. https://doi.org/ 10.3390/rs13101928

Drius M, Jones L, **Marzialetti F**, de Francesco MC, Stanisci A, Carranza ML (2019) Not just a sandy beach. The multi-service value of Mediterranean coastal dunes. *Sci. Total Environ.* 668, 10, 1139-1155 https://doi.org/10.1016/j.scitotenv.2019.02.364

Carranza ML, Drius M, **Marzialetti F**, Malavasi M, de Francesco MC, Acosta ATR, Stanisci A (2020) Urban expansion depletes cultural ecosystem services: an insight into a Mediterranean coastline. *Rendiconti Lincei. Scienze Fisiche e Naturali* 31, 103-111. htps//doi.org/10.1007/s12210-019-00866-w

Lozano V, **Marzialetti F**, Carranza ML, Chapman D, Branquart E, Dološ K, Große-Stoltenberg A, Fiori M, Capece P, Brundu G (2020) Modelling Acacia saligna invasion in a large Mediterranean island using PAB factors: A tool for implementing the European legislation on invasive species *Ecol. Indic.* 116, 106516. https//doi.org/10.1016/j.ecolind.2020.106516

Giulio S, Cao Pinna L, Carboni M, **Marzialetti F**, Acosta ATR (2021) Invasion success on European coastal dunes. *Plant Sociology* 58(1), 29-39. https//doi.org/0.3897/pls2021581/02

Giulio S, Carboni M, **Marzialetti F**, Acosta ATR, Garbolino E, Jucker T (Major Revision) Invasion dynamics of Euphorbia paralias from Europe and potential further spread across Australian coastal dunes *J. Biogeogr.*